13482

RD&E CENTER

Technical Report

No. 13482

STANDARD SCENES PROGRAM FOR ESTABLISHING
A NATURAL SCENES DATA BASE

CONTRACT NO. DAAE07-85-G-R007

DECEMBER 1989

By William R. Reynolds
Anne Marie L. LaHaie
Robert K. Baratono
Keweenaw Research Center
Michigan Technological University
Houghton, MI 49931

U.S. ARMY TANK-AUTOMOTIVE COMMAND
RESEARCH, DEVELOPMENT & ENGINEERING CENTER
Warren, Michigan 48397-5000

NOTICES

REPORT DOCUMENTATION PAGE

Form Approved
OMB No. 0704-0188
Exp. Date: Jun 30, 1986

1a. REPORT SECURITY CLASSIFICATION
Unclassified

1b. RESTRICTIVE MARKINGS

2a. SECURITY CLASSIFICATION AUTHORITY

2b. DECLASSIFICATION / DOWNGRADING SCHEDULE

3. DISTRIBUTION / AVAILABILITY OF REPORT
Approved for Public Release.
Distribution is Unlimited.

4. PERFORMING ORGANIZATION REPORT NUMBER(S)

5. MONITORING ORGANIZATION REPORT NUMBER(S)

6a. NAME OF PERFORMING ORGANIZATION
KEWEENAW RESEARCH CENTER

6b. OFFICE SYMBOL (If applicable)

7a. NAME OF MONITORING ORGANIZATION
U.S. ARMY TANK-AUTOMOTIVE COMMAND

6c. ADDRESS (City, State, and ZIP Code)
Michigan Technological University
Houghton, MI 49931

7b. ADDRESS (City, State, and ZIP Code)
Attn: AMSTA-RSA
Warren, MI 48397-5000

8a. NAME OF FUNDING / SPONSORING ORGANIZATION
USA TACOM

8b. OFFICE SYMBOL (If applicable)
AMSTA-RSA

9. PROCUREMENT INSTRUMENT IDENTIFICATION NUMBER
DAAE07-85-G-R007 D.O. #0012

8c. ADDRESS (City, State, and ZIP Code)
Warren, MI 48397-5000

10. SOURCE OF FUNDING NUMBERS

PROGRAM ELEMENT NO.	PROJECT NO.	TASK NO.	WORK UNIT ACCESSION NO.

11. TITLE (Include Security Classification)
Standard Scenes Program for Establishing a Natural Scenes Data Base

12. PERSONAL AUTHOR(S)
William R. Reynolds, Anne Marie L. LaHaie & Robert K. Baratono

13a. TYPE OF REPORT
Final

13b. TIME COVERED
FROM 3/31/86 TO 1/31/87

14. DATE OF REPORT (Year, Month, Day)
1989 December

15. PAGE COUNT
166

16. SUPPLEMENTARY NOTATION

17. COSATI CODES

FIELD	GROUP	SUB-GROUP

18. SUBJECT TERMS (Continue on reverse if necessary and identify by block number)
Infrared
Natural Backgrounds
Thermal Imaging
Background Modeling
Thermal Clutter

19. ABSTRACT (Continue on reverse if necessary and identify by block number)

An understanding of spatial & temporal variations of radiance in natural terrains is fundamental to accurate modeling & prediction of infrared target detection capabilities. To this end, six tracts of land in Northern Michigan were selected and extensively characterized in terms of their topography, soil, vegetation, & other physical features. Thermal imagery of these scenes & of military vehicles was recorded concurrently with weather data to provide a data base that covers a wide range of conditions. Selected clutter statistics & spectral analysis techniques were tested on this data base, in order to gain an insight to possible relationships between physical and meteorological parameters of the scene & image descriptive measures.

20. DISTRIBUTION / AVAILABILITY OF ABSTRACT
☐ UNCLASSIFIED/UNLIMITED ☒ SAME AS RPT. ☐ DTIC USERS

21. ABSTRACT SECURITY CLASSIFICATION
Unclassified

22a. NAME OF RESPONSIBLE INDIVIDUAL
Wallace Mick

22b. TELEPHONE (Include Area Code)
(313) 574-5788

22c. OFFICE SYMBOL
AMSTA-RSA

DD FORM 1473, 84 MAR

83 APR edition may be used until exhausted.
All other editions are obsolete.

SECURITY CLASSIFICATION OF THIS PAGE
UNCLASSIFIED

PREFACE

The work described in this technical report was sponsored by the Countermeasure Function, AMSTA-RSC, of the U. S. Army Tank-Automotive Command under contract number DAAE07-85-G-R007, delivery order 012. For further information contact:

Keweenaw Research Center
Attn: William R. Reynolds
Michigan Technological University
Houghton, Michigan 49931

Department of the Army
U. S. Army Tank-Automotive Command
Attn: AMSTA-RSA (Wally Mick)
Warren, Michigan 48397-5000

TABLE OF CONTENTS

TABLE OF CONTENTS (Continued)

LIST OF ILLUSTRATIONS

LIST OF ILLUSTRATIONS (Continued)

LIST OF ILLUSTRATIONS (Continued)

LIST OF TABLES

1.0. FORWARD

This report represents a final comprehensive discussion of the Standard Scene program. The test and analysis activity conducted under this program includes four years in which multiseasonal diurnal thermal infrared imagery was recorded for standard background scenes. In addition to thermal data acquisition, first principles thermal models were developed to simulate the Infrared (IR) signature of simple background scenes and validated with the Standard Scenes thermal imagery.

This report will describe in detail each of the six standard scene sites. Emphasis will be placed on the clutter routines developed for this program[1] and the results of the clutter analysis performed with the multiseasonal Standard Scene imagery.

The background models developed as part of this program have been presented in detail in the previous Standard Scene report[2], so they will not be discussed extensively in this report. The interested reader is referred to the previous report for more information.

2.0. INTRODUCTION

2.1. Backgrounds

2.1.1. Infrared (IR) Backgrounds. Military vehicles, equipment and sensors operate within the context of an environment whose properties may serve to enhance or degrade target detection capabilities, to improve or endanger vehicle survivability, to complement or compromise the effectiveness of a given countermeasure. In terms of infrared detection, the background against which a target is observed is dynamic, both spatially and temporally, and interactive with the target. Scenario components that determine or influence variation in background IR characteristics include the scene composition, from such gross distinctions as between natural versus urban scenes, to finer details of soil and ground cover characteristics. Temporal and meteorological parameters also affect IR variation in a scene. A related consideration is the viewing direction. Because of the dynamics of solar heating during diurnal cycles, viewing direction will have a major influence on target-background signatures: south-facing treelines will receive more solar radiation than north-facing ones and hence appear very different in infrared imagery. In order to assess vehicle IR signatures, it is important to have an understanding of the thermal behaviour of the natural surroundings in which the vehicle operates. It is therefore necessary to analyze and identify not only the IR properties

of the target but also those properties of its background that change, enhance, or disquise the target's signature.

2.1.2. Natural Scenes. Infrared detection frequently involves trying to distinguish between targets and natural terrain elements. Countermeasures are often designed with the objective of making an artificial object appear as similar to natural objects and foliage as possible. The Standard Scenes program has therefore concentrated on investigating natural backgrounds. Battlefield natural scenes may be described in terms of two areas of interest: the foreground and the background. The foreground is defined here as that portion of the scene between the sensor and the outer boundary where a vehicle may operate. The size of the foliage in the foreground region is constrained to plants and bushes that will not completely obstruct ground-to-ground viewing of a vehicle. The background is defined as the outer boundary of the scene. In the type of terrain emphasized in the Standard Scenes program, the background typically is composed of a treeline of taller vegetation in which the line of sight is no more than several meters.

2.2. The Standard Scene

2.2.1. The Standard Scene Program. The Standard Scene program was established as a data base development effort. Although a large body of thermal background data already exists,[3,4,5] it typically does not include weather data or a detailed characterization of the terrain. Yet, for many applications of interest to the IR community, such information is essential. The Standard Scene program was originated to address this problem by providing simultaneous thermal imagery and weather data for scenes of well-characterized terrain. Of course, there are a great many factors involved in defining and collecting a complete data base, so the Standard Scene program necessarily included some compromises and limitations. For example, the scenes selected for the program have foreground lengths ranging from 300 to 800 meters. In a typical battlefield scenario, distance to the enemy is generally taken as being in the 1 to 8 kilometer range. This is compensated for by the fact that military thermal imagers generally have a narrower field of view than the commercial imagers used in this program; the shorter ranges of the Standard Scenes thus can provide an equivalent length of treeline, while minimizing the problem of atmospheric degradation affecting longer range viewing. Selection of scenes was also limited to areas accessible to the data acquisition vans and target vehicles used in the study. Finally, the data collection effort was also limited to the meteorological conditions that occurred on test days. A very good range of weather conditions was acquired,

overall, but getting a full range of conditions for each scene would have been beyond the scope of the project.

2.2.2. The Standard Scene Environment. Each standard scene is located within the general area of the Keweenaw Research Center (KRC) which operates out of the Keweenaw Field Station located in the Houghton County Memorial Airpark, in the northern part of Michigan's Upper Peninsula. The area in the vicinity of the Keweenaw Research Center is characterized by a low human population density, varied terrain, and a seasonal climate that exhibits a wide variety of meteorological conditions.

2.2.3. Data Base Development. Natural scenes were selected and characterized in terms of their individual topography, soil and vegetation type. For each scene, calibrated thermal imagery was recorded on a diurnal basis, i.e., once each hour for a twenty-four hour period. Sets of thermal imagery were recorded for each scene at different times of the year in order to include information about seasonal variations in IR properties of natural scenes.

Nearly every field test in the Standard Scene Program also includes supplementary thermal imagery showing reference "targets" (ground vehicles) positioned in the standard scene. This imagery is useful in the analysis of vehicular IR signatures and thermal contrasts against well-characterized backgrounds. Reference vehicles used in various field tests included a jeep with visual camouflage paint markings, an M113-APC (Armored Personnel Carrier), an M60, and a Bradley M2-IFV (Infantry Fighting Vehicle).

This extensive set of data is compiled into a data base structure that may be used by the IR community as a validation tool in thermal modeling. The Standard Scenes data base can also serve as an analytical data source in efforts to better understand the thermal physics within natural scenes.

On the basis of climatological comparisons between Houghton County and the Giessen/Fulda region of West Germany[6], it may be concluded that significant similarities exist between the climates of these regions. The standard scene data may therefore be used to simulate West German climates and backgrounds.

2.2.4. Supporting Weather Data. Meteorological variables significantly influence thermal behaviour of natural scenes. In addition to characterizing the physical features of the scene, it is important to track changes in time-dependent factors that may aid in predicting changes in IR images of

the scene. All thermal imagery of standard scenes is therefore supported by an extensive on-site meteorological characterization, which is collected using a portable weather station. Observations for many of the meteorological variables are recorded at five minute intervals throughout the 24-hour period covered by the field test. Additional weather data, recorded hourly, are collected from the NOAA (National Oceanic and Atmospheric Administration) Flight Service Station at the Houghton County Memorial Airport.

2.3. Clutter

2.3.1. Clutter Definition. Thermal clutter is a function of the magnitude, spatial variations, and radiance variations of the background imagery relative to a target of interest. In this context, note that "background imagery" includes any part of the imagery that is not a target. Since the IR signature of both target and background changes across time and changing environmental conditions, the concept of clutter is also time-dependent. It would be desirable to have a measure that would characterize scene clutter at a given time. It would, furthermore, be useful if the measure correlated well with easily measured temporal or physical variables that influence the IR characteristics of target and background. Generalizations or predictions of the "state" of scene clutter under given conditions could then be made.

2.3.2. Selected Clutter Metrics. Two related image metrics were selected as being the most illustrative of the changing nature of thermal clutter as pertinent to a human observer using an infrared imager. Using Standard Scenes thermal imagery, this report examines these scene metrics and how they correlate to and range with meteorological conditions present at the time the imagery was obtained. These metrics were employed to evaluate the thermal clutter characteristics of the standard scenes under the several seasonal variations recorded as part of this program. The probability of detection of a target versus the Signal to Clutter Ratio (SCR), as will be defined in Section 5.8.1, has also been investigated[7].

3.0. OBJECTIVES

3.1. Standard Scene Characterization

The basic objective of this project was to establish the Standard Scene test sites and thoroughly document them. Physical characterization of the scenes consists of detailing: scene orientation, location, and layout; topography; vegetative cover and content; and soil type. This characterization results in a well defined area in which

controlled thermal measurement and analysis can be accomplished.

3.2. Thermal Imagery Documentation

Infrared imagery for all Standard Scenes was to be recorded under varying seasonal and meteorological conditions and incorporated to a comprehensive data base package. This data base was conceived to include accessible temperature frames for each scene, supported with coinciding meteorological documentation, topographical mapping, and botanical and geological surveys. Data would be formatted or reformatted as necessary to make it amenable to various applications of interest to the IR community, which would conceivably include thermal modeling, scene simulation, validation, and the evaluation of image metrics used to train automatic target recognizer (ATR) algorithms.

3.3. Aids to Radiometric Prediction

Having obtained a large body of thermal imagery from well-characterized scenes, it was considered possible to relate meteorological and scene variables to the radiometric properties of the image. This opens the possibility of developing background signature models that describe or predict changes in radiometric properties of natural scenes as a function of weather and seasonal inputs. In the context of the Standard Scene program, clutter metrics were to be selected and investigated to determine whether they correlated significantly with measured scene parameters.

3.4. Development of Thermal Clutter Computer Programs

The investigation of the relationship, if any, between image clutter and measured scene parameters requires the development of computer programs to calculate scene statistics and clutter metrics from digitized temperature maps of the thermal imagery and to compute correlations or other measures of association between the clutter value and variables of interest. Computer programs for characterizing or predicting thermal clutter based on the imagery observations would also be considered.

4.0. CONCLUSION

4.1. Standard Scene Data

The thermal imagery data base for Standard Scenes has been established and is described in detail in Appendix A. The supporting documentation for each scene includes complete meteorological data, topographical, geological and botanical

maps. Imagery and supporting data have been organized into formats that should be compatible with or easily adaptable to formats currently in use in the IR modeling community.

4.2. Thermal Background Models

4.2.1. Model Development. Thermal background models have been developed to predict the thermal behavior of the terrain and of the vegetative canopy in the foreground. A detailed discussion regarding mathematical representations used in the models, the model structure, and validation data were given in the interim Standard Scene report[8].

4.2.2. PRISM Implementation. The terrain and canopy thermal models have been incorporated to the TACOM/KRC Physically Reasonable Infrared Signature Model (PRISM). PRISM Version 2.0 fully implements these models as subroutines and, given the required initial inputs, automatically predicts terrain temperature in a way that takes into account both soil and vegetation properties. Details on these subroutines and their associated input files can be obtained by referring to the PRISM user's manual[9].

4.3. Results of Clutter Analysis

4.3.1. Clutter Analysis Summary. Thermal imagery for Standard Scenes I, IV, and V from the 1984 test sequence were used to evaluate the relationship between two clutter measures and scenario parameters. The target, treeline and foreground areas were defined in each image. Clutter and Signal-to-Clutter Ratios (SCR) were then computed separately for the foreground and treeline areas.

The computed clutter measure C was deemed to be consistent with the interpretation of a human observer, i.e., imagery that is highly cluttered in appearance yields clutter values that are high. During periods of low perceived clutter, e.g., late night, the clutter values are also low. For the observation ranges typical in Standard Scene imagery, the clutter measure C has different values for separate background components; it is for this reason that foreground and treeline clutter values have here been analyzed separately.

4.3.2. Correlation of Clutter and Scenario Parameters. The temperatures of target and background are highly dependent on scenario parameters, e.g., weather and time. Clutter measures computed for image foreground and treeline are also dependent on these parameters. The clutter in the scenes presented can be reasonably well explained by the values of the following independent variables: solar irradiance, humidity, time of

day and wind speed. The actual independent variables which are important and their order of importance depends upon whether one is looking at a treeline or earthy foreground. There is a correlation between SCR and clutter in both treeline and foreground during daylight hours. However, the SCR variation during night time is too random to correlate well with clutter.

4.4. Spectral Analysis and Probability Distributions. Power spectral densities and probability densities were computed for a selected subset of standard scenes thermal imagery. In the spatial domain, frequency distributions of pixel temperature values were used to define the probability density function (PDF) of temperatures for the treeline and foreground regions, respectively, of each thermal image. Multimodal, skewed distributions were observed, particularly during afternoon hours when the temperature range was greatest. This suggests that non-Gaussian distributions may be applicable to temperatures in natural scenes. The presence of multiple modes conceivably relates to heterogeneous scene composition. In the frequency domain, the spectral content of images was evaluated across time to provide information about the relative stationarity of the signal.

5.0. DISCUSSION

The Standard Scenes Program developed in three distinct phases of effort. The first, groundwork phase involved defining the criteria for the scenes to be included in the study and selecting sites that met those criteria. Section 5.1 below describes the Standard Scene selection process. Once selected, each Standard Scene was surveyed and its soil, vegetation and physical features analyzed and inventoried in order to characterize the scene. Scene characterization is described in Sections 5.2 through 5.4, below. Finally, a sequence of field tests was performed at each Standard Scene. Each field test involved collecting thermal imagery of the scene, itself, plus a reference vehicle, concurrently with measurements of meteorological and other time-dependent variables that would conceivably influence the infrared characteristics of the scene. Sections 5.5 and 5.6 provide descriptions of the imagery and data collected during Standard Scene field tests.

5.1. Standard Scene Selection

The scenes that were chosen for this program have foreground lengths ranging from 300 to 800 meters. The scene foregrounds are relatively flat, with a maximum elevation change of approximately 14 meters, and open. Vegetation in the foreground areas ranges from low mosses and grasses, to

shrubs of varying heights and small trees. Some scene foregrounds also include areas of bare soil or sand. The type and uniformity of foliage in the foreground was one consideration in scene selection, as was the type of trees (deciduous or coniferous) in the background. The background is generally composed of taller wooded vegetation in which the line of sight is no more than several meters. The viewing direction was of concern in the scene selection because of the dynamics of solar heating during diurnal cycles, especially in treelines. It was also necessary to have scenes that are accessible to vehicles, inasmuch as data acquisition vans and reference target vehicles must be able to reach and maneuver in the vicinity of the site.

5.2. Standard Scene Description

All standard scenes were surveyed and mapped in terms of their topography, elevation, soils, and vegetation. Figures 5-1 through 5-4 show maps prepared for Standard Scene I; maps and details of the botanical and geophysical surveys for all scenes can be found in Appendix A. A brief description of each scene is provided in the following sections. The centerline in each scene is physically defined by the placement of permanent markers. Standard Scenes I through V are located in the vicinity of the KRC main installation; Standard Scene VI is at a remote site approximately 30 miles away from KRC.

5.2.1. Standard Scene I. Scene I has a 39^{o} field of view, with a centerline viewing direction of 2^{o} from north. The background is a deciduous treeline, and the foreground is composed of several different vegetation types, occurring in patches. Areas of bare earth are also visible, along with rocks up to 10 centimeters (cm) in diameter. The terrain is undulating, with a 5 meter (m) peak-to-valley maximum. Figures 5-5 and 5-6 are visible photographs of Standard Scene I taken during the October 1986 test procedures.

5.2.2. Standard Scene II. Scene II is a southward-looking view of Scene I, so it shares the same foreground. The field of view is 28^{o}, with a centerline viewing direction of 191.6^{o} from north. The background is also a deciduous treeline. Figures 5-7 and 5-8 are October 1986 photographs of Standard Scene II.

5.2.3. Standard Scene III. Scene III is a southwest view of the same foreground terrain, using the same viewpoint as Scene II, and looking at the side of a hill 15 m high which has patches of disturbed soil. The field of view is 40^{o} from north. The background is a deciduous treeline. Figures 5-9 and 5-10 again show October 1986 photographs of this scene.

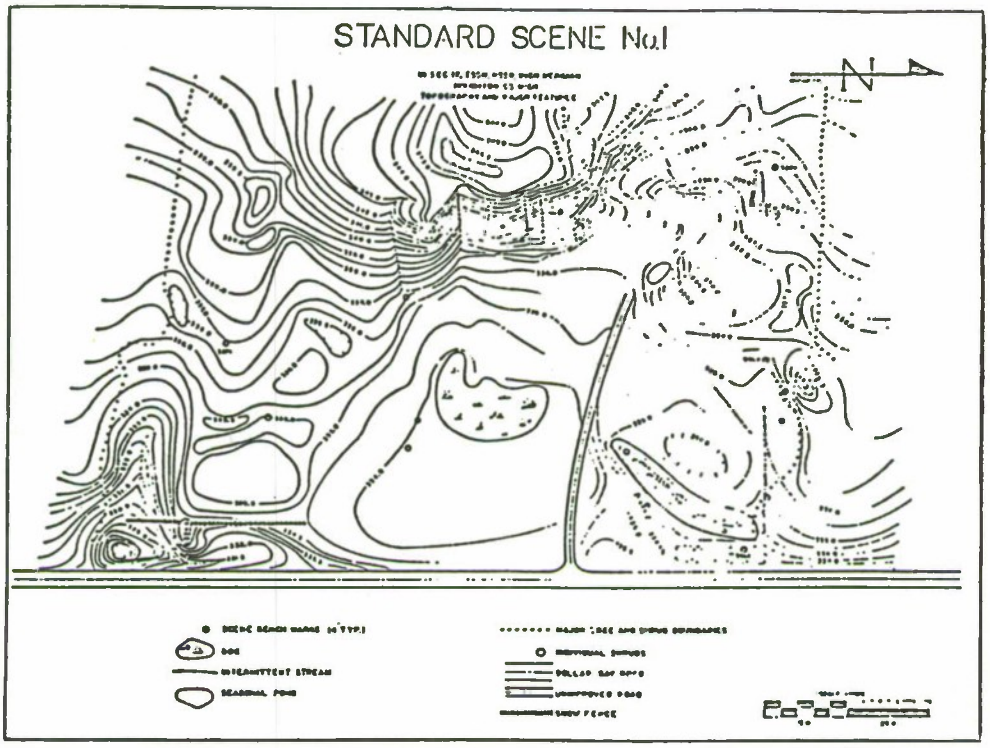

Figure 5-1. Standard Scene I Topographical Map

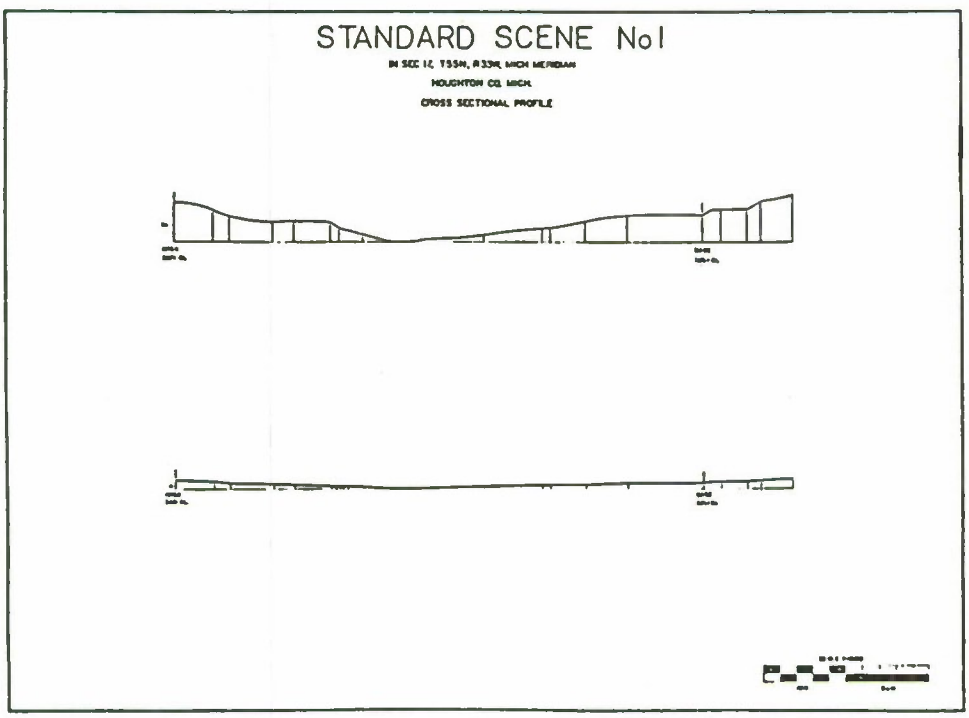

Figure 5-2. Standard Scene I Cross-sectional Elevation Map

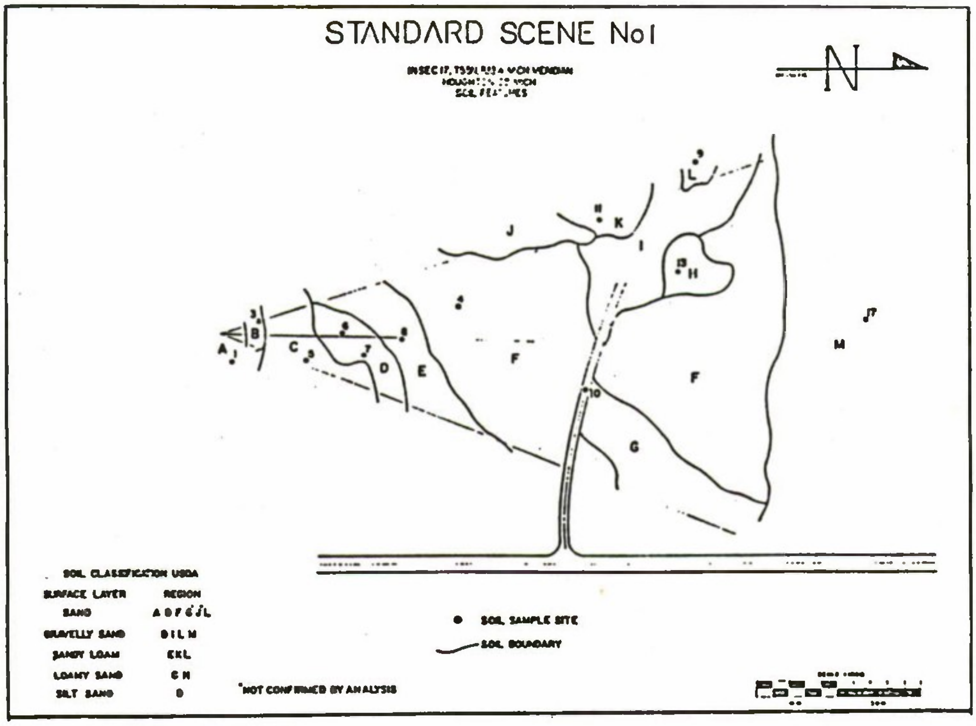

Figure 5-3. Standard Scene I Soil Classification Map

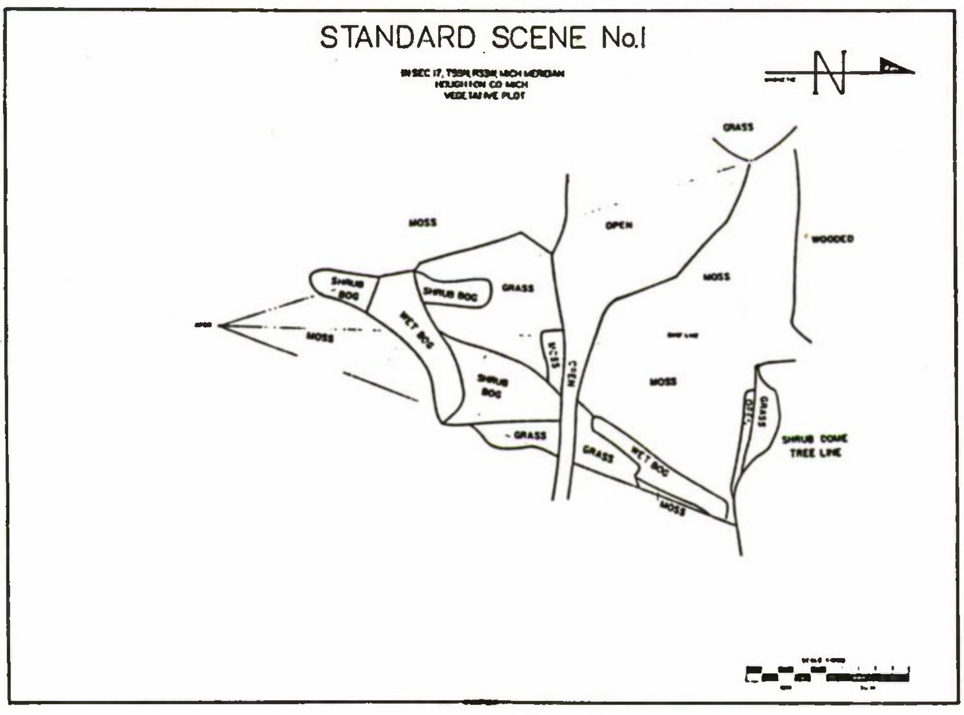

Figure 5-4. Standard Scene I Vegetation Map

Figure 5-5. Standard Scene I, with M113-APC

Figure 5-6. Standard Scene I, detail, with M2

Figure 5-7. Standard Scene II, with M113-APC

Figure 5-8. Standard Scene II, mossy foreground, West edge

Figure 5-9. Standard Scene III, with black bodies and jeep

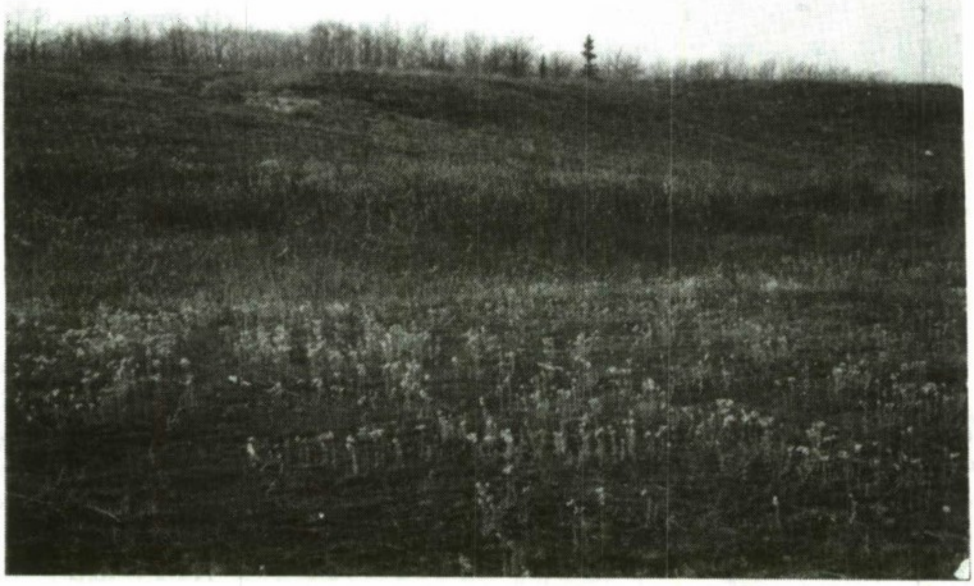

Figure 5-10. Standard Scene III, view of ridge

5.2.4. Standard Scene IV. Scene IV has a viewing direction due east, on flat terrain. The centerline viewing direction is 98.9^{o} from north and the field of view is 14^{o}. Vegetation consists of tall grass and scattered bushes (mainly tag alder). No bare earth or rock is visible. No clear distinction between foreground and background is possible in Standard Scene IV, because of the tall, dense shrubbery present in the scene. At a range of a few hundred meters, viewing is effectively obscured in any direction within the scene's field of view. Figures 5-11 and 5-12 provide fall and spring photographs of Standard Scene IV.

5.2.5. Standard Scene V. Scene V is a view along a dirt trail, looking south. The field of view is 2^{o} with the centerline viewing direction of 181^{o} from north. The trail is visible for 750 m, making this the scene with the longest unobstructed view. Vegetation consists of deciduous bushes 3 to 5 meters high along both sides of the trail in the foreground, and taller deciduous vegetation in the background. The viewpoint is on a rise 5 meters high. Figures 5-13 and 5-14 show the visual detail of this standard scene.

5.2.6. Standard Scene VI. Scene VI features a coniferous treeline viewed toward the west. The field of view for this scene is defined by the capability of the imager used; however, the centerline viewing direction is set at 175.4^{o} from north.

The foreground is a very uniform field which is mowed twice per year. The unique attribute of Scene VI is that the image recording position is 30 m above ground providing a 10.5^{o} look-down point of view to the base of the background treeline 89 m away. Figures 5-15 and 5-16 are photographs of Standard Scene VI as seen from the tower, and of the tower facility itself.

5.2.7. Summary of Scenes. Table 5-1 provides a table summary of salient physical characteristics and composition of the standard scenes.

5.3. Soil Analysis

Whether exposed or covered with a vegetative canopy, the soil plays an important role in the thermal dynamics of the Standard Scene. It is therefore important that the soil be characterized, and its properties taken into account. A soil analysis was made at several locations within each of the Standard Scene areas. Several sample bore holes at each scene were analyzed to determine soil particle-size distribution. This characterization was accomplished using

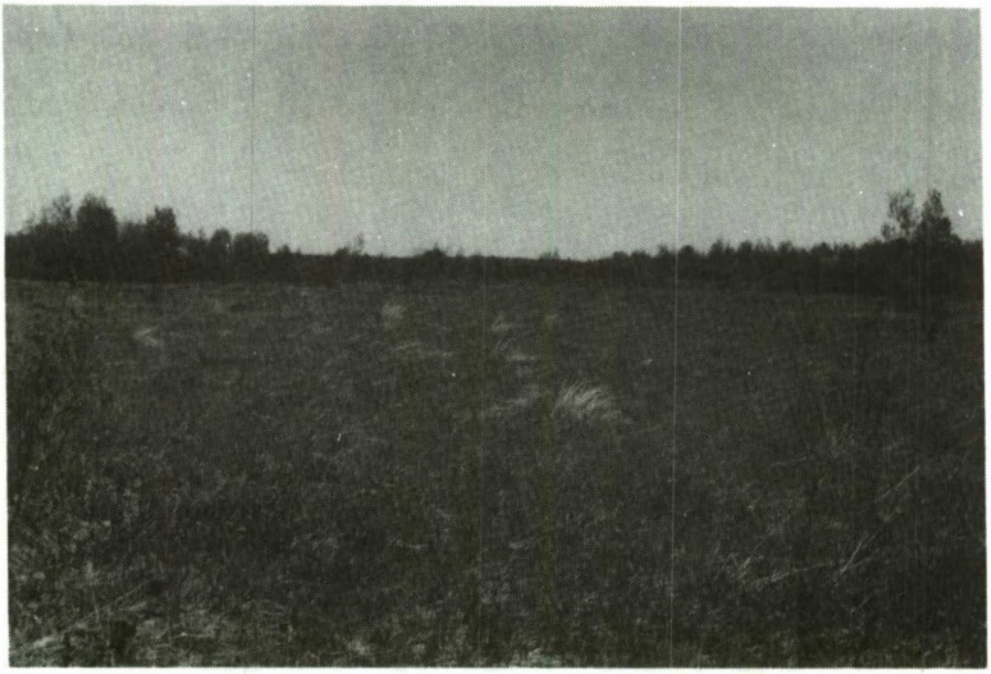

Figure 5-11. Standard Scene IV, Spring

Figure 5-12. Standard Scene IV, with black bodies, Autumn

Figure 5-13. Standard Scene V, with M113-APC, Spring

Figure 5-14. Standard Scene V, with black bodies, Autumn

Figure 5-15. Standard Scene VI, viewed from tower

Figure 5-16. Standard Scene VI Tower Facility

Table 5-1. Summary: Standard Scenes Characterization

SCENE	DIRECTION OF VIEW	RANGE TO TREELINE	TREELINE TYPE/HEIGHT	FOREGROUND COMPOSITION	SOIL COMPOSITION
I[1]	2°	360 m	Deciduous 10-15 m	Grasses Shrubs, Moss	Sand
II[1]	192°	380 m	Deciduous 10-15 m	Grasses Shrubs, Moss	Sand Loamy sand
III[1]	240°	280 m	Deciduous 10-15 m	Grasses Shrubs, Moss	Gravelly sand Sand
IV	99°	170 m	Deciduous 3- 5 m	Grasses High bushes	Loamy sand Sand
V[2]	18°	873 m	Deciduous 3-15 m	Grass Dirt Road	Gravelly sand Sand
VI[3]	175°	217 m*	Deciduous 8-10 m	Grasses Clover	Loamy Sand Sand

Notes:
1 Scenes I, II, and III look across same field.
2 Dirt road runs through center of Scene V.
3 Scene VI observed from 30m high tower (8° slant angle)
* Slant range.

standard American Society for Testing and Materials (ASTM) Sieve and Hydrometer analysis procedures.

5.3.1. General Procedure. A bore sample 50 cm deep is taken at each of several locations within the standard scene. The analysis is performed on soil from the top section of the sample and again on soil from the bottom section. In addition to determining the soil particle size, the soil type is defined using the United States Department of Agriculture Textural Classification system. Table 5-2 lists a summary of the results of the Sieve and Hydrometer analysis for each Standard Scene.

5.4. Vegetative Survey

A complete vegetation inventory was made of the Standard Scenes using the Step-point Transect Method. This method was adapted from the Soil-Vegetation Inventory Methods used by the Bureau of Land Management[10] in extensive range inventories conducted throughout the Western United States. The Step-Point Transect Method involves traversing a vegetative community type across its longest axis, thus defining a transect or sample area in the form of a long strip. Information about the ground cover is recorded at each point, or pace. A more thorough characterization of plant types and development is made every 10 toe-points along the transect line. The goal of the Step-point Transect Method is to select the minimum number of transects needed to adequately characterize existing vegetation within each community type in a given scene.

5.4.1. Surveying Procedure. The survey that was carried out consisted of the complete standard scene area being divided into transected areas and further subdivided into 1 square meter plots. As may be noted in the vegetation maps in Appendix A, the survey extended past the standard scene area into areas seen beyond the standard scene range line. Each plot was thoroughly characterized as follows:

a) Each plant is identified and recorded according to genus and species
b) Each plant is given a stratification symbol
   - S - shrubs
   - H - herbaceous forbs
   - G - grass and grasslike plants
   - M - mosses
   - B - bare ground or rocks
   - L - litter (any organic ground cover not fitting in other categories)
c) Each plant's phenological state of development was recorded.

Table 5-2. Sieve and Hydrometer Analysis

Scene	Hole	Soil Description	Gravel	Sand	Silt	Clay
1,2	8a	Sandy Loam	10.1	58.5	40.9	0.6
1,3	9	Loamy Sand	4.0	82.3	17.0	0.6
1,3	8	Sandy loam	10.14	58.5	40.9	0.6
1,2	6b	Sand	10.4	93.5	6.3	0.2
1,2	5 top	Sandy Loam	0.8	69.8	30.2	0.0
1,2	4	Sand	0.7	98.3	1.7	0.0
1,2	4	Silt Loam	.75	24.7	72.2	1.1
1,2	5 top	Clay Loam	18.17	92.6	7.4	0.0
1,2	5b	Loamy Sand	0.66	85.1	14.5	0.4
1,3	6a top	Gravelly Sand	25.21	95.85	4.15	0.0
1,3	6a bottom	Gravelly Sand	23.5	91.8	6.8	1.4
1,2,3	17	Gravelly Sand	67.5	94.2	5.4	.4
1,2	1a top	Gravelly Sand	48.92	94.64	5.36	0.0
1,2	1a bottom	Fine sand	.99	99.35	.65	0.0
1	2 top	Gravely sand	30.58	93.1	6.0	0.9
1	2 bottom	Clay Loam	7.28	52.7	45.35	1.94
1	3a top	Loamy Sand	0.42	95.0	5.0	0.0

TABLE 5-2. Sieve and Hydrometer Analysis, Continued

Scene	Hole	Soil Description	Gravel	Sand	Silt	Clay
1	3a bottom	Sand	0.93	98.1	1.9	0.0
1	3b top	Sandy Loam	18.0	80.0	20.0	0.0
1	3b bottom	Sand Loam	.4	90.5	9.5	0.0
3	15	Clay Loam				
3	15	Sandy Loam	4.4	89.4	10.5	0.1
3	15	Sandy Gravel	2.1	63.9	35.9	.2
4	2 top	Sand	12.2	90.4	8.2	1.4
4	1 top	Sandy Loam	11.7	86.6	13.0	0.4
4	1 bottom	Sandy Loam	15.2	82.5	13.8	3.7
5	1 top	Sandy Loam	10.5	81.6	16.4	2.0
5	2 bottom	Loamy Sand	8.8	87.9	10.7	1.4
5	3 bottom	Sandy Loam	11.8	84.9	15.1	0.0
5	4	Sandy Clay Loam	1.7	69.0	31.0	0.0
6	1 bottom	Loamy Sand	14.3	84.6	14.2	1.2
6	2 top	Loamy Sand	60.0	85.9	13.3	.8
6	2 bottom	Sand Clay Loam	10.1	72.3	7.1	.6
6	1 top	Loamy Sand	11.8	85.1	13.6	1.2

1 - beginning growth
2 - vegetation stage
3 - mature (flowering or fruiting)
4 - seed ripe
5 - dormant

d) Measure and record average height for each species
e) Count and record number of plants per unit area by species
f) Measure and record percent cover per species using the Line Intercept Method[11].

Tables 5-3, 5-4, and 5-5 summarize the results of the vegetation inventory taken at Standard Scenes I, II, and III, respectively. As an example of the plant types that were encountered in the study, Table 5-6 is a listing, by species, of those plants that were found in Standard Scene I, transect 5. Transect 5 is located roughly in the center of Standard Scene I. This same detailed analysis is available for each transect survey at each of the standard scenes shown above.

Photographic documentation includes a general view of each transect, taken at the beginning of the transect run. For each plot (5 plots are generally done along each transect line), vertical and horizontal photographs are taken. Plot label forms are displayed in each photograph to identify it. Figures 5-17 and 5-18 are examples of the photographs of transection areas used to identify and map botanical characteristics of each standard scene.

Such a detailed survey is not considered necessary for most infrared applications. A general survey that includes treeline and shrub studies as well as generic ground cover vegetation density measurements would be sufficient to properly characterize a scene for the purposes of infrared study.

5.5. Image Recording

All standard scene data is recorded on a diurnal basis with an image recorded on the hour for 24 hours. Each image is recorded on VHS format video tape for a time period of about 30 seconds. After the target image is recorded, the imaging system is aimed (with no changes in sensitivity or black level) at an ambient temperature blackbody and its image is also recorded, again for about 30 seconds. The temperature of the black body is recorded for use as a reference body in image calibration. The calibration isotherm curves for this model were measured at the factory and were used in conjunction with a blackbody standard to convert each pixel to its corresponding radiance or equivalent blackbody temperature.

Table 5-3. Vegetation Inventory: Standard Scene I

Vegetation Type	Standard Scene to Rangeline: M^2 Area	Standard Scene to Rangeline: % Total to Range	Extension (Beyond Range): M^2 Area	Extension (Beyond Range): % Total in Exten.
Disturbed grass	6326.93	17.5	812.81	6.6
Moss dominate	15853.10	43.9	4935.40	40.4
Shrub-bog	3530.86	9.8		
Open	7237.28	20.1	448.67	3.7
Treeline			2236.86	18.3
Wet Bog	3127.70	8.7	13.00	.01
Shrub line			3777.95	30.9

Treeline Heights

Composition: Oldeiz populus tremuloides, acer saccharum, understory of ostrya virginiana, acer saplings

height:

height:	Populus	14-16 m
	Pinus	
	Acer	11-14m
	Quercus	
	Shrubline	3.5m

Table 5-4. Vegetation Inventory: Standard Scene II

Vegetation Type	Standard Scene to Rangeline: M^2 Area	Standard Scene to Rangeline: % Total to Range	Extension (Beyond Range): M^2 Area	Extension (Beyond Range): % Total in Exten.
Disturbed grass	2900.12	9.9	3654.40	29.2
Moss dominate	19858.64	67.7	3855.98	30.8
Shrub-bog	3647.90	12.4		
Open	676.26	2.3		
Treeline			3283.76	26.3
Wet Bog	2269.37	7.7		
Shrub line			1716.66	13.7

Treeline Heights

Composition: Acer saccharum, scattered old populus tremuloides, understory of ostrya virginiana and acer samplings (small clearing with fraxinus and betula

height:
- Populus 13-15m
- Pinus
- Acer 11-14m
- Quercus
- Shrubline

Table 5-5. Vegetation Inventory: Standard Scene III

Vegetation Type	Standard Scene to Rangeline: M^2 Area	Standard Scene to Rangeline: % Total to Range	Extension (Beyond Range): M^2 Area	Extension (Beyond Range): % Total in Exten.
Disturbed grass	4688.30	19.2	4278.65	31.1
Moss dominate	9129.51	37.4	2087.30	15.1
Open	10605.58	43.4	318.62	2.3
Treeline			7087.72	51.5

Treeline Heights

Composition: Pinus strobus, populus tremuloids, acer saccharum, quercus rubrum, understory of thuja occidentalis, abies, balsamca and saplings

height:

Populus	12-15m
Pinus	14-17m
Acer	12-14m
Quercus	11-14m
Shrubline	

Table 5-6. Plant Species Listing for Standard Scene I Transect 5

SS #1 Transect 5
Plot 1,2,3

Plantago lanceolata	English/lanceleaf plaintain	Herbaceous

****

triflorium pratense	red clover	herbaceous
melilotus officinalis	sweet clover	herbaceous
hieracium spp.	hawkweed	herbaceous
chrysanthemum spp.	chrysanthemum	herbaceous
aster spp.	aster	herbaceous
carex spp.	sedge	grass
agrostis spp.	tickle grass	grass
poa compressa	Canada bluegrass	grass
moss		
litter		
fragaria virginiana	common strawberry	herbaceous
bromus spp.	brom	herbaceous
achillea millefolium	yarrow	herbaceous
chrysanthemum leucanthemum	Qx-eye daisy	herbaceous
trifolium repens	white clover	herbaceous
habenaria spp.	tway blade	herbaceous

Figure 5-17. Horizontal Photograph of Transect 1, Plot 4
Standard Scene I

Figure 5-18. Horizontal Photograph of Transect 6, Plot 4
Standard Scene I

5.5.1. Summary of Standard Scene Imagery. Diurnal thermal imagery for the Standard Scene program was collected across four years - 1983 through 1986 - and for three different seasons. Table 5-7 is a summary of the thermal IR data that was generated over the course of this program, including information on the seasons in each year which imagery covers and the reference vehicles imaged in each scene. As an example of the imagery recorded for each Standard Scene during each test year, a 24-hour sequence of thermal IR pictures from the October 1986 test in Standard Scene V is depicted in Figures 5-19 through 5-41.

The 1983 and 1985 Standard Scene data acquisition program was conducted by OptiMetrics, Inc.; their test reports are provided in Appendix B. However, no weather data was recorded during the 1983 testing activity; hence, the 1983 test is considered inconsistent with the Standard Scene program. Therefore, imagery from 1983 has not been reduced to temperature frames and is not included in the Standard Scenes data base package.

5.5.2. Weather Data Summary. During each time period in which thermal imagery of standard scenes is recorded, an extensive set of physical and meteorological measurements is also recorded on-site by a portable weather station. Because of changes and improvements made in the data gathering procedure across the course of the study, data for certain variables is not complete for the entire study. However, data from the various field tests have been organized in as consistent a format as possible.

The weather parameters that are recorded and included as part of the Standard Scene data package are listed below. Solar irradiance data is sampled once per minute; all other quantities are sampled 12 times per hour.

- global solar irradiance (0.285 - 2.8 micrometers)
- longwave incoming radiation (3.0 - 50.0 micrometers)
- air temperature (0,1,2,3, and 5 meters above ground)
- wind speed (0, 2, and 8 meters above ground)
- wind direction (8 meters above ground)
- dew point
- barometric pressure
- soil temperature (0, 1, 5, 10, 20, and 50 cm depths)

Table 5-8 is a listing of the sensor types used as part of the KRC portable weather station and used to collect the data listed above.

Additional weather data are obtained from NOAA (National Oceanic and Atmospheric Administration) surface weather

Table 5-7. Standard Scenes Thermal Frame Inventory

STANDARD SCENE	DATE	TIME	NO. OF FRAMES	TARGET
Contract DAAE07-83-G-R007 D.O. 0006*				
I	11/11-11/12, 1983	1130-1430	85	M60
II	11/15, 1983	1200-1730	14	M60
III	11/15, 1983	1200-1730	5	-
II	11/16, 1983	1000-1700	20	M60
III	11/16, 1983	1000-1700	7	-
IV	11/17, 1983	1300-2230	24	M60
IV	11/18, 1983	0730-1200	6	M60
Contract DAAE07-83-G-R007 D.O. 0018**				
II	07/19-07/20, 1984	0700-0800	52	-
III	07/19-07/20, 1984	0700-0800	52	-
I	07/25-07/26, 1984	0600-0600	75	M2-APC
IV	08/01-08/02, 1984	0600-0600	75	M2-APC
V	08/09-08/10, 1984	0600-0600	25	M2-APC
Contract DAAE07-83-G-R007 D.O. 0024***				
I	05/12-05/13, 1985	0800-0700	23	M113-APC
IV	05/14-05/15, 1985	0800-0800	12	M113-APC
V	05/16-05/17, 1985	0700-0700	32	M113-APC
II	05/18-05/19, 1985	0630-0700	32	M113-APC
III	05/19-05/20, 1985	0800-0700	31	M113-APC
VI	05/21-05/22, 1985	0700-0700	18	M113-APC
Contract DAAE07-85-G-R007 D.O. 0012****				
V	10/21-10/22, 1986	0700-0700	50	M113-APC
IV	10/23-10/24, 1986	0700-0700	25	M113-APC
II	10/27-10/28, 1986	0600-0600	50	M113-APC
III	10/27-10/28, 1986	0600-0600	25	-
I	10/29-10/30, 1986	0600-0600	50	M113-APC
VI	11/04-11/05, 1986	0600-0600	50	M113-APC

Notes: * Hourly weather, incomplete solar irradiance data.

** 48 thermocouples placed on the M2-APC;
right side of M2-APC visible in Scenes I and IV;
front side of M2-APC visible in Scene V.

*** Gaps exist in the imagery;
43 thermocouples placed on the M113-APC.

**** Local time change from EDT to EST after SS IV test.

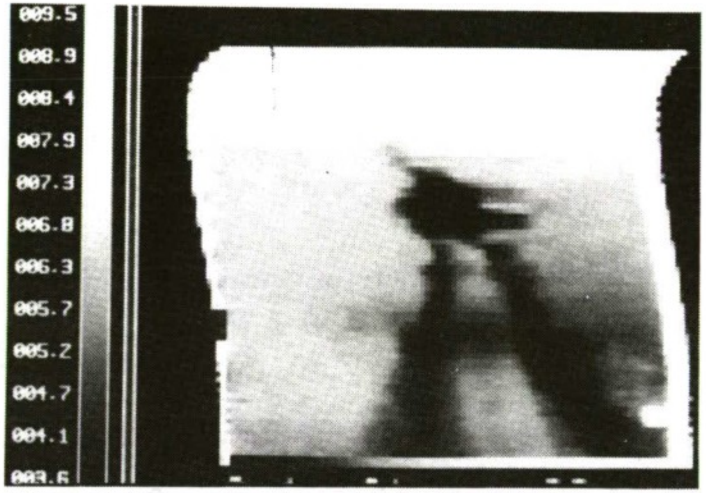

Figure 5-19. Scene V at 0700 hours 10/21/86, Thermal Range 10°

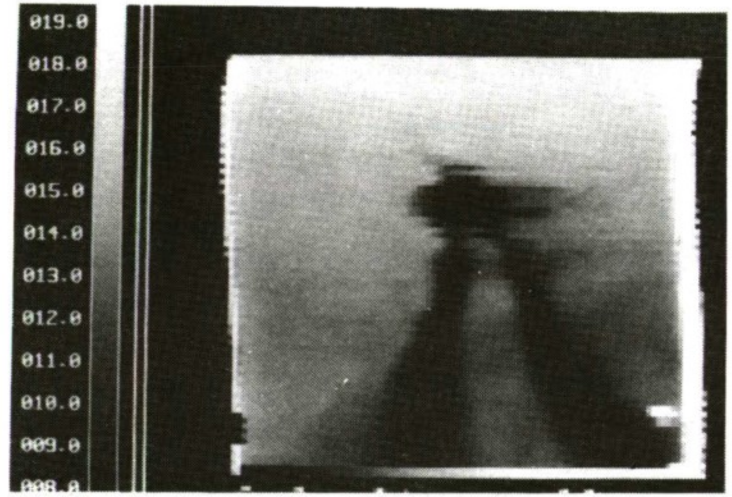

Figure 5-21. Scene V at 0900 hours Thermal Range 20°

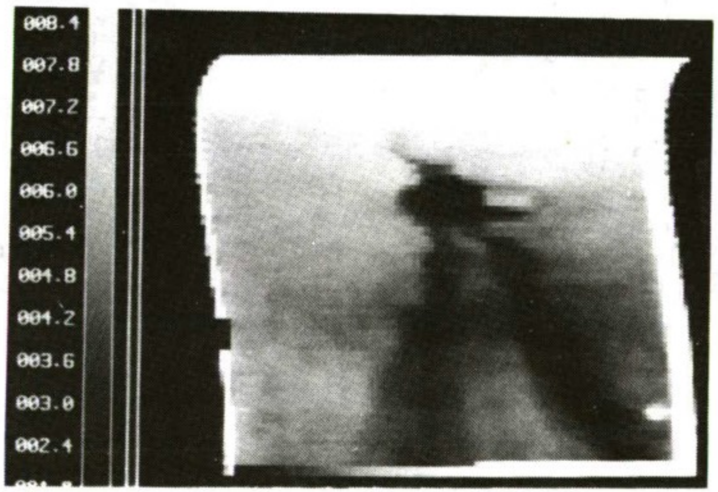

Figure 5-20. Scene V at 0800 hours Thermal Range 10°

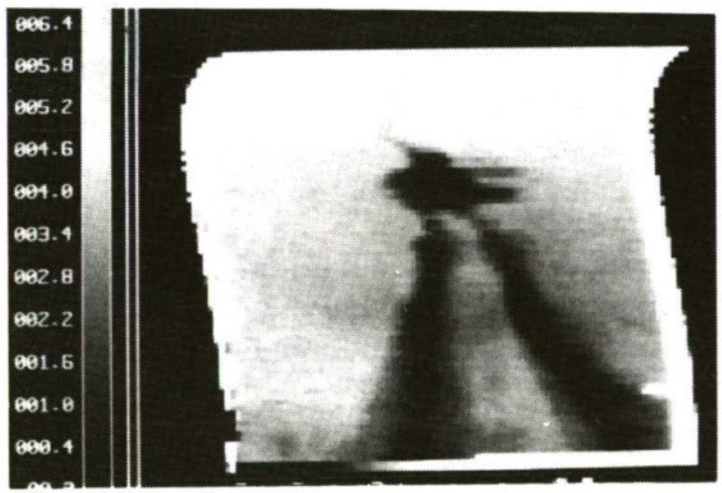

Figure 5-22. Scene V at 1100 hours Thermal Range 20°

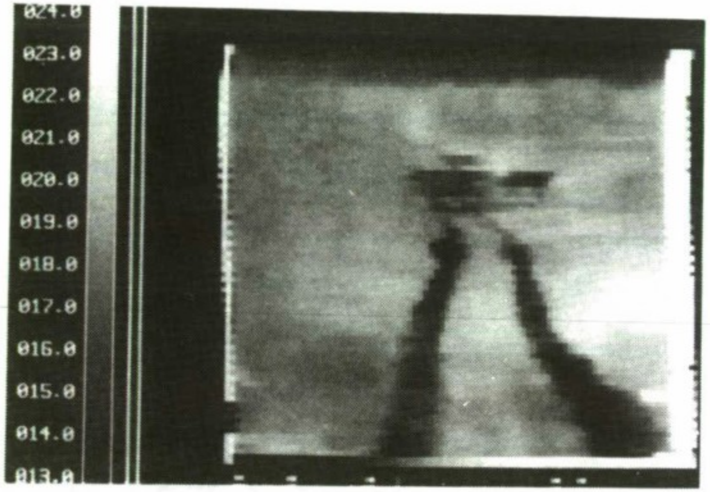

Figure 5-23. Scene V at 1200 hours Thermal Range 20°

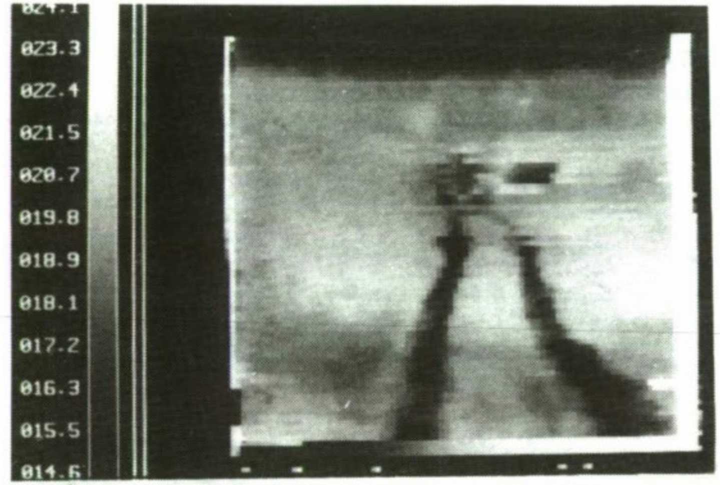

Figure 5-25. Scene V at 1400 hours Thermal Range 20°

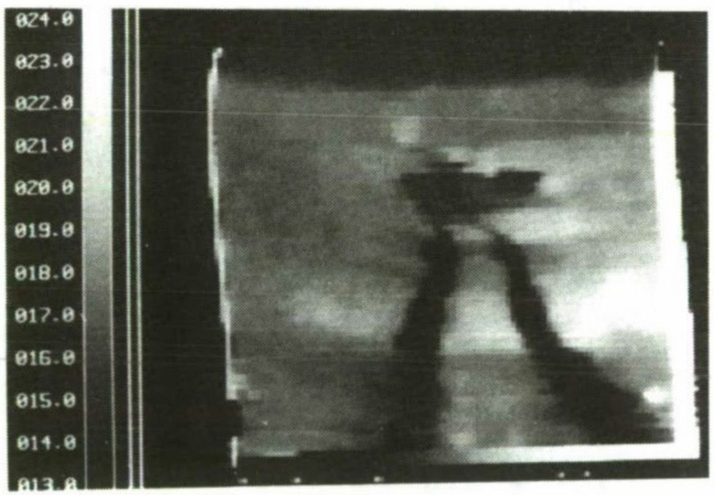

Figure 5-24. Scene V at 1300 hours Thermal Range 20°

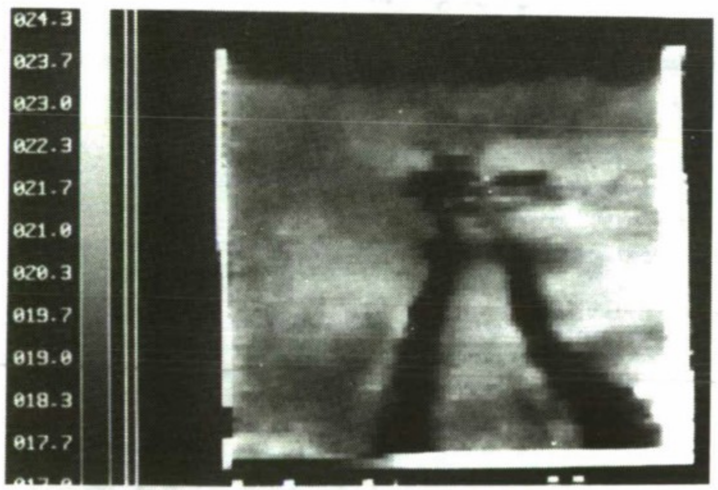

Figure 5-26. Scene V at 1500 hours Thermal Range 20°

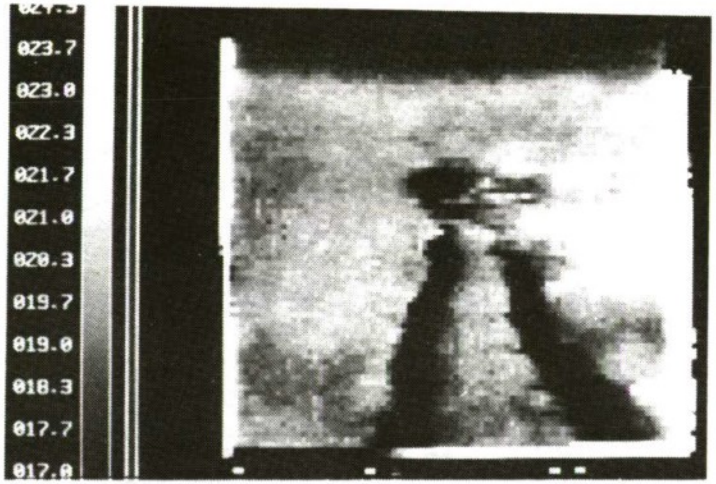

Figure 5-27. Scene V at 1600 hours
Thermal Range 50^{o}

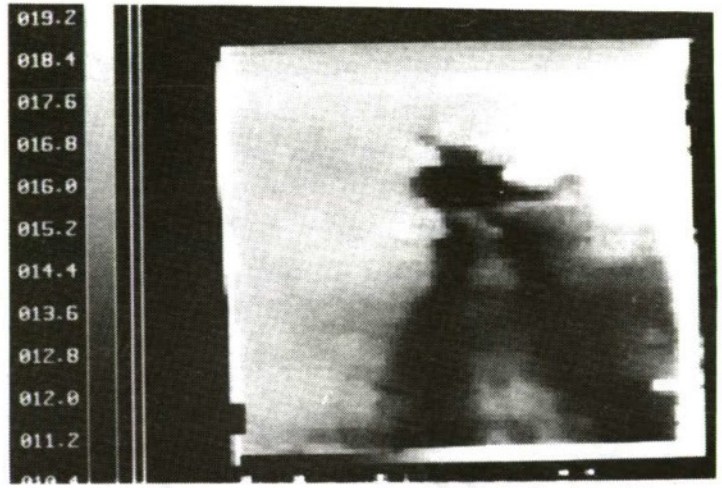

Figure 5-29. Scene V at 1800 hours
Thermal Range 20^{o}

Figure 5-28. Scene V at 1700 hours
Thermal Range 50^{o}

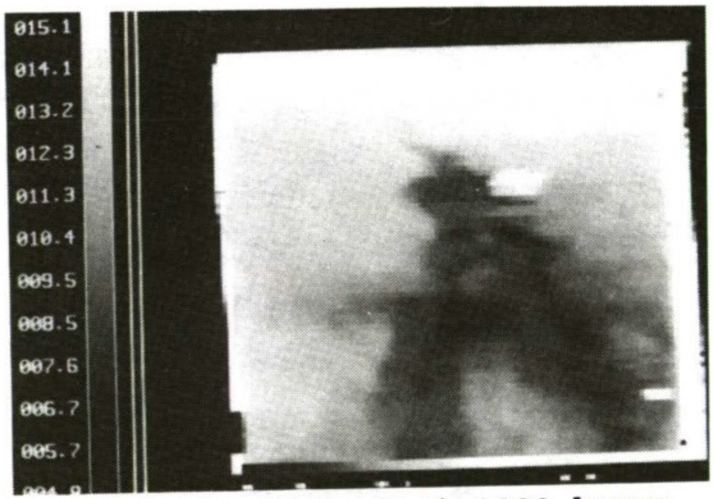

Figure 5-30. Scene V at 1900 hours
Thermal Range 20^{o}

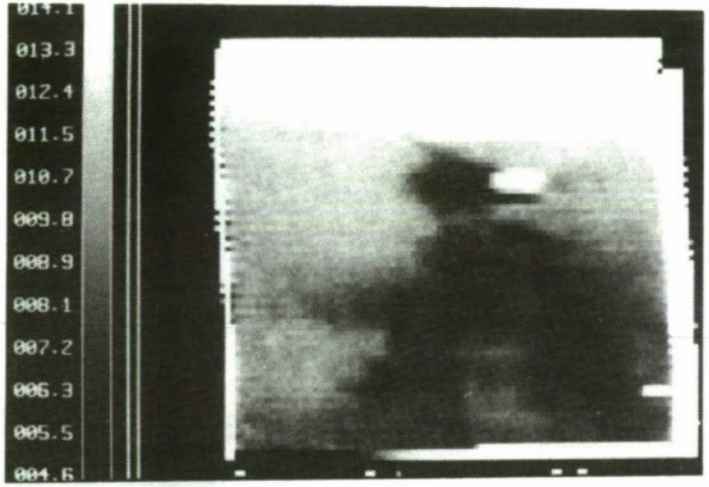

Figure 5-31. Scene V at 2000 hours
Thermal Range 50°

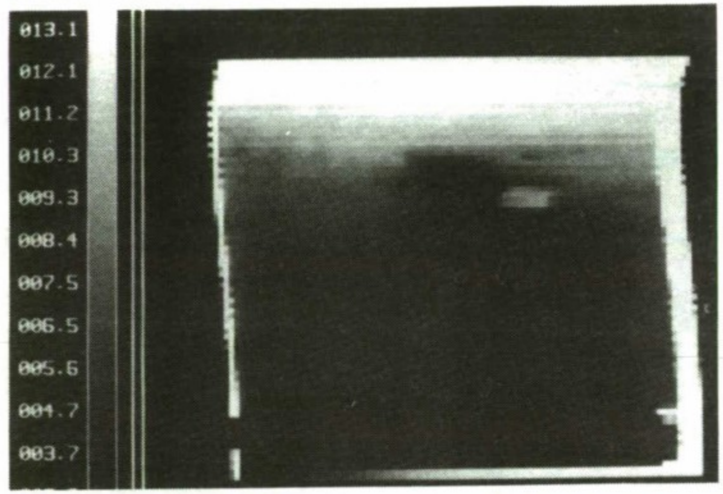

Figure 5-33. Scene V at 2200 hours
Thermal Range 20°

Figure 5-32. Scene V at 2100 hours
Thermal Range 20°

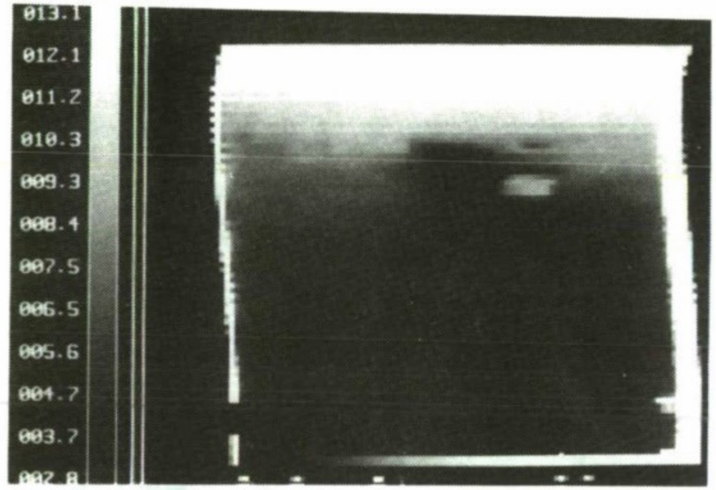

Figure 5-34. Scene V at 2300 hours
Thermal Range 20°

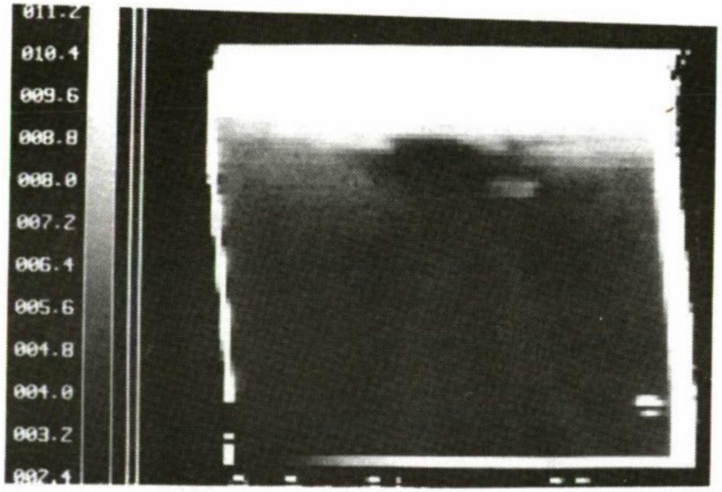

Figure 5-35. Scene V at 0000 hours
10/22/86, Thermal Range 20°

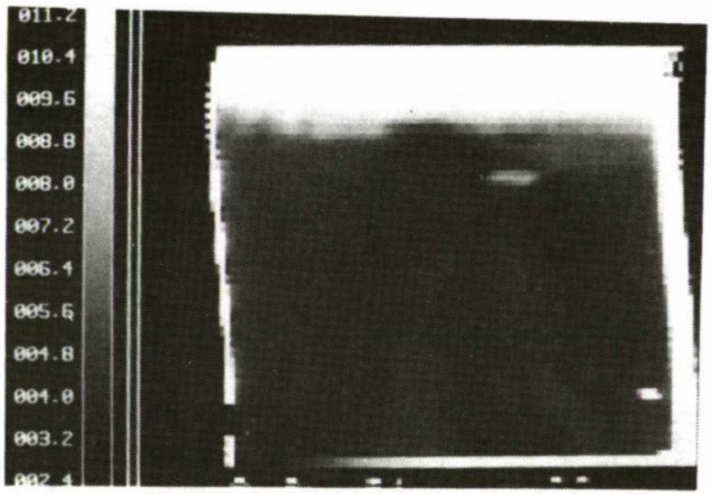

Figure 5-36. Scene V at 0200 hours
Thermal Range 20°

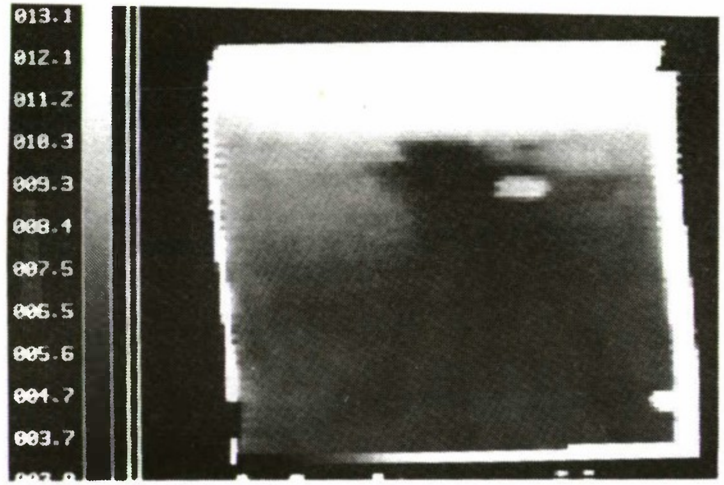

Figure 5-37. Scene V at 0300 hours
Thermal Range 20°

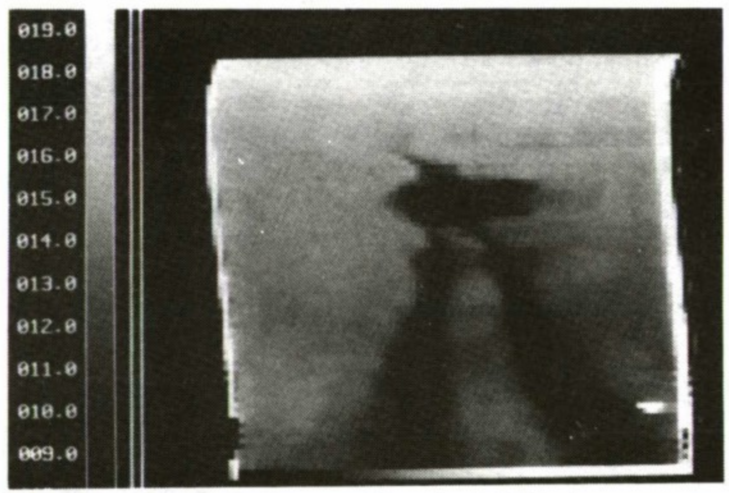

Figure 5-38. Scene V at 0400 hours
Thermal Range 20°

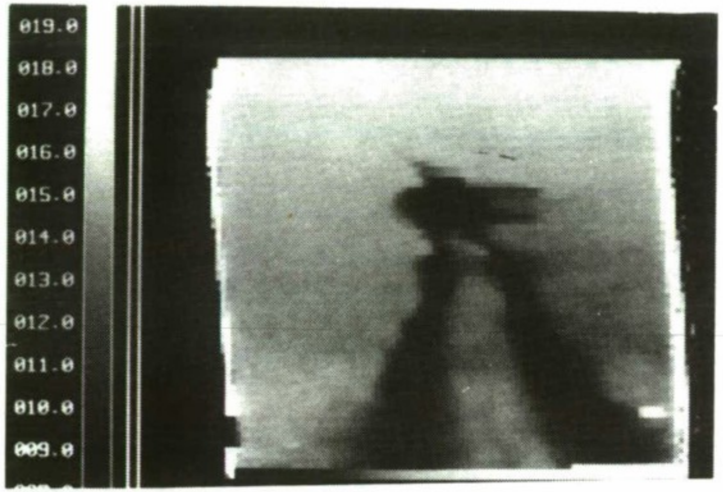

Figure 5-39. Scene V at 0500 hours
Thermal Range 20°

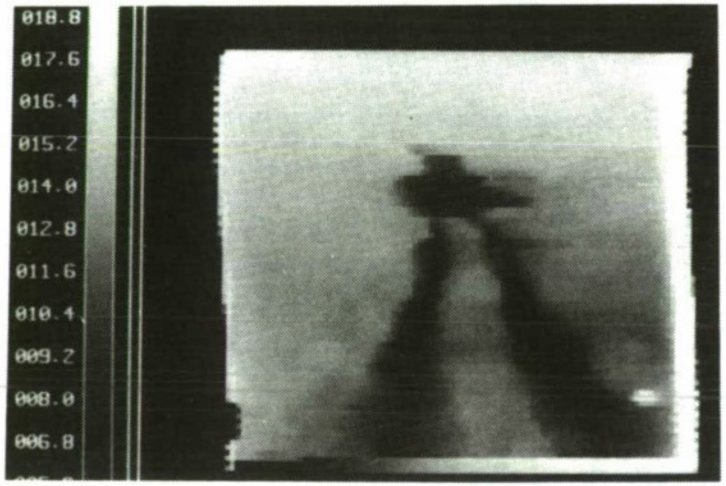

Figure 5-40. Scene V at 0600 hours
Thermal Range 20°

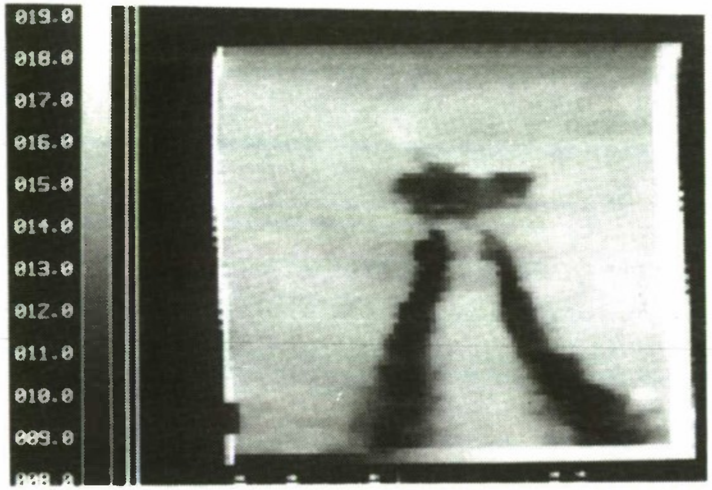

Figure 5-41. Scene V at 0700 hours
Thermal Range 20°

Table 5-8. Standard Scenes Program Automated Weather Acquisition

Sensors and units of measurement are specified for meteorological and physical parameters recorded for the Standard Scenes Program.

Sensors	Measurements
Pyranometer	global solar irradiance (0.285 - 2.8 um) one sample per minute*
Pyrgeometer	longwave incoming irradiance (3 to 50 um)
Shielded type K thermocouple	ambient air temperature profile at 0.1, 1,2,3, and 5 meters above ground plane
Anemometer	wind speed profile at 0.1 and 2 meters above ground plane
Propeller	wind speed profile at 8 meters above ground plane
Vane	wind direction 8 meters above ground plane
Dew point	lithium chloride salt
Barometer	barometric pressure (millibars)
Soil probe	soil temperature profile at 0, 0.01, 0.05, 0.10, 0.20, and 0.50 meter depths

The sensor data are supplemented with hourly NOAA Surface Weather Observations from the Houghton County Memorial Airport.

*All other sensors are sampled 12 times per hour.

observations, which are collected at the Flight Service Station at the Houghton County Memorial Airport. These data are recorded hourly from 0600 to 2200 hours local time on NOAA form MF1-10C, Surface Weather Observations, and include the following information:

- sky condition (National Weather Service abbreviations)
- cloud ceiling (hundreds of feet)
- surface visibility (miles)
- precipitation (inches)
- temperature (^{o} F)
- wind direction (10^{o} increments)
- wind speed (knots)
- total sky cover (tenths)

Several soil samples were also taken at each scene during the 1985 field tests to analyze soil moisture content. For each sample taken, soil was described, and percent moisture determined at the surface and at depths of 1, 5, 10, 25, and 50 cm.

5.6. Data Base Format

The formats used to establish the IR imagery data base package and supporting documentation have been prepared with an eye to the types of formats commonly used in IR modeling applications. Software has been produced or modified to accomplish several aims: (1) to handle all formats in which data was collected, since recording formats and equipment changed from one year's test to the next; (2) inasmuch as possible, to adapt each year's test data to a single, common format; and (3) to generate new, special interest formats. Formats have thus been specified for each of the main types of data included in the data base: maps, meteorological parameters, and imagery.

5.6.1. Reformatting Procedure. IR image models typically input information about the physical structure of a scene in a gridded format. However, the Standard Scenes maps were created from surveyor's data, which does not provide a uniform distribution of points across the scene. KRC has written software incorporating Akima's surface fitting method of interpolating from scattered data[12] to create gridded versions of the Standard Scenes topological maps. Data from the geological and botanical surveys have also been adapted to gridded overlays on the scene.

Files containing information on all measured meteorological parameters have been merged into weather files of the type currently used in PRISM. The PRISM files contain a subset of weather parameters that are most influential in IR modeling,

and give actual measured or interpolated values of these parameters at five minute intervals.

Table 5-9 lists the imaging hardware used during each phase including the application data for each system. As may be seen, several different imagers were used during the various tests included in the Standard Scenes program. All thermal imagery from tests during 1984, 1985, and 1986 has been digitized and converted into temperature data expressed in degrees Kelvin. Data files for the 1984 and 1986 tests are stored in 128-by-128 pixel format, and files for 1985 are 256-by-256 pixels. KRC's OS7 imaging software has been adapted to read, display and calculate pixel statistics for both of these resolutions.

5.6.2. Sample Formats. Appendix A is written as a stand-alone section for use as a Standard Scenes data base user's manual. Topographical information is depicted there in the form of contour maps, and background on the gridded files are also given. Geological and botanical information are presented in a similar manner, with map drawings shown and descriptions of the corresponding gridded and tabled data files included. Descriptions of both the complete and PRISM-formatted weather files can be found in Appendix A. Summary information about available thermal imagery and its format is also repeated there. The reader with special formatting requirements may consult Appendix A, to see if current Standard Scenes data base formats can meet or be adapted to those needs.

5.7. Thermal Models

There are three specific models developed under the Standard Scene program. Brief descriptions of two background thermal models developed in the context of the Standard Scenes program will be provided here. The third model - thermal clutter - will be discussed in detail, and clutter analysis of the standard scene data will be presented.

5.7.1. The Terrain Model. The terrain model was developed as the initial background model and was released as a subroutine in the first release of PRISM. This model will simulate the radiometric temperature of homogeneous and non homogeneous soil layers including any non soil type that can be described using its standard thermal properties, such as concrete roads.

The Standard Scene Thermal Frame Inventory terrain is modeled as a semi-infinite solid in which time dependent heat conduction occurs along a one dimensional path described by the heat transfer equation that follows:

Table 5.9. Standard Scenes Program Thermal Imager Specifications

Date	Imager	FOV	IFOV	Absolute Temp Error	MRT	Dynamic Range	Frame Size	Spectral Range
Fall '83	Inframetrics Model 525	14° x 18°	2 mr	±1° C	0.1° C	64 (6 bits)	200 x 250	8-12 μm
Summer 84	AGA Model 780	3.5° x 3.5°	0.5 mr	±1° C	0.1° C	256 (8 bits)	128 x 128	8-14 μm
Spring '85	TMI Model 910	33° x 33°	1.5 mr	±1° C	0.05° C	64 (6 bits)	250 x 250	8-14 μm
Fall '86	AGA Model 680	8° x 8°	1.3 mr	±1° C	0.2° C	64 (6 bits)	128 x 128	8-14 μm

$$\frac{d^2T(x,t)}{dx^2} = \frac{1}{\alpha}\frac{T(x,t)}{dt} \qquad (1)$$

where: α is the material thermal diffusivity.
$T(x,t)$ represents the temperature as a function of depth and time.

The solution of the equation is controlled by the boundary conditions at the top and bottom surfaces of the terrain plot. The bottom surface is described as a constant temperature boundary set by the diurnal temperature of the soil. The top surface is subject to continuously varying thermal inputs due to its exposure to local meteorological events such as convection forces, solar radiation, and thermal radiation exchanges.

5.7.2. The Canopy Model. The canopy model (CANOPY) is the expanded version of the background model and has been integrated into PRISM. Minor changes to the terrain model were required to integrate with CANOPY. A change to the expression used to describe the environment thermal input at the terrain surface (Q_s) was instituted to account for radiation exchange with the vegetation, degraded incident solar radiation, degraded air flow, and corrected local air temperature. PRISM now calls CANOPY as a subroutine, and CANOPY calls the terrain model. CANOPY input variables are read from the PRISM terrain input file.

Because the layer is assumed to be a bulk layer without heat storing capacity, a simple energy budget can be performed. This budget is a summation of all external environmental factors acting on the layer such as is described in this heat flow equation:

$$QT = QSW + QR - QC - QL \qquad (2)$$

where

QT is the net heat flow
QSW is the short wave solar radiation term
QR is the long wave thermal radiation term
QC is the convective heat term
QL is the latent heat term

With the assumption that the canopy layer does not store energy, QT must be a balance between all the thermal forces and, therefore, will sum to zero.

5.7.3. Model Validation. Model validation was performed using the thermal imagery recorded as part of the Standard

Scene program. As a brief introduction to the results of the background models, Figures 5-42 through 5-45 are provided. Figure 5-42 presents modeled versus measured foliage temperatures plotted for Standard Scene IV on August 1, 1984; Figure 5-43 shows the underlying soil surface temperature for the same scene. Figures 5-44 and 5-45 show the same results for the October 23, 1986 test data.

5.8. Clutter Analysis

The strong interest in autonomous target recognition (ATR) in recent years has led to the development of a variety of software algorithms designed to distinguish potential targets from surrounding background and nontarget objects. Objects and background areas in the image that may be confused or confounded with actual targets constitute "clutter" and, although the meaning of clutter in terms of human perception is intuitively clear, this concept is not easy to quantify. It is desirable not only to quantify clutter but also to relate it to other known scene parameters, in order to predict how cluttered imagery will be under given conditions and to relate clutter measures to target recognition performance. As part of the Standard Scenes program, two clutter measures were calculated for a sequence of thermal images, and their values were related to corresponding scene and meteorological variables to see if clutter could reasonably be predicted for the conditions present when the imagery was taken.

5.8.1. Clutter Metrics. The size of a given target within the sensor field of view is typically quite well defined. Hence, many image metrics use a sampling window that is approximately the same size as the target. Thus, target-sized segments of the background are sampled and compared with actual target areas as a means of quantifying the amount of clutter present in the image. For the clutter measure C used in this report, the sampling window is a square cell, with the length of the cell side set equal to the longest horizontal or vertical dimension of the target vehicle.

Other possible dimensions for the sampling window are described in other studies, in which a cell side equal to twice the height of the vehicle,[13] or a double window[14] are utilized. Actual cell sizes used in this report range from 12 pixels to a side for imagery from Standard Scene V, to 22 pixels to a side for Standard Scene IV and 25 pixels to a side for imagery from Standard Scene I.

Having established the cell size and divided the area of interest into cells, Clutter C is then defined in terms of the rms of the sum of cell variances, as in equation (3). This quantity incorporates both intensity and spatial

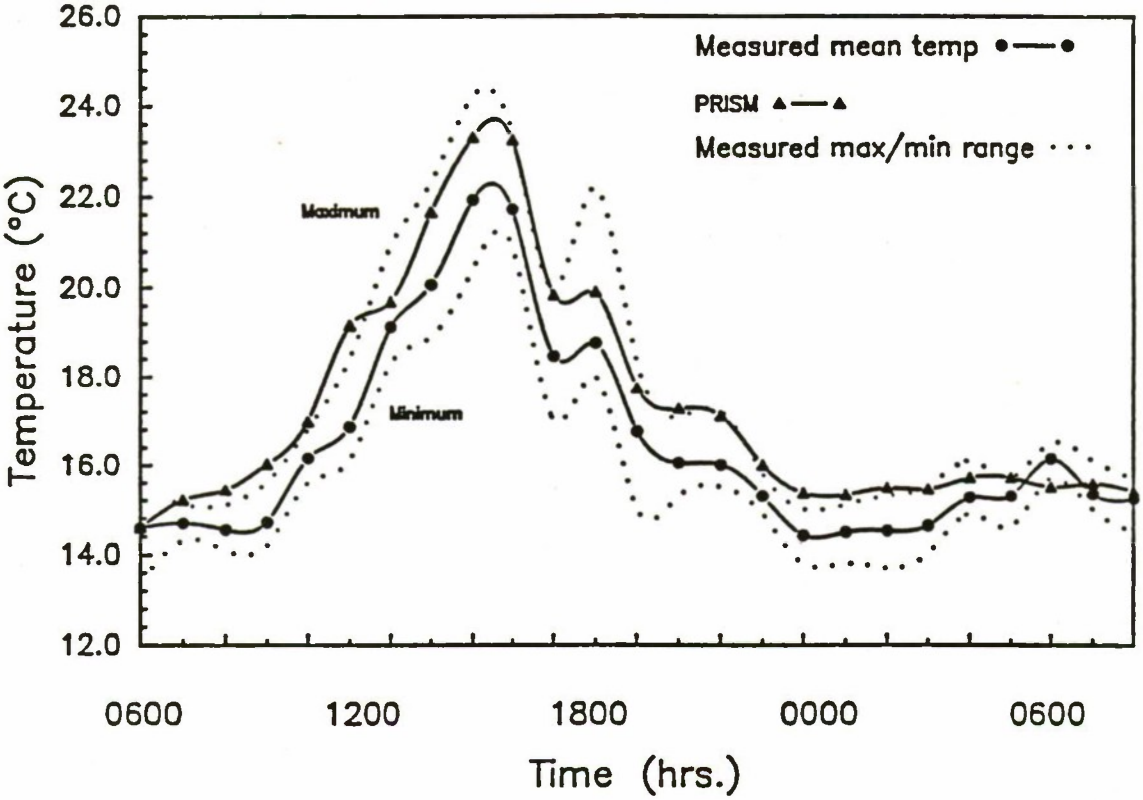

Figure 5-42. PRISM Validation of Foliage Temperature.
Verification: Standard Scene IV, August 1, 1984

Measured and modeled mean temperature of foliage are compared across a 24-hour period for vegetation canopy in Standard Scene IV. The actual range of temperatures is also indicated by plotting the minimum and maximum foliage temperatures measured throughout the period.

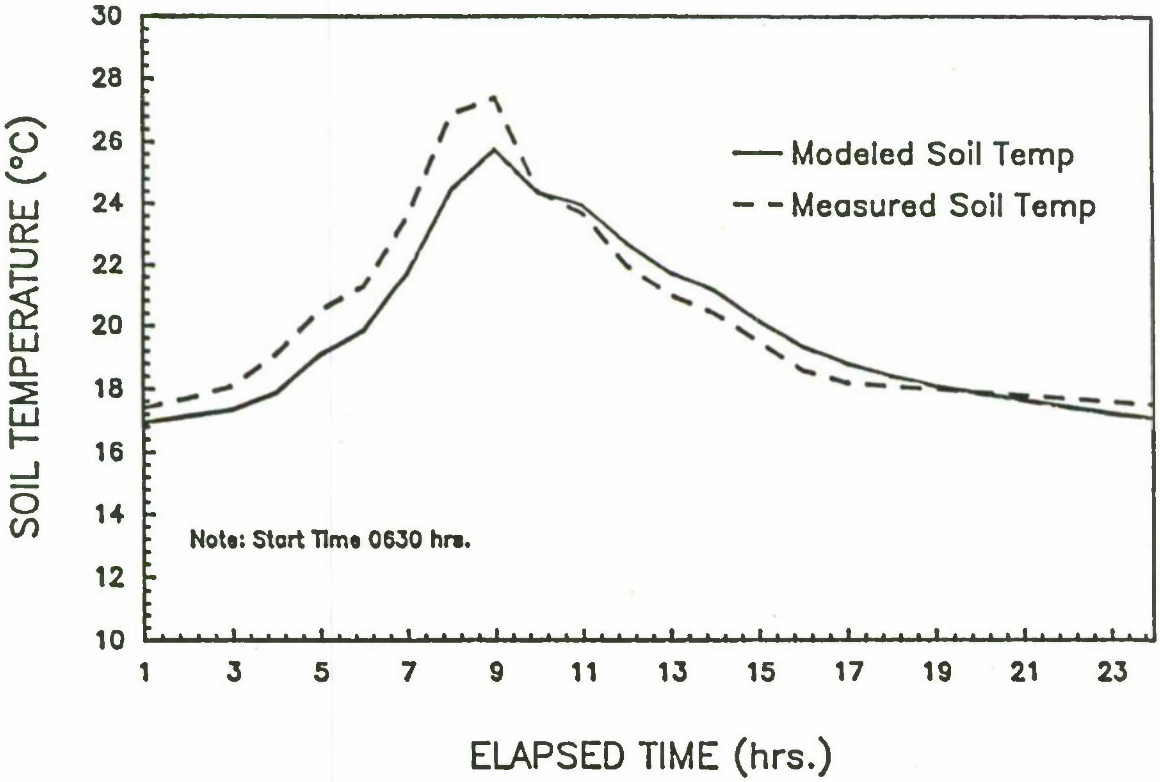

Figure 5-43. PRISM Validation of Soil Surface Temperature.
Verification: Standard Scene IV, August 1, 1984

Measured and modeled soil surface temperatures are compared across a 24-hour period in summer, for a soil probe placed in Standard Scene IV.

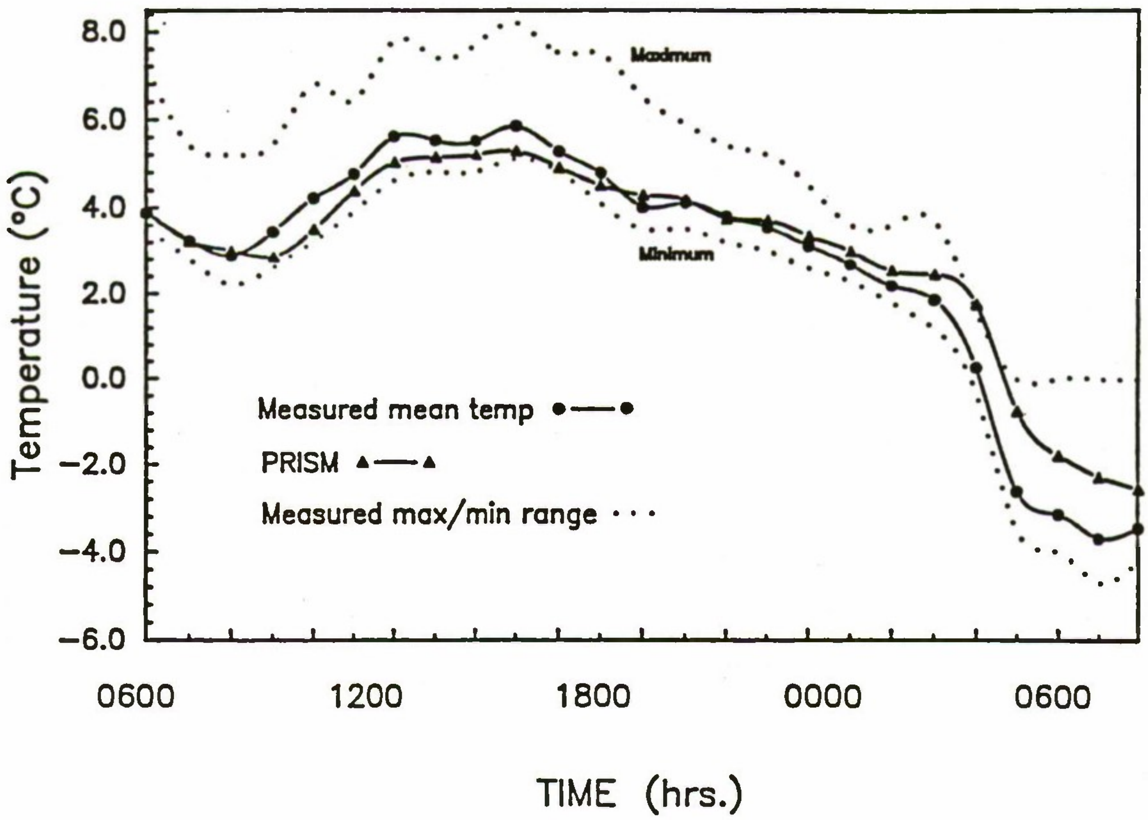

Figure 5-44. PRISM Validation of Foliage Temperature.
Verification: Standard Scene IV, October 23, 1986

Measured and modeled mean temperature of foliage are compared across a 24-hour period, in late October, for vegetation canopy in Standard Scene IV. The actual range of temperatures is also indicated by plotting the minimum and maximum foliage temperatures measured throughout the period.

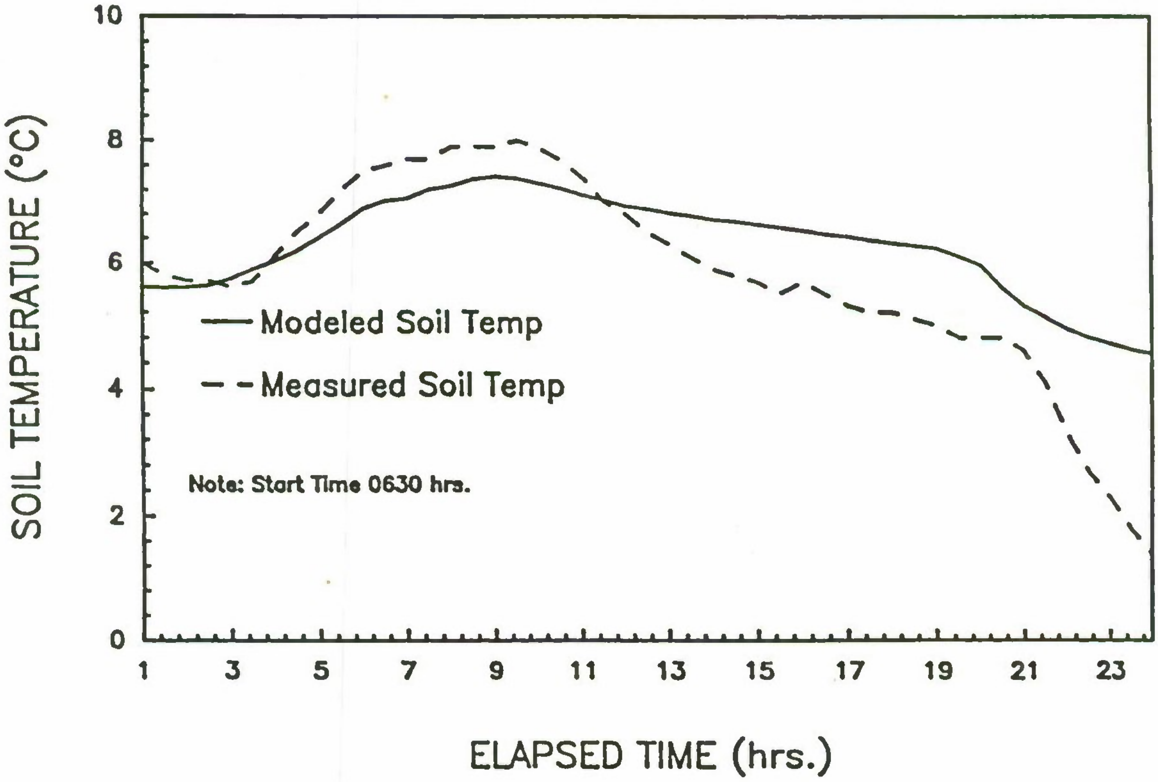

Figure 5-45. PRISM Validation of Soil Surface Temperature.
Verification: Standard Scene IV, October 23, 1986

Measured and modeled soil surface temperatures are compared across a 24-hour period in late October, for a soil probe placed in Standard Scene IV. In this example, the model assumed a more dense vegetation canopy than existed in reality. As a result, measured soil temperatures change more in response to environmental conditions, whereas the modeled soil surface is not as exposed and thus shows less variation across the diurnal cycle.

components of clutter, inasmuch as it uses information about the distribution of (temperature-equivalent) radiances in each target-sized area.

$$C = \frac{\sum_{i=1}^{N} \left(s_i^2 \right)^{1/2}}{N} \tag{3}$$

where

s_i is the standard deviation of the ith cell, and
N is the total number of cells in the image.

A signal to clutter ratio (SCR) is defined using the above definition of clutter. It is based on the difference between average background temperature and vehicle temperature extrema. For the positive contrast case in which the average vehicle temperature is greater than the average background temperature:

$$SCR = \frac{\text{Max Target Temp} - \text{Bkgrd Mean Temp}}{C} \tag{4}$$

Alternately, for negative contrast, i.e., average target temperature less than the average background temperature:

$$SCR = \frac{\text{Min Target Temp} - \text{Bkgrd Mean Temp}}{C} \tag{5}$$

In the case of negative contrast the sign is carried along to indicate that the contrast is negative.

5.8.2. Clutter Calculations in Standard Scene Imagery. A statistical analysis was performed on three sets of hourly readings, each over twenty-five consecutive hours, taken on July 25, August 1, and August 9 of 1984. Thus a total sample of 75 hourly readings was analyzed to determine the sensitivity of two image clutter measures or metrics to time dependent meteorological conditions. The scenes consist of a foreground area of low foliage bordered by a prominent treeline. An M3 Bradley is parked at various aspect angles in the scene and is included in the thermal imagery. Meteorological conditions were monitored simultaneously and in close proximity of the background being imaged.

Once thermal imagery was mapped to discrete temperature frames, scene statistics and clutter metrics were computed. For the purposes of this study, the foreground and treeline were analyzed separately. This approach was adopted because,

at the close viewing range existing in the Standard Scenes, differences in the statistics for these areas are clearly distinguished, and either the foreground or treeline dominates the imager field of view (FOV) in individual frames. For Standard Scenes I and IV, clutter and SCR values were calculated from three separate, calibrated frames for each time period: one frame showed the foreground, one treeline, and one the target. The entire scene was in the imager FOV for Standard Scene V, so only one frame was used for each time period.

Each frame is called for viewing on a graphics workstation. Specific areas of interest in the frame - i.e., the target, foreground, and treeline - are defined using a bit pad. The pixels contained in a specific area can then be isolated from the remainder of the frame and all calculations performed using only their values.

Once the target, treeline and foreground are defined, the mean and standard deviation of the temperature in these areas are directly computed in the image processing software along with a portion of clutter calculation. Target mean temperature is required to compute SCR values for the background areas. Final calculation of the clutter and SCR are then made in a second pass on the intermediate clutter data.

5.8.3. Clutter Correlated to Scenario Parameters. Four dependent variables were computed for each hourly reading included in the analysis. These were: (1) clutter of treeline, (2) SCR of treeline, (3) clutter of foreground and (4) SCR of foreground. The set of independent variables or scenario parameters consisted of: date, time of day, air-temp, solar irradiance, cumulative solar irradiance for the past six hours, relative humidity, cloud cover, and wind speed.

Frequency charts were plotted for the data, as well as for the means and standard deviations of all variables. Graphs showing the time dependency of the variables were also generated. Scatter graphs of various pairs of variables, both dependent and independent, were plotted. The Pearson product moment correlation coefficient was calculated for each plotted pair. Finally, a regression analysis was performed using the variables which were statistically significantly correlated.

The scatter graphs and correlation coefficients showed the following variables to be significantly correlated at the one percent (0.01) level of significance. Clutter was correlated with air temperature, solar irradiance, humidity, cloud cover

and wind speed in both the treeline and foreground. Air temperature, solar load and humidity were strongly correlated with each other, which suggests the possibility of partial correlations. The SCR was not significantly correlated with the independent variables or the clutter variables.

5.8.4. Clutter Regressed on Scenario Parameters. Stepwise linear regression was applied to predict clutter as a function of the independent variables. By this method, treeline clutter is found to be a function of relative humidity RH, hour of the day HOUR, and cloud cover CLD (1=clear sky,...,10=complete overcast). The following regression equation explains 72.83% of the variation in treeline clutter C_t values:

$$C_t = 1.5810 + (-0.00161)RH + (-0.00011)HOUR + (0.0177)CLD \quad (6)$$

Foreground clutter C_f is a function of solar irradiance SOL, relative humidity RH, and windspeed WND with the regression equation explaining 84.17% of the variation in foreground clutter:

$$C_f = 1.0205 + (0.00076)SOL + (-0.001050)RH + (0.11600)WND \quad (7)$$

Variables are listed in their order of importance in the regression equations. As was already noted, several of the independent variables are strongly correlated, which implies one may be substituted for the other without loss of accuracy. The regression equations provide a reasonable interpretation of factors influencing clutter. For example, solar load is most significant in explaining clutter in the foreground, which is mostly exposed soil, whereas relative humidity is more important in the vegetative treeline. Forcing other independent variables into the regression equations did not appreciably improve their accuracy.

The signal to clutter (SCR) metric failed to correlate well with any of the environmental parameters examined or with clutter when evaluated over the entire diurnal cycle. Examination of results showed that a great deal of random variation in the SCR values occurred at night. To remove this noise, the data was reexamined using only readings from 0700 to 2100 hours. Forty-five readings were available for this analysis. When restricted to this time period, the correlation coefficients between SCR and clutter in both the treeline and foreground were statistically significant at the five percent (0.05) level of significance. These correlation values were negative, as would be expected. Regression of clutter against the independent variables did not result in any change.

5.8.5. Clutter Analysis Results. In summary, it appears that the clutter in a scene can be fairly well explained by the values of the independent variables: solar load (instantaneous), humidity, cloud cover, time of day and wind speed. The actual independent variables (which are important) and their order of importance depends upon whether one is looking at a treeline or earthy foreground. There is a correlation between SCR and clutter in both treeline and foreground during daylight hours. But the SCR variation during nighttime is too random to correlate well with clutter.

5.9. Spectral Analysis

As an additional means of presenting the information contained in thermal imagery of natural scenes, selected signal processing techniques were applied to Standard Scenes imagery. In the spatial domain, distributions of pixel values were examined and used to define the probability density function (PDF) of temperatures in an image or segment of an image. Examination of temperature distributions and PDF provides descriptive statistics such as temperature mean and variance, and also helps to determine what assumptions - e.g., normality, stationarity, or ergodicity - may reasonably be applied to image analysis involving natural scenes.

The power spectral density (PSD) function was also computed for image segments, by way of analysis in the frequency domain. In the context of this paper, the PSD is the spreading or decomposition of the total mean square power of the radiometric signal as a function of frequency and is calculated via fast Fourier transform (FFT) techniques applied to the digitized data.

5.9.1. Calculation of FFTs and PSDs. For each digitized image analyzed, an area of interest was first defined and truncated to have even numbers of rows and columns of pixels. To "center" the distribution, the temperature mean was computed for the area, and then subtracted from the value of each pixel in the area. Correspondingly, the PSDs that result are centered at 0 radians^{-1}, as is seen in the following figures. Calculations were performed on a row-by-row or column-by-column basis. If necessary, pixel rows or columns in the area were padded with an equal number of zero-value pixels at each end in order to obtain N = 256 pixels, or data points, in each. Given a sampling interval of T = 4.7724 x 10^{-4} radians (i.e., one pixel per T radians), the power spectral density obtained from the transform is a complex one-dimensional array containing 128 points

$$X(0), X(1), X(2), \ldots, X(127)$$

with a spacing of $F = 8.1851$ radians^{-1}. The frequency spacing F is obtained from

$$F = 1/P \tag{8}$$

where the period P is the total record length

$$P = NT = 256 \cdot (4.7724 \times 10^{-4}) = 0.12217 \tag{9}$$

in radians. The Fourier coefficients X(k), k=1,2,...,127 are obtained from the fast Fourier transform (FFT)

$$X(k) = T \cdot \sum_{i=0}^{N-1} [x(i) \cdot \exp(-j(2\pi/N)ik)] \tag{10}$$

The computer program that was written to compute FFTs for the Standard Scene data utilizes the Cooley-Tukey algorithm[15,16].

Having computed the Fourier coefficients X(k), a Goodman spectral window is applied for spectrum averaging, to suppress leakage. The adjusted value X(k) that results is

$$X(k) = X(k) + \sum_{i=1}^{3} b(i) \cdot [X(k-i)+X(k+i)] \tag{11}$$

where

$$k = 0,1,2,\ldots,N-1$$
$$b(1) = -0.35$$
$$b(2) = -0.8750$$
$$b(3) = -0.0625$$

and the values X(k) are the original values of the coefficients represented by equation (10). For k=0, the terms X(k-i), i=1,2,3 require special definitions: let

$$X(0-i) = X((N-1)-i) \tag{12a}$$

Similarly, for k=N-1, the terms X(k+i), i=1,2,3 must be specially defined: let

$$X((N-1)+i) = X(i) \tag{12b}$$

Estimates of the power spectral density $\tilde{s}(k)$ can then be computed and normalized by the equation

$$\tilde{s}(k) = (2G/P) \cdot |\tilde{X}(k)|^2 \tag{13}$$

where

$$|X(k)| = X(k) \cdot X^*(k)$$

$X^*(k)$ is the complex conjugate of $X(k)$
$k = 0,1,2,\ldots,(N/2)$
G = Goodman normalization = 1.267
P = record length = 0.010865 radians

Values of $\tilde{s}(k)$ are accumulated until all rows or columns are completed. Individual PSDs for each row or column are averaged and values plotted.

5.9.2. Probability Densities for Standard Scenes Imagery. The distribution and relative frequency of temperature values in foreground and treeline sections of images were also examined via probability density function plots. As is evident from the plots shown in Figures 5-46 and 5-47, temperature distributions during daytime hours frequently show multiple modes and some skewness, with extended tails on the upper end of the curve. During the night, the range of temperatures predictably decreases, producing a narrow, spikey distribution. Although goodness-of-fit of these PDFs to specific distributions was not evaluated, observed shape characteristics suggest that distributions from the Weibull family, rather than the Gaussian, might be used to describe the temperature distribution for natural scenes.

For all scenes, the temperature means for foreground and treeline were comparable throughout the diurnal cycle. However, temperature variances behaved differently, and these differences were not consistent from scene to scene. In general, the variability of treeline and foreground temperatures were comparable and relatively low during the night. Temperature variability typically increased during daylight hours, with the notable exception of the north-facing treeline in Standard Scene V. In Scenes I and V, variances for the foreground were much higher than those for the treeline; this is probably explained by the variety of ground cover present in the foregrounds of these scenes. In contrast, variances for foreground and treeline areas of Scene IV are more comparable, with the treeline showing somewhat more variability during the day. It will be recalled that Scene IV has more uniform, dense vegetation throughout.

5.9.3. Power Spectra for Standard Scenes Imagery. A sampling of power spectral densities calculated from row-by-row averaging for treeline and foreground areas are shown in Figures 5-48 and 5-49, respectively. These PSDs correspond to the same sequence of thermal images for which probability density functions were depicted in Figures 5-46 and 5-47. Whereas the difference between PDFs of foreground and treeline were of particular interest, it is the similarity in spectral content between the various figures that is worth noting.

Figure 5-46. Probability Density Function, Treeline Example

Sample PDFs calculated for sequence of Standard Scene I thermal imagery, treeline area. Date: 25 July, 1984.

a. Time: 1200

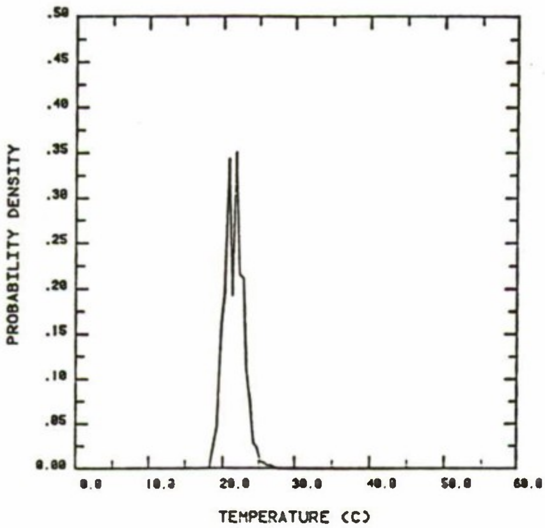

b. Time: 1300

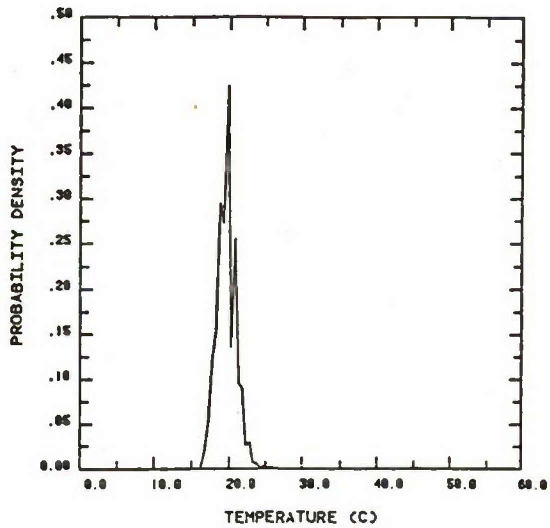

c. Time: 1400

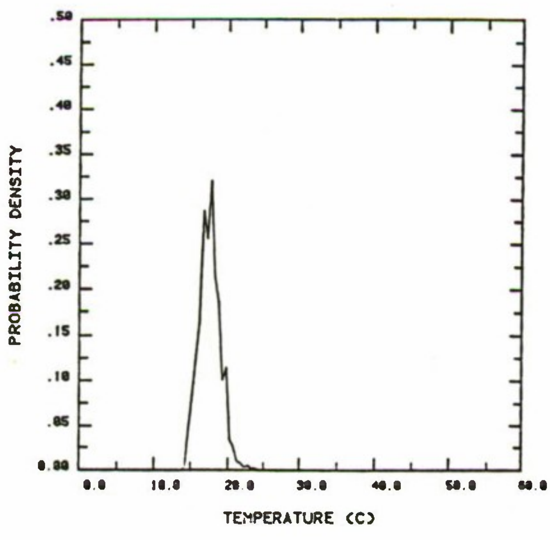

d. Time: 1500

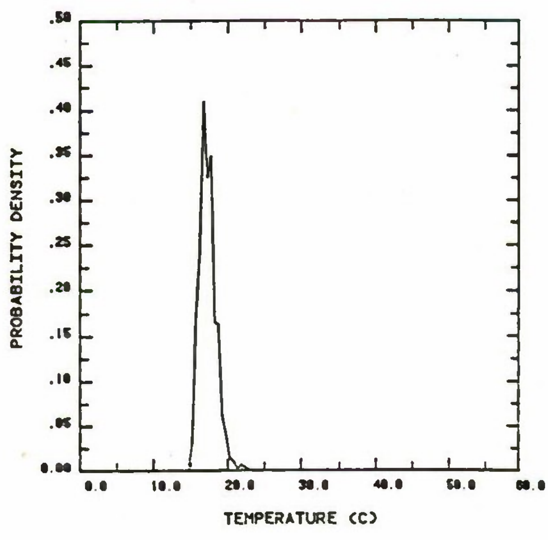

Figure 5-47. Probability Density Function, Foreground Example

Sample PDFs calculated for sequence of Standard Scene I thermal imagery, foreground area. Date: 25 July, 1984. Note change of scale for probability density in plot b.

a. Time: 1200

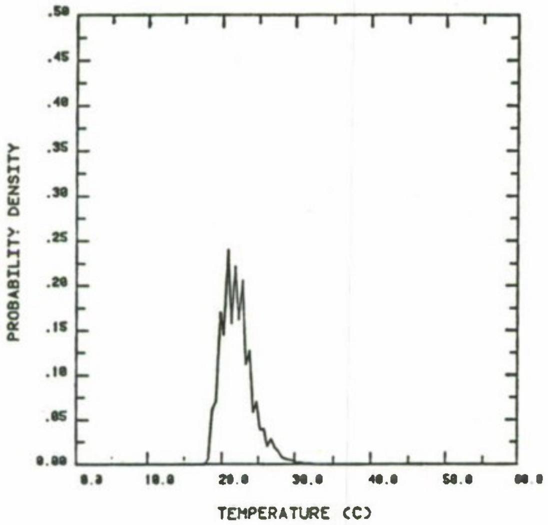

b. Time: 1300

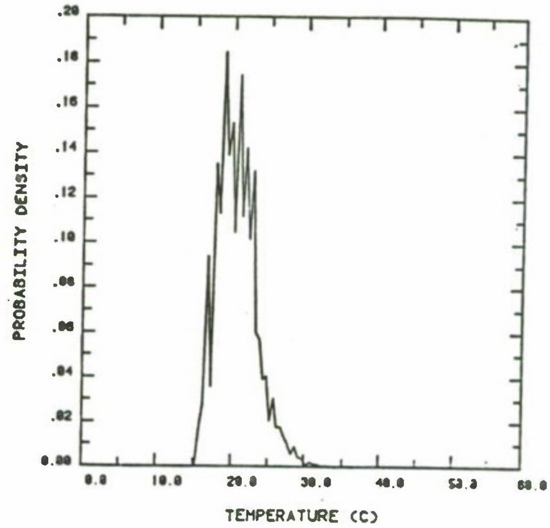

c. Time: 1400

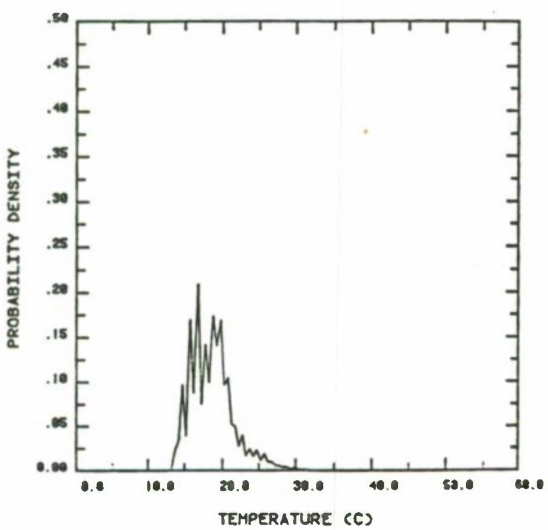

d. Time: 1500

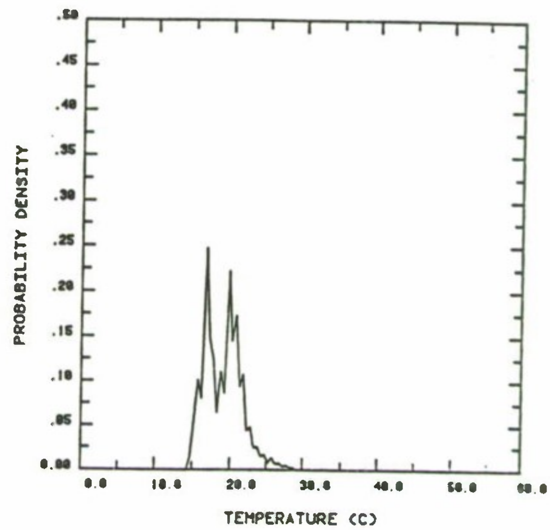

Figure 5-48. Power Spectral Density, Treeline Example

Sample PSDs calculated for sequence of Standard Scene I thermal imagery, treeline area. Date: 25 July, 1984. Note change of scale for power variable in plot c.

a. Time: 1200

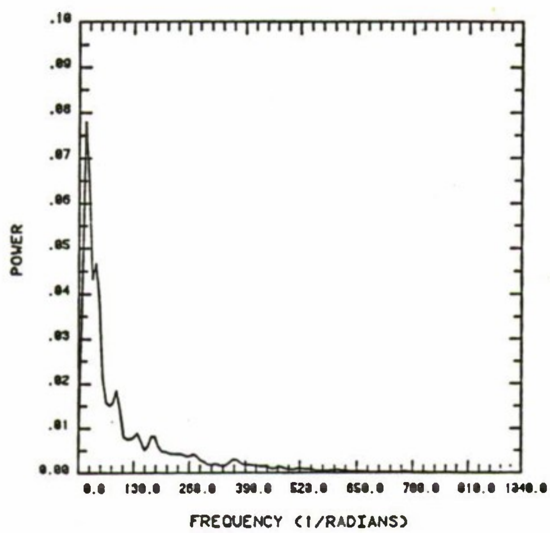

b. Time: 1300

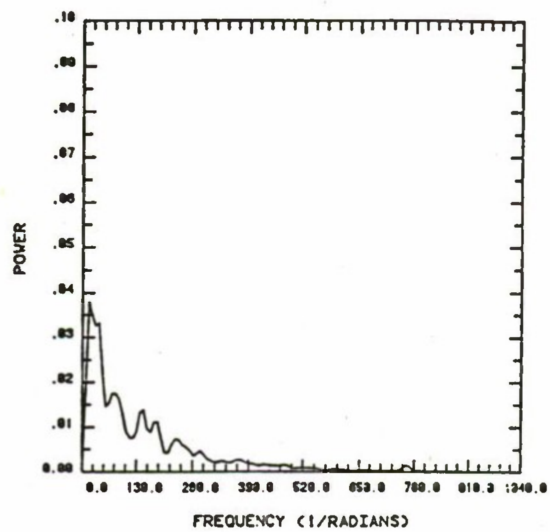

c. Time: 1400

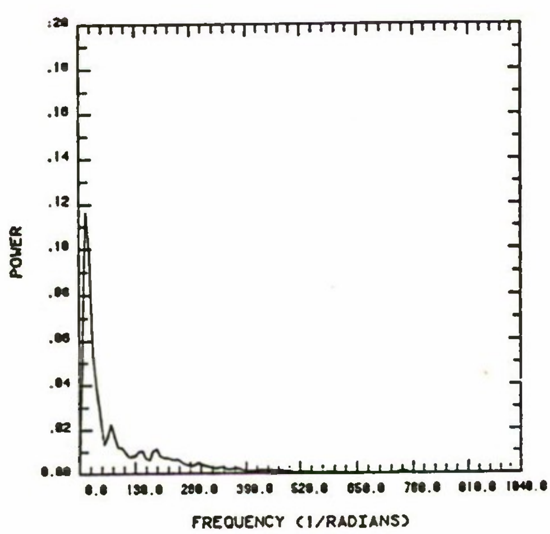

d. Time: 1500

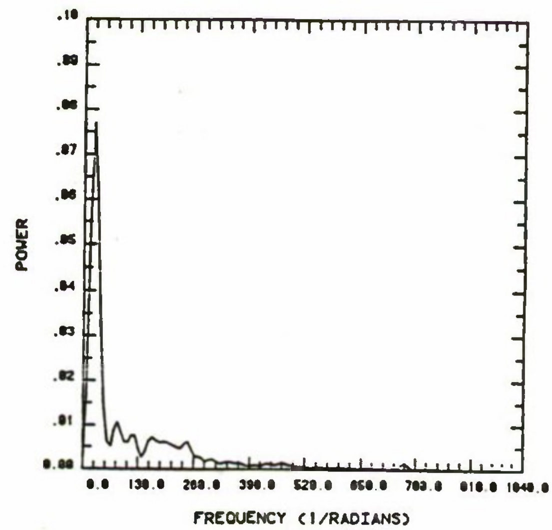

Figure 5-49. Power Spectral Density, Foreground Example

Sample PSDs calculated for sequence of Standard Scene I thermal imagery, foreground area. Date: 25 July, 1984. Note change of scale for power variable in plot d.

a. Time: 1200

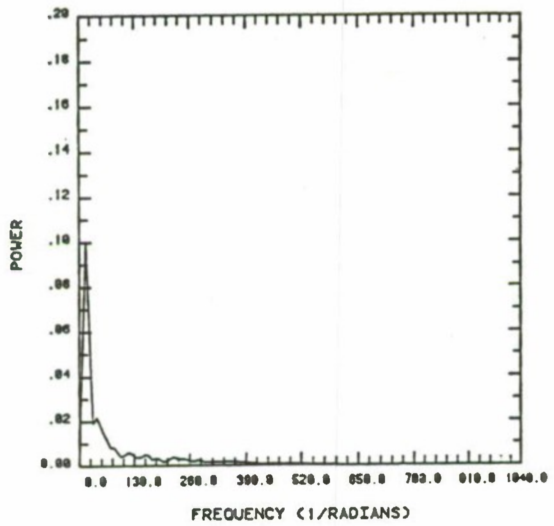

b. Time: 1300

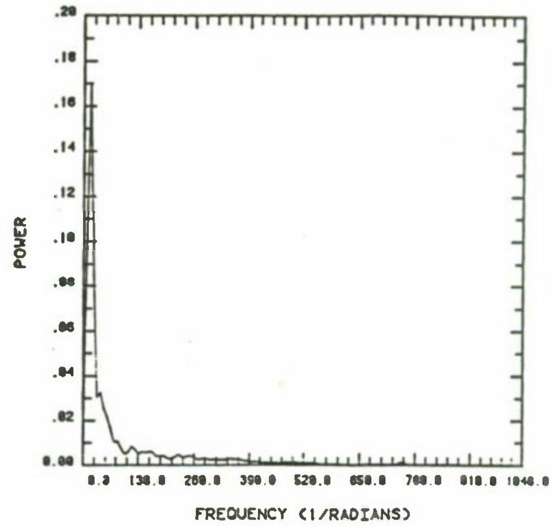

c. Time: 1400

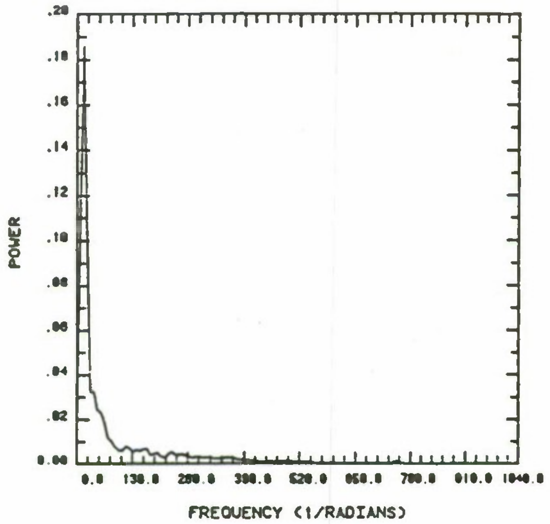

d. Time: 1500

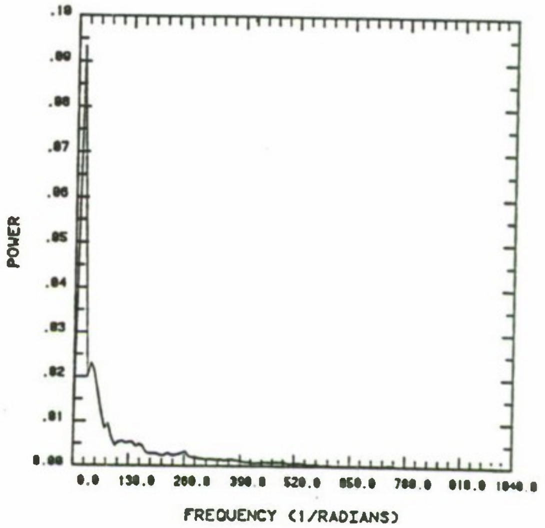

REFERENCES

1. Reynolds, W. R., Beckwith, J. P., and Baratono, R. K., "Infrared Clutter Analysis of Standard Scenes Image Data," Proceedings of the Seventh Annual Symposium on Ground Vehicle Signatures, Keweenaw Research Center, 1985.

2. Howard, G. B., Reynolds, W. R., and Baratono, R. K., "Modeling and Measurement of Standard Scenes," U. S. Army Tank-Automotive Command Technical Report No. 13306, 1987.

3. Maxwell, J. R., "Statistical Analysis of Selected Terrain and Water Background Measurements Data," Final Report No. 132300-1-F, Infrared and Optics Division, Environmental Research Institute of Michigan, July 1978.

4. LaRocca, A. N. and Witte, D. J., "Handbook of the Statistics of Various Terrain and Water (Ice) Backgrounds from Selected U. S. Locations," 139900-1-X, Infrared and Optics Division, Environmental Research Institute of Michigan, Jan. 1980.

5. Carmer, D. C., Coleman, E. N., Dell'Eva, M., Due, C., and Swonger, C., "Data Base, Image Characterization and Algorithm Characterization For Autonomous Infrared Techniques Program (AIRT)," 176000-7-T, Environmental Research Institute of Michigan, Dec. 1984.

6. Hayes, M. J., "Climatological Comparison of Houghton, Michigan with the Giessen/Fulda Region of West Germany," Institute of Snow Research, Keweenaw Research Center, Houghton, Michigan, August, 1985.

7. Schmieder, D. E., Weathersby, M. R., Finlay, W. M., and Doll, T. J., "Clutter and Resolution Effects on Observer Static Detection Performance," AFWAL-TR-82-1059, Engineering Experiment Station, Georgia Institute of Technology, June 1982.

8. Howard, G. B., Reynolds, W. R., and Baratono, R. K., "Modeling and Measurement of Standard Scenes," U. S. Army Tank-Automotive Command Technical Report No. 13306, 1987.

9. Physically Reasonable Infrared Signature Model (PRISM) User's Manual, Version 2.0, Keweenaw Research Center, Houghton, Michigan, 1989.

10. U. S. Department of Interior, "Physical Resource Studies," Bureau of Land Management Manual 4412, 1979.

11. Mueller-Dombois, D., and Ellenberg, H., "Aims and Methods of Vegetation Ecology," John Wiley and Sons, New York, New York, 547 pages, 1974.

12. Akima, H., "A Method of Bivariate Interpolation and Smooth Surface Fitting for Irregularly Spaced Data Points," ACM Transactions on Mathematical Software, Vol. 4, 1978. Pages 148-159.

13. Schmieder, D. E., Weathersby, M. R., Finlay, W. M., and Doll, T. J., "Clutter and Resolution Effects on Observer Static Detection Performance," AFWAL-TR-82-1059, Engineering Experiment Station, Georgia Institute of Technology, June 1982.

14. Carmer, D. C., Coleman, E. N., Dell'Eva, M., Due, C., and Swonger, C., "Data Base, Image Characterization and Algorithm Characterization For Autonomous Infrared Techniques Program (AIRT)," 176000-7-T, Environmental Research Institute of Michigan, Dec. 1984. Pages 103-109.

15. Otnes, R. K., and Enochson, L., <u>Applied Time Series Analysis</u> Vol. 1, John Wiley and Sons, New York, 1978. P. 239ff.

16. Pickett, R. C., Lindgren, G. E., and Anderson, R. K., "An FFT-based Signal Processor for 6502 Microcomputers," American Journal of Physics, Vol. 52, No. 8, August 1984. Pp. 713-719.

SELECTED BIBLIOGRAPHY

1. Akima, H., "A Method of Bivariate Interpolation and Smooth Surface Fitting for Irregularly Spaced Data Points," ACM Transactions on Mathematical Software, Vol. 4, 1978. Pages 148-159.

2. Carmer, D. C., Coleman, E. N., Dell'Eva, M., Due, C., and Swonger, C., "Data Base, Image Characterization and Algorithm Characterization For Autonomous Infrared Techniques Program (AIRT)," 176000-7-T, Environmental Research Institute of Michigan, Dec. 1984.

3. Hayes, M. J., "Climatological Comparison of Houghton, Michigan with the Giessen/Fulda Region of West Germany," Institute of Snow Research, Keweenaw Research Center, Houghton, Michigan, August, 1985.

4. Howard, G. B., Reynolds, W. R., and Baratono, R. K., "Modeling and Measurement of Standard Scenes," U. S. Army Tank-Automotive Command Technical Report No. 13306, 1987.

5. LaRocca, A. N. and Witte, D. J., "Handbook of the Statistics of Various Terrain and Water (Ice) Backgrounds from Selected U. S. Locations," 139900-1-X, Infrared and Optics Division, Environmental Research Institute of Michigan, Jan. 1980.

6. Maxwell, J. R., "Statistical Analysis of Selected Terrain and Water Background Measurements Data," Final Report No. 132300-1-F, Infrared and Optics Division, Environmental Research Institute of Michigan, July 1978.

7. Mueller-Dombois, D., and Ellenberg, H., "Aims and Methods of Vegetation Ecology," John Wiley and Sons, New York, 1974.

8. Otnes, R. K., and Enochson, L., <u>Applied Time Series Analysis</u> Vol. 1, John Wiley and Sons, New York, 1978.

9. Physically Reasonable Infrared Signature Model (PRISM) User's Manual, Version 2.0, Keweenaw Research Center, Houghton, Michigan, 1989.

10. Pickett, R. C., Lindgren, G. E., and Anderson, R. K., "An FFT-based Signal Processor for 6502 Microcomputers," American Journal of Physics, Vol. 52, No. 8, August 1984. Pp. 713-719.

11. Reynolds, W. R., Beckwith, J. P., and Baratono, R. K., "Infrared Clutter Analysis of Standard Scenes Image Data," Proceedings of the Seventh Annual Symposium on Ground Vehicle Signatures, Keweenaw Research Center, 1985.

12. Schmieder, D. E., Weathersby, M. R., Finlay, W. M., and Doll, T. J., "Clutter and Resolution Effects on Observer Static Detection Performance," AFWAL-TR-82-1059, Engineering Experiment Station, Georgia Institute of Technology, June 1982.

13. U. S. Department of Interior, "Physical Resource Studies," Bureau of Land Management Manual 4412, 1979.

APPENDIX A

Standard Scenes Imagery Data Base

APPENDIX A: TABLE OF CONTENTS

A.1.0. Overview of Standard Scenes

A.1.1. General Description of Standard Scenes. Summary descriptions of the areas included in the Standard Scenes Program are provided in Table A-1.

A.1.2. Maps of Standard Scenes. A set of maps was prepared for each Standard Scene to graphically portray the following information:

- Topology and salient physical features and boundaries.
- Soil types by area, within established field of view.
- Principal vegetation types by area, within established field of view.
- Elevation of a cross-section of the scene, with both a 1:1000 scale (meters) and a 5X magnification shown.

In the following sections, each of these maps are shown, respectively, for each of the six Standard Scenes.

A.1.3. Photographs of Standard Scenes. Extensive photographic documentation exists for all Standard Scenes and for specific field tests conducted at them. To augment the visual views of the Standard Scenes included in the program's final report, photographs of each of the Standard Scenes are included here in Figures A-1 through A-6.

Table A-1. Summary: Standard Scenes Characterization

SCENE	DIRECTION OF VIEW	RANGE TO TREELINE	TREELINE TYPE/HEIGHT	FOREGROUND COMPOSITION	SOIL COMPOSITION
I[1]	2°	360 m	Deciduous 10-15 m	Grasses Shrubs, Moss	Sand
II[1]	192°	380 m	Deciduous 10-15 m	Grasses Shrubs, Moss	Sand Loamy sand
III[1]	240°	280 m	Deciduous 10-15 m	Grasses Shrubs, Moss	Gravelly sand Sand
IV	99°	170 m	Deciduous 3- 5 m	Grasses High bushes	Loamy sand Sand
V[2]	18°	873 m	Deciduous 3-15 m	Grass Dirt Road	Gravelly sand Sand
VI[3]	175°	217 m*	Deciduous 8-10 m	Grasses Clover	Loamy Sand Sand

Notes:
1 Scenes I, II, and III look across same field.
2 Dirt road runs through center of Scene V.
3 Scene VI observed from 30m high tower (8° slant angle)
* Slant range.

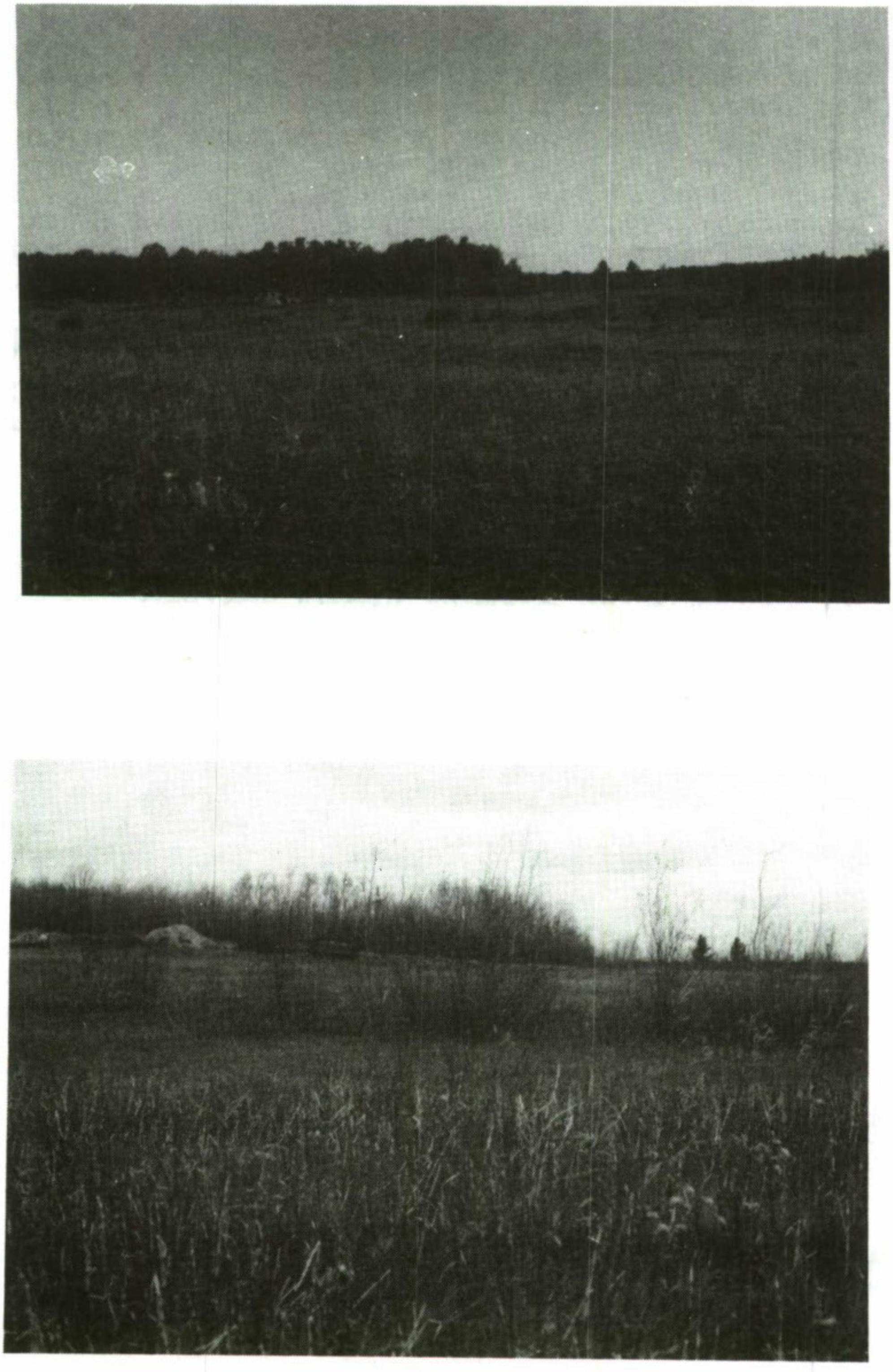

Figure A-1. Photographic views of Standard Scene I

Figure A-2. Photographic views of Standard Scene II

Figure A-3. Photographic views of Standard Scene III

Figure A-4. Photographic views of Standard Scene IV

Figure A-5. Photographic views of Standard Scene V

Figure A-6. Photographic views of Standard Scene VI

A.2.0. Topography

A.2.1. Physical Survey. Each Standard Scene was initially surveyed by transit, using known, permanent benchmarks established in the vicinity. These surveys constituted the basis for creating the contour maps shown in the following Figures A-7 through A-12. Cross-sectional maps of each scene, showing both a scale matched to the topographical maps and a 5X magnification, are presented in Figures A-13 through A-18. The original survey information defines points in the scene in terms of stations, horizontal and vertical angles, and stadia, along with physical referents or verbal descriptions of the location of the point. This information is combined with the elevation of the known benchmark(s) to calculate elevations at specified points in the scene.

One corner of each scene was arbitrarily chosen as the origin and all survey points were assigned Cartesian (x-y) coordinates. The basic computer file of topographical data thus consists of the set x and y coordinates and corresponding elevations (in meters) of scattered, surveyed points in the scene.

A.2.2. Grid Format for Elevation Data. Some applications of the Standard Scenes database of potential interest are in the areas of synthetic image generation, and scene modeling. The programs being developed for these purposes often assume a rectangular grid format for the input data. The Army Training Simulation System (ARTBASS) terrain database supplied by the Defense Mapping Agency (DMA) is one such example. In order to make Standard Scenes data more adaptable to these applications, elevations for a rectangular grid of points have been extrapolated from survey data.

A.2.3. Elevation File Format and Description. The elevation data file header provides information on the standard scene represented, the assumed grid spacing (typical values are 10 meters or 12.5 meters), and the row and column location of the origin in the data file. At present, the main body of elevation data is given in an x, y, z format, where x and y are the coordinates, expressed in meters, for an intersection point on the grid overlaying the scene, and z is elevation above sea-level, in meters, at that point.

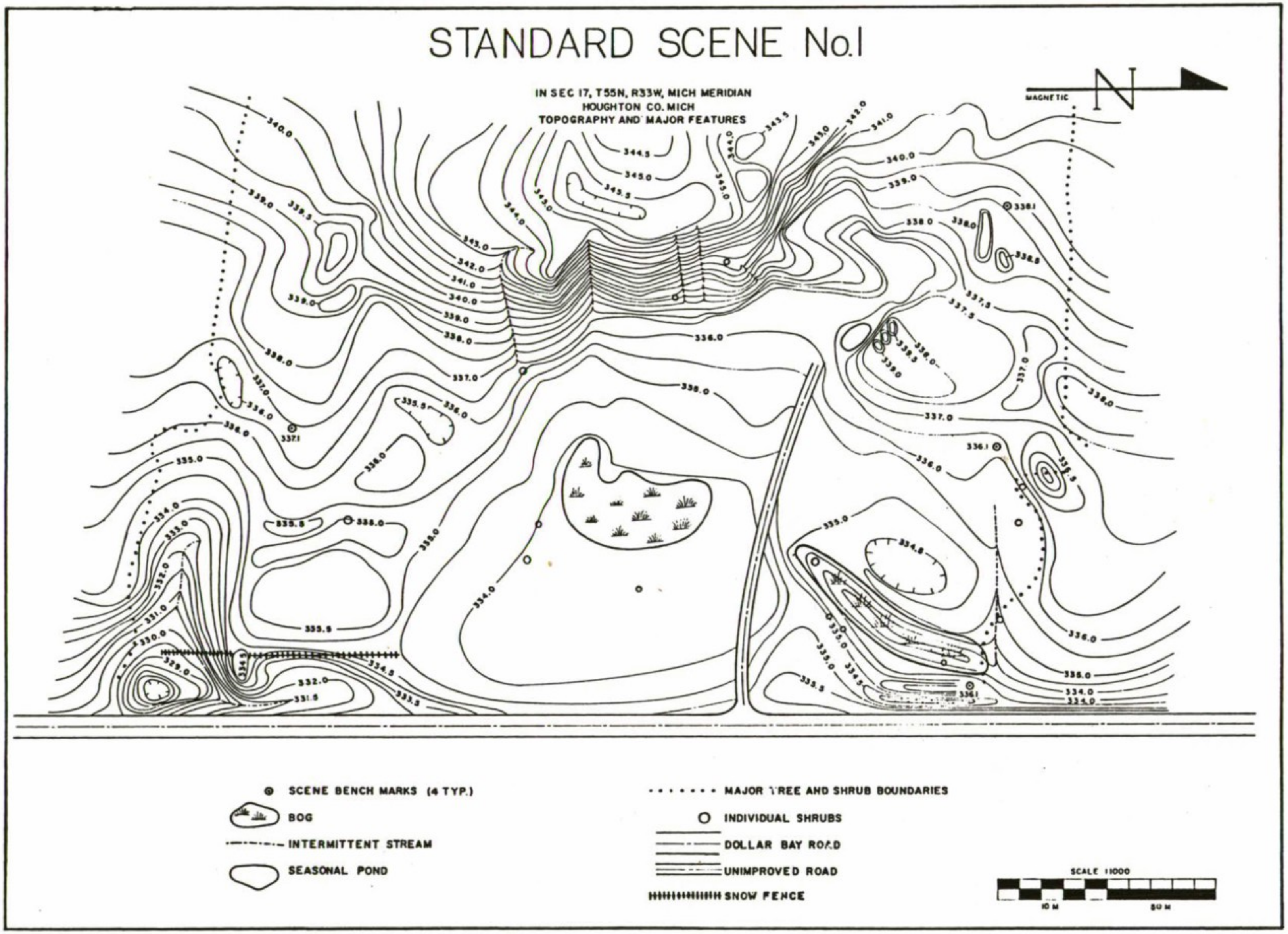

Figure A-7. Topographical Map of Standard Scene I

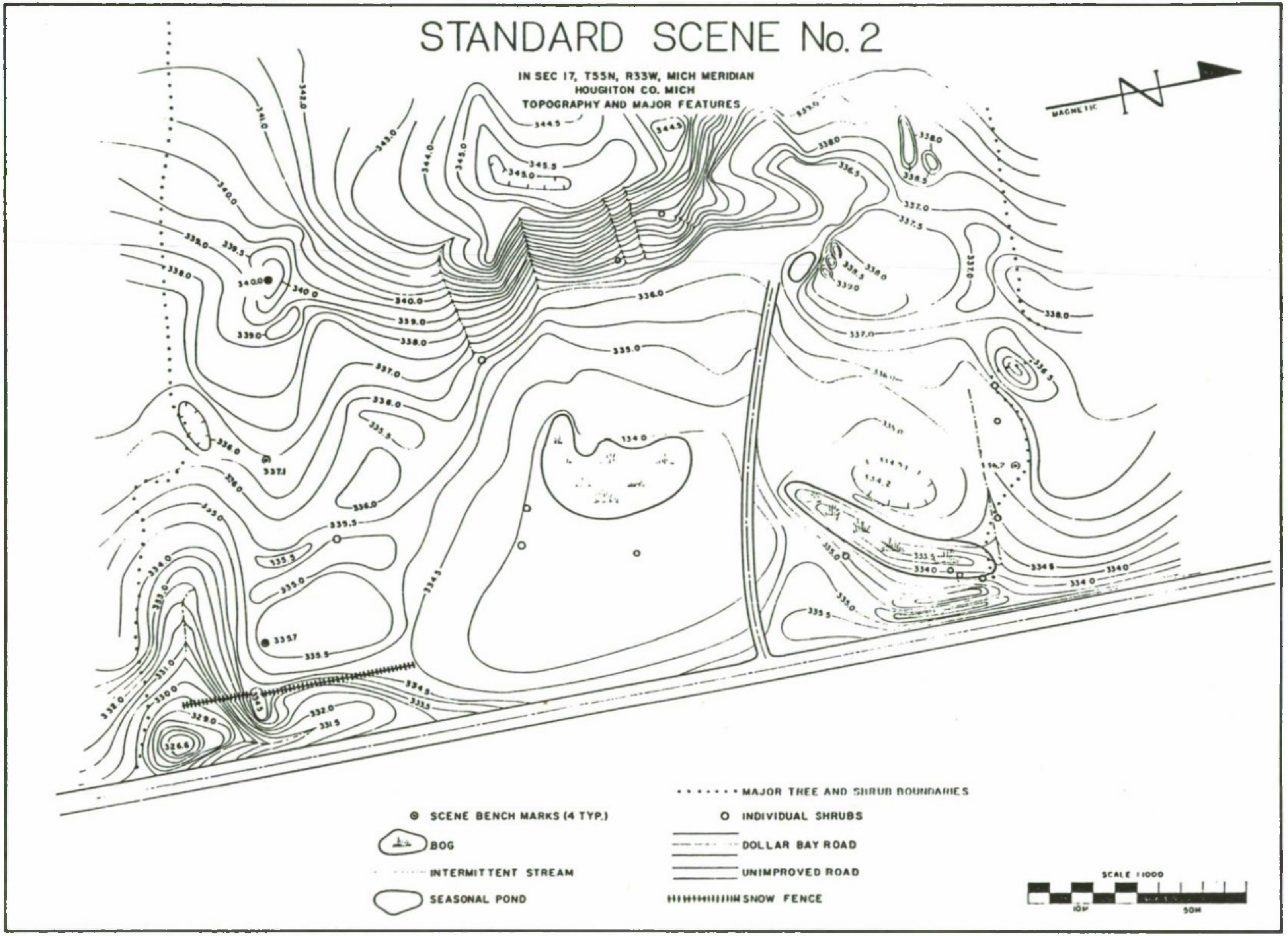

Figure A-8. Topographical Map of Standard Scene II

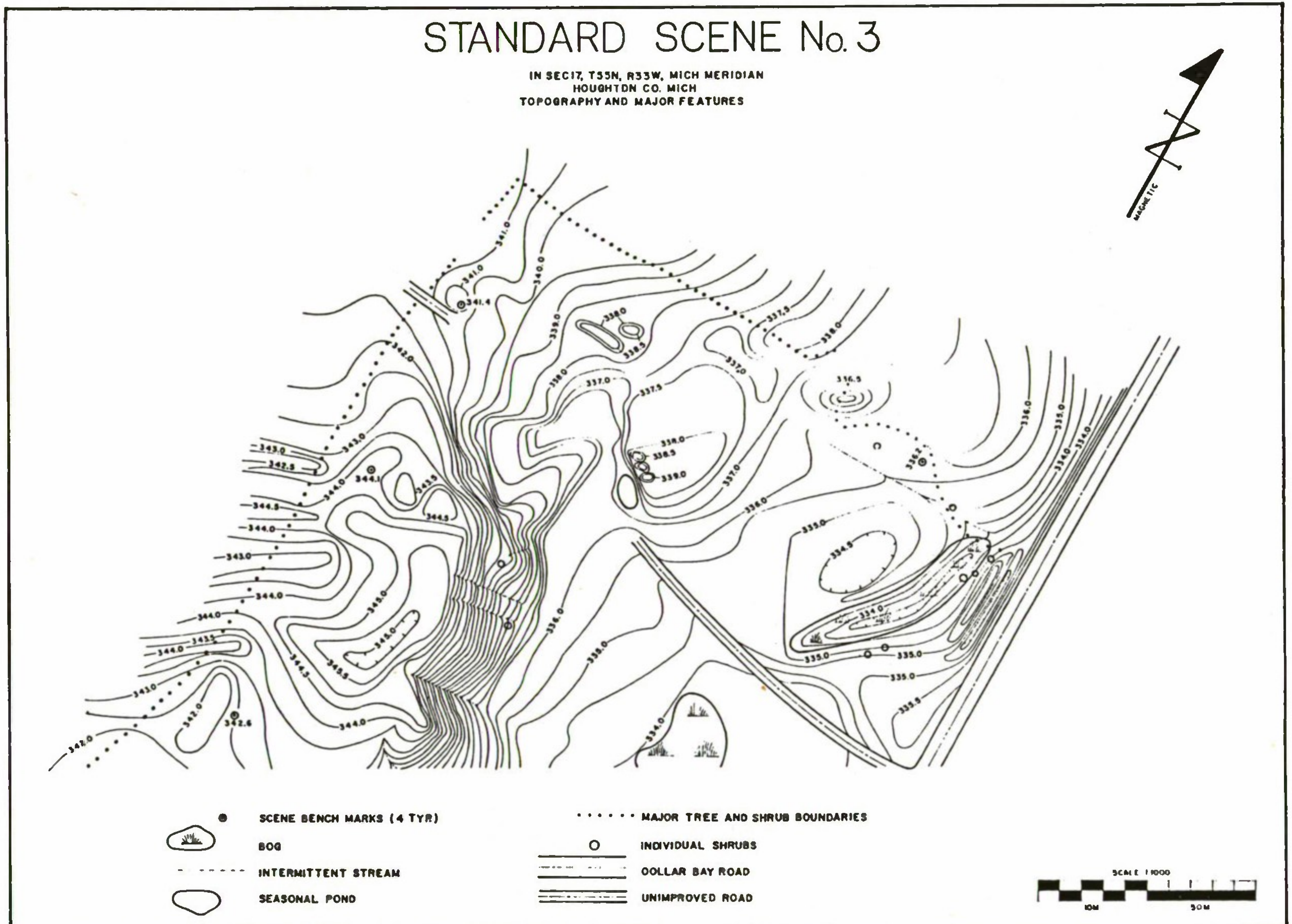

Figure A-9. Topographical Map of Standard Scene III

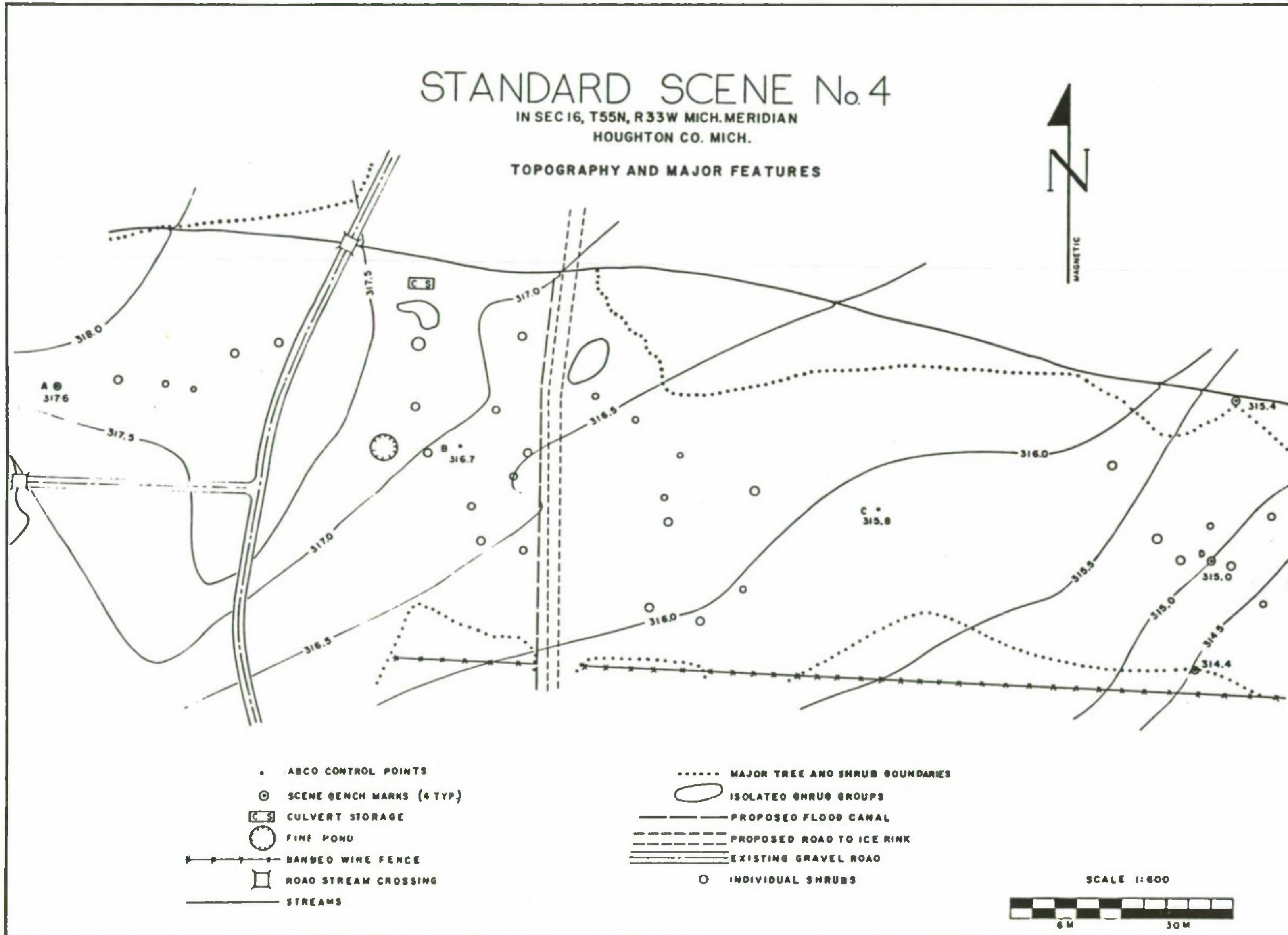

Figure A-10. Topographical Map of Standard Scene IV

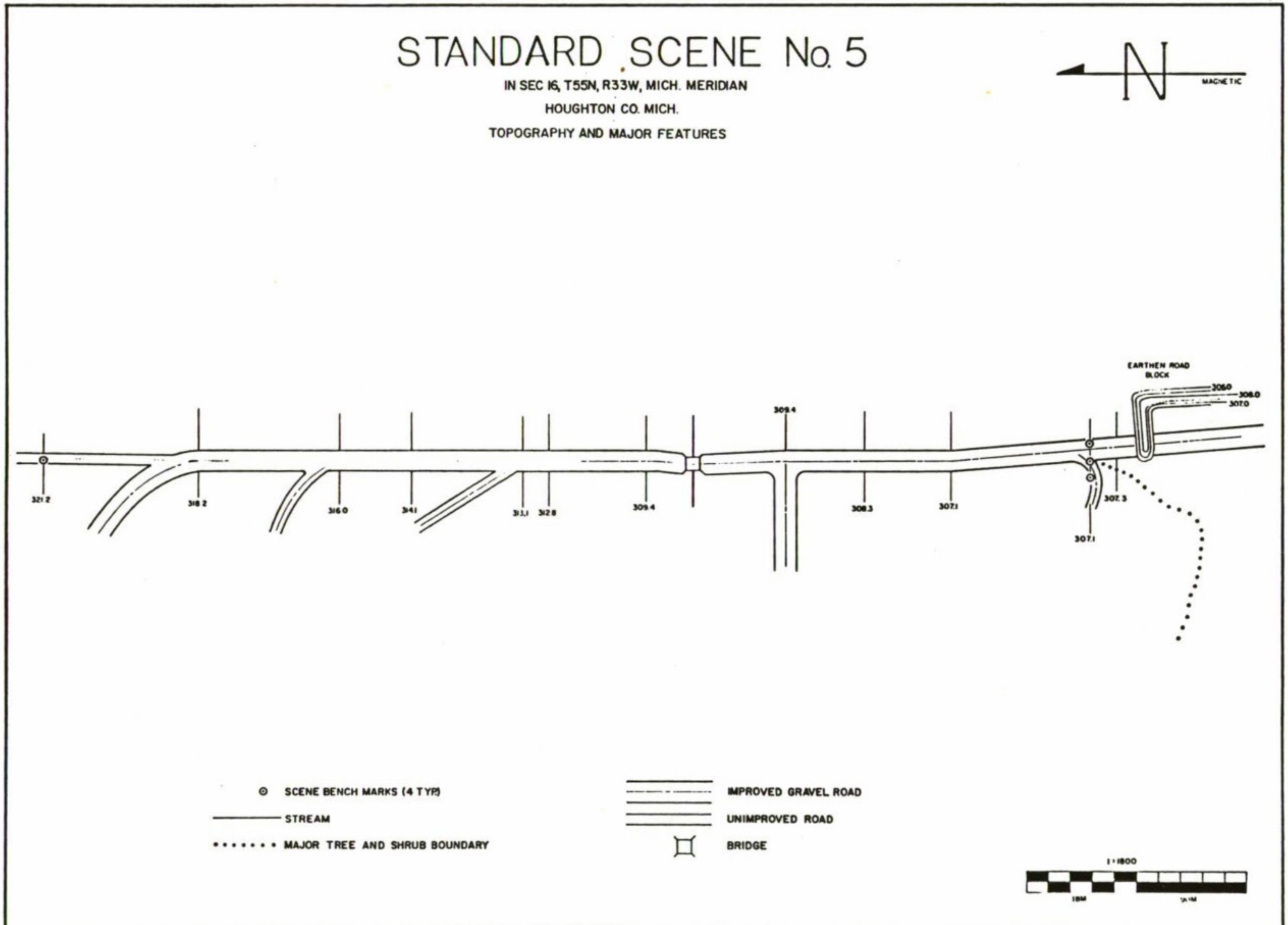

Figure A-11. Topographical Map of Standard Scene V

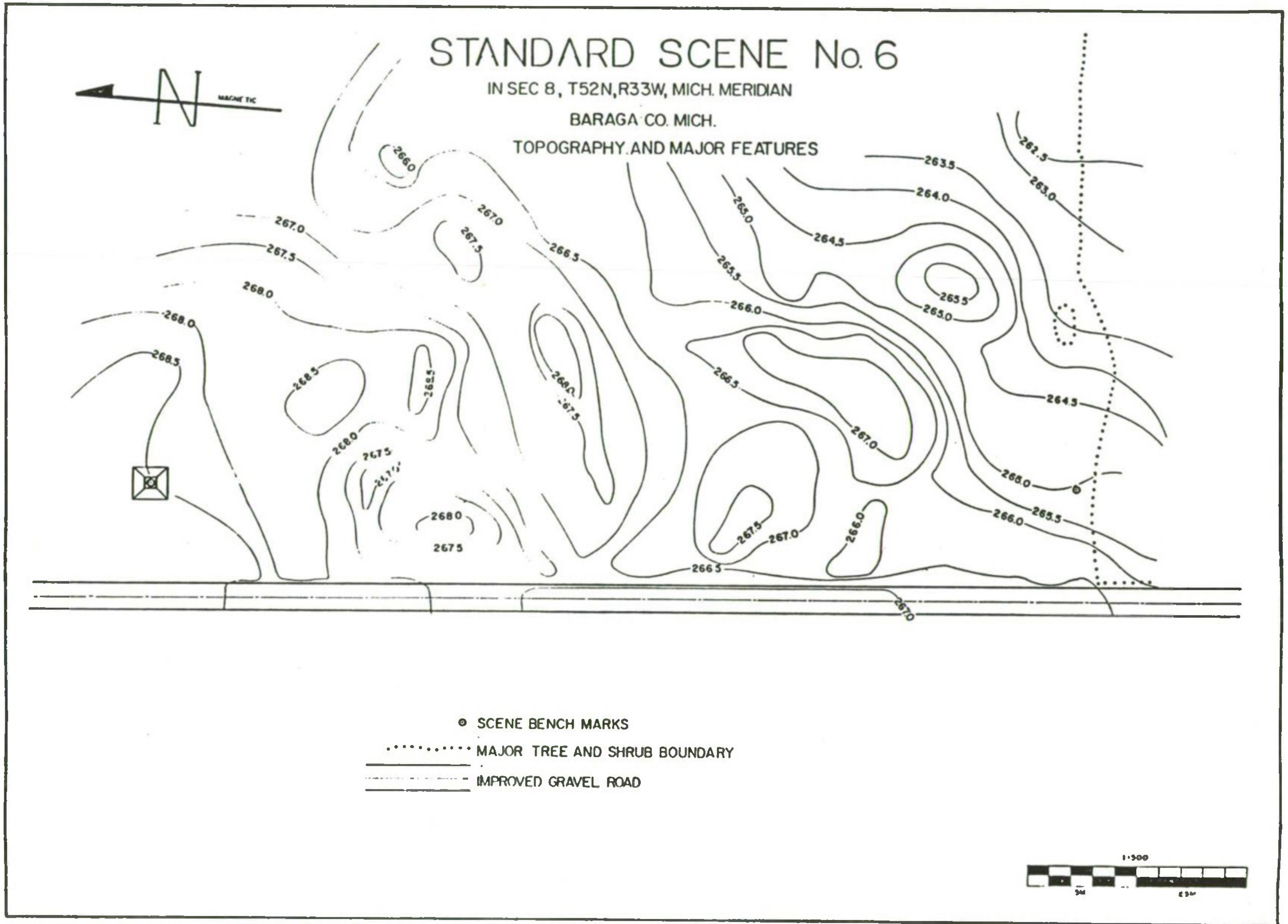

Figure A-12. Topographical Map of Standard Scene VI

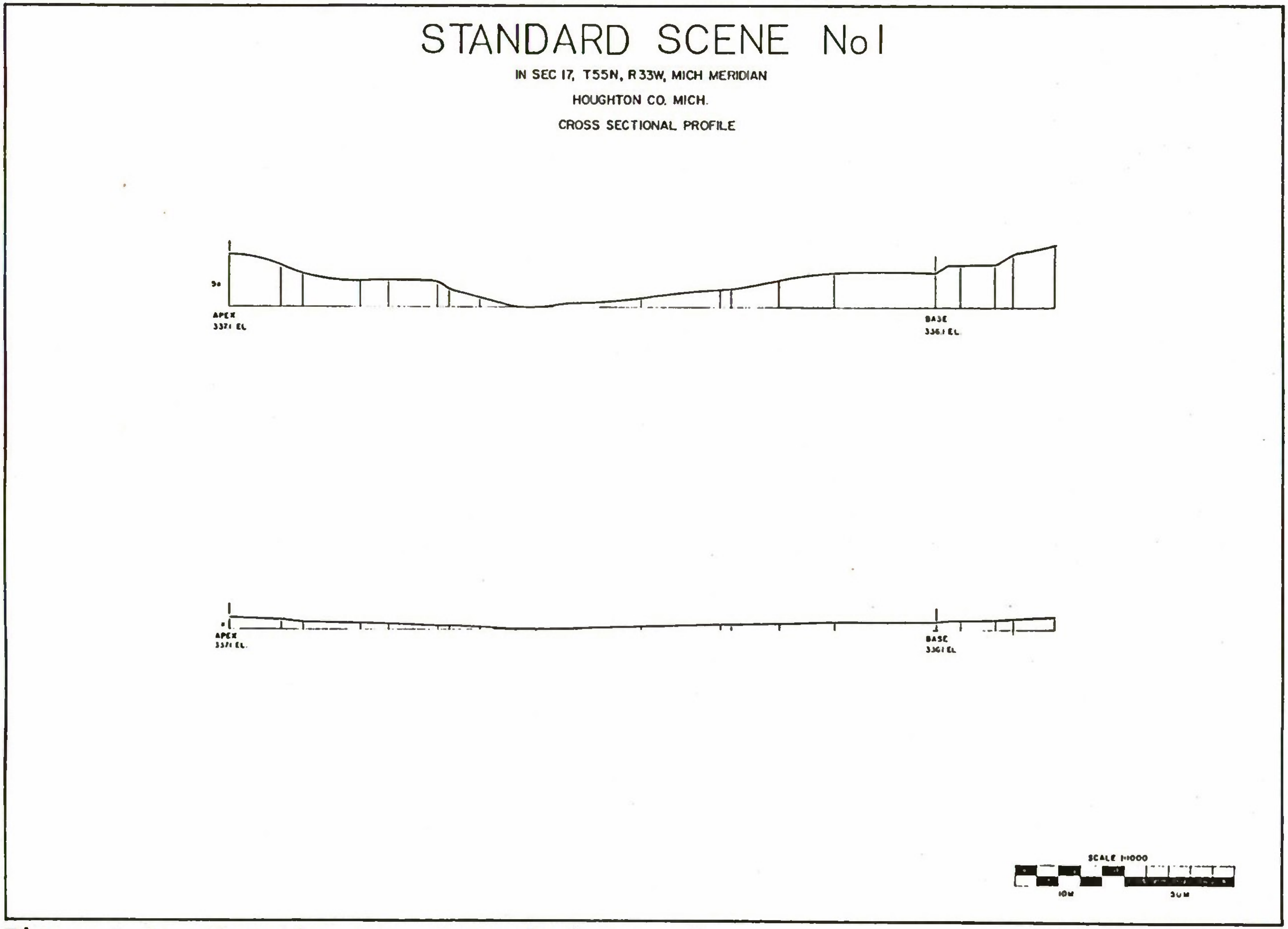

Figure A-13. Elevation Map of Standard Scene I

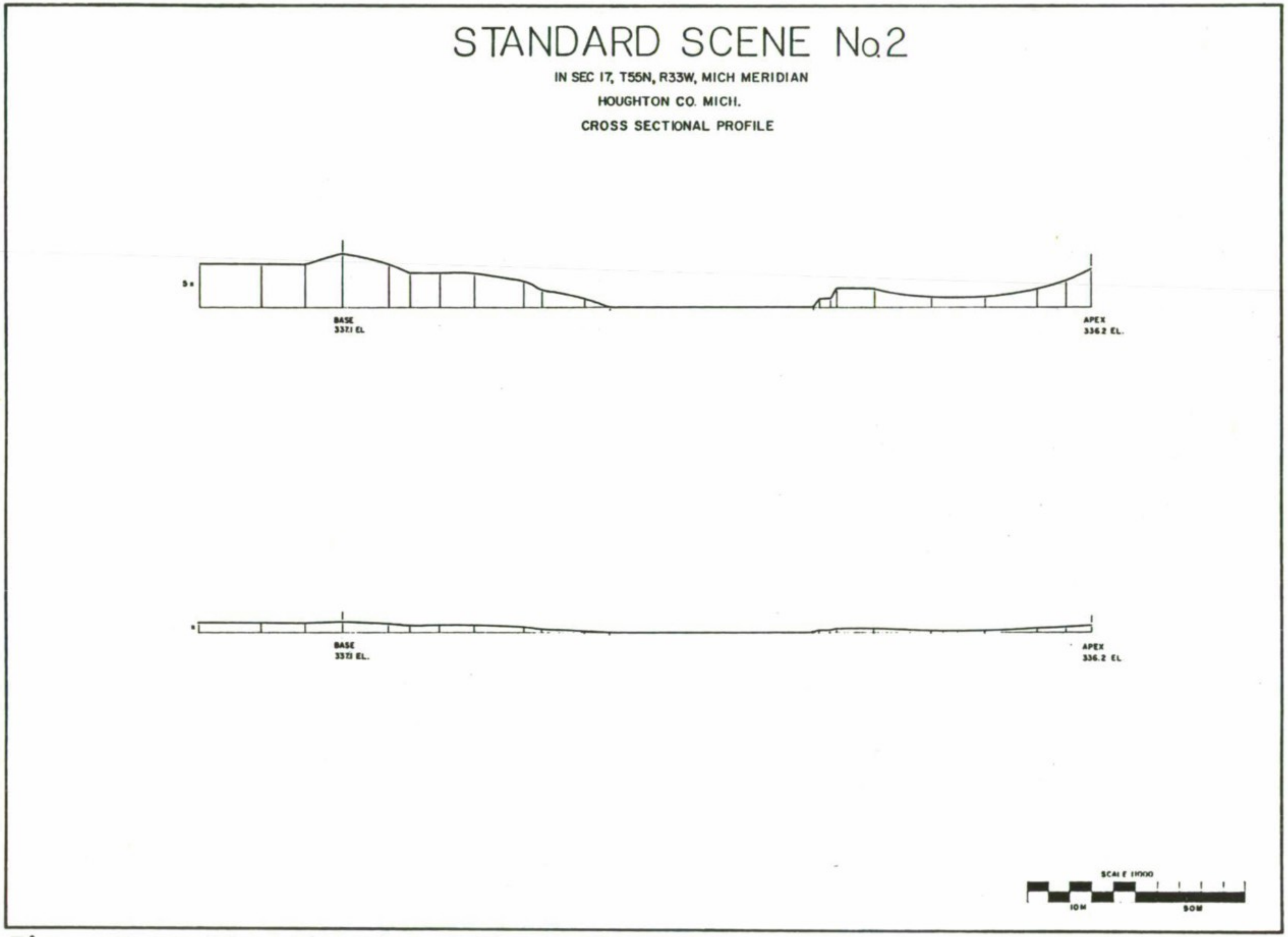

Figure A-14. Elevation Map of Standard Scene II

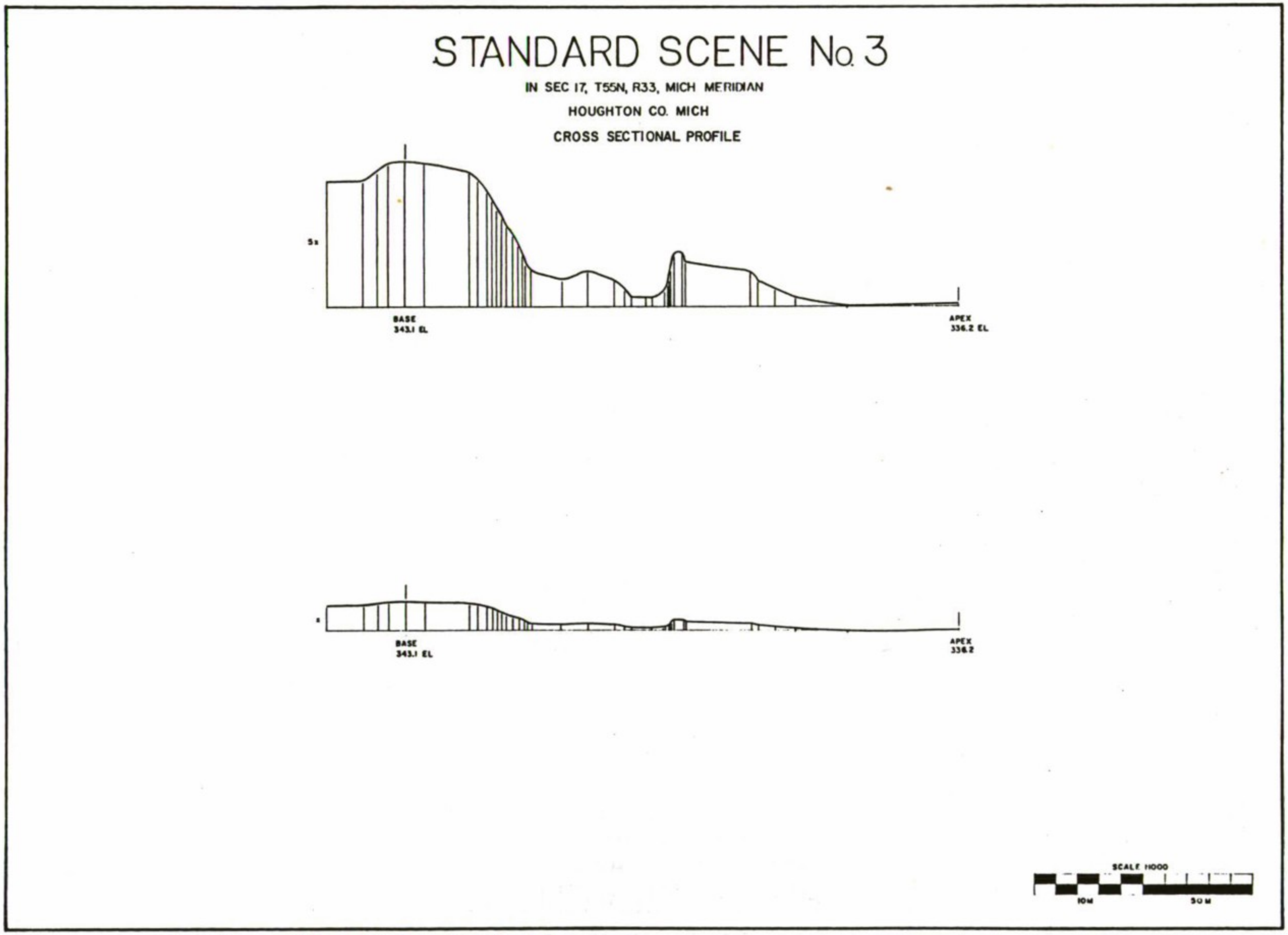

Figure A-15. Elevation Map of Standard Scene III

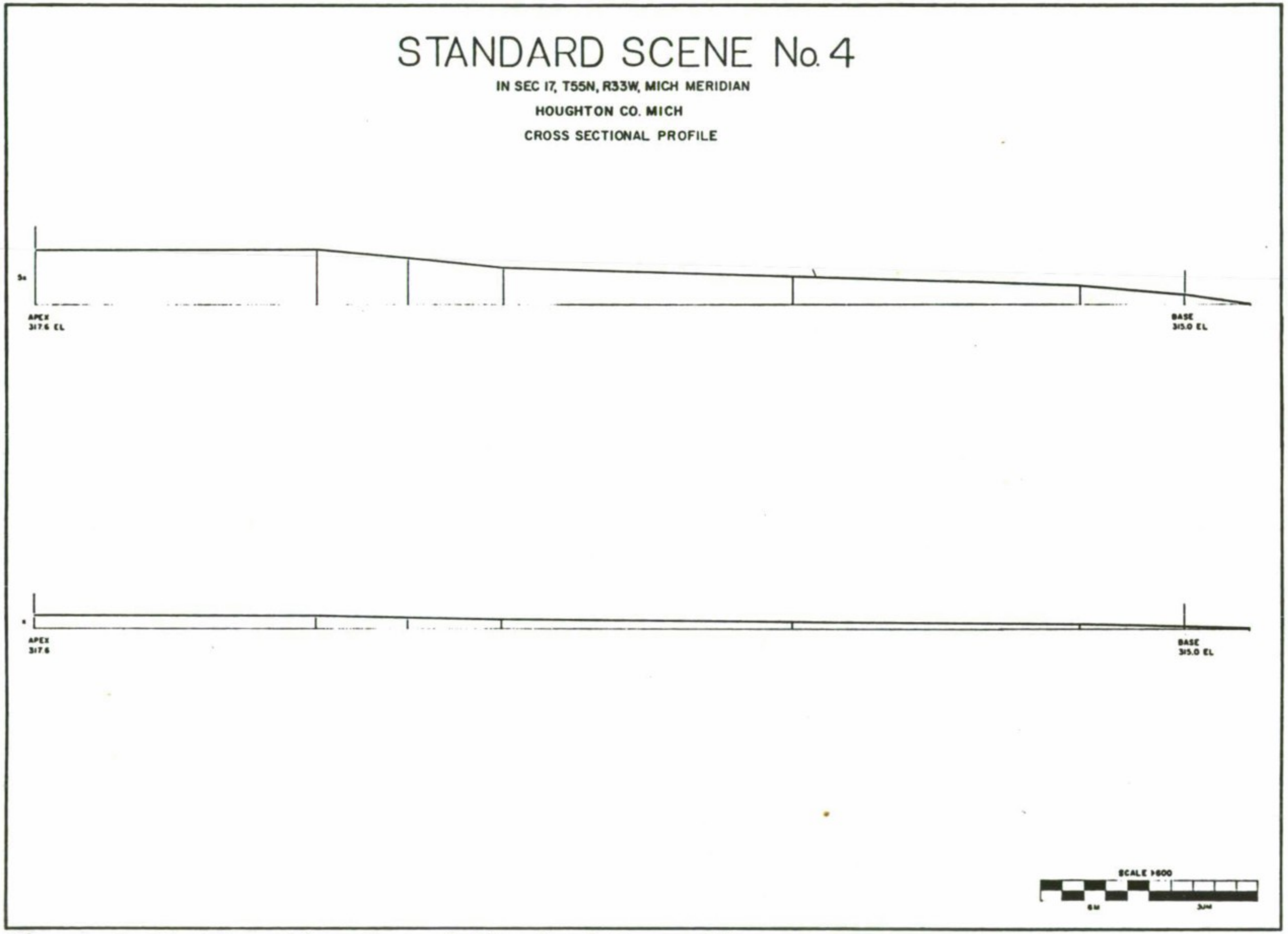

Figure A-16. Elevation Map of Standard Scene IV

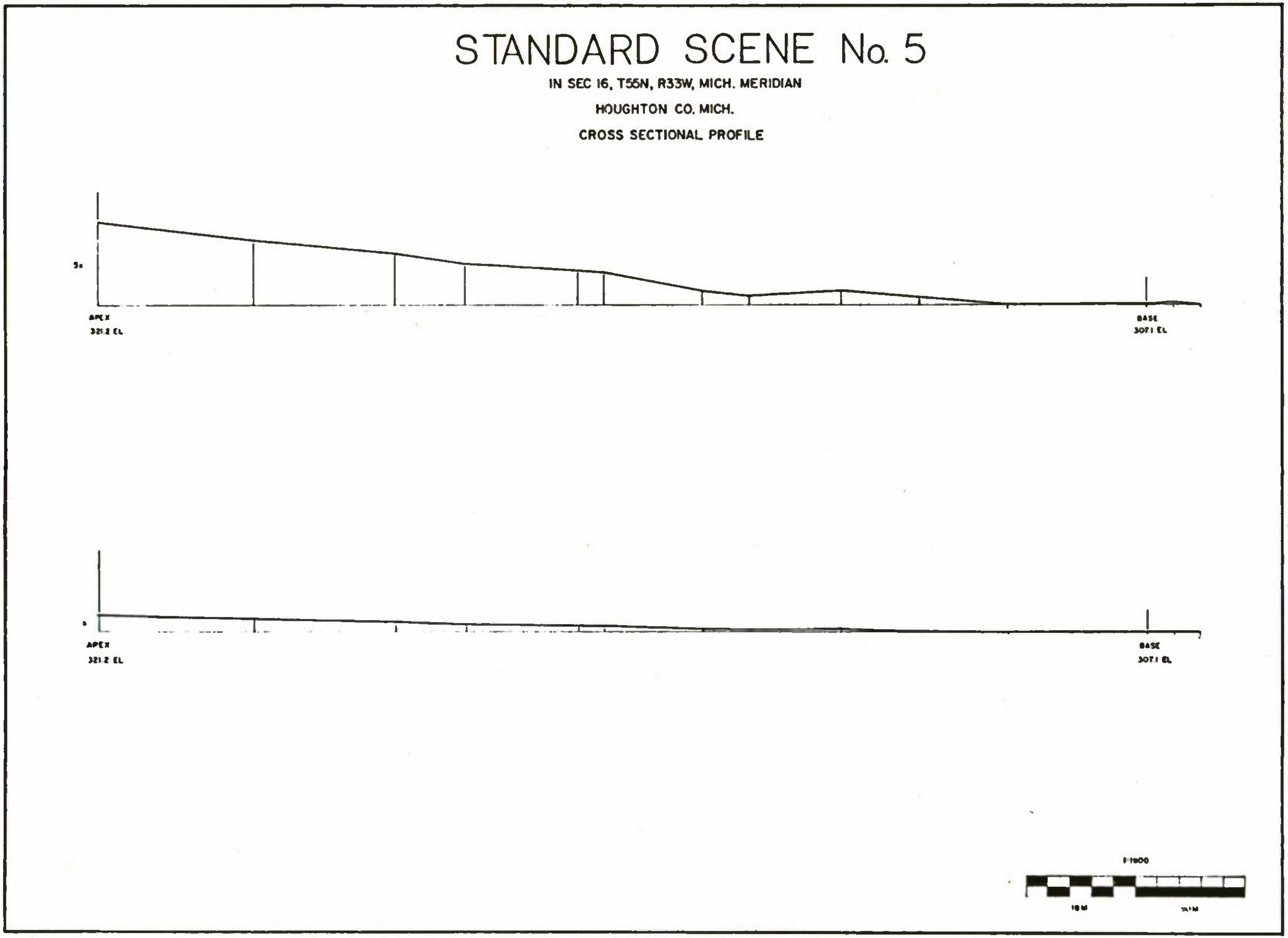

Figure A-17. Elevation Map of Standard Scene V

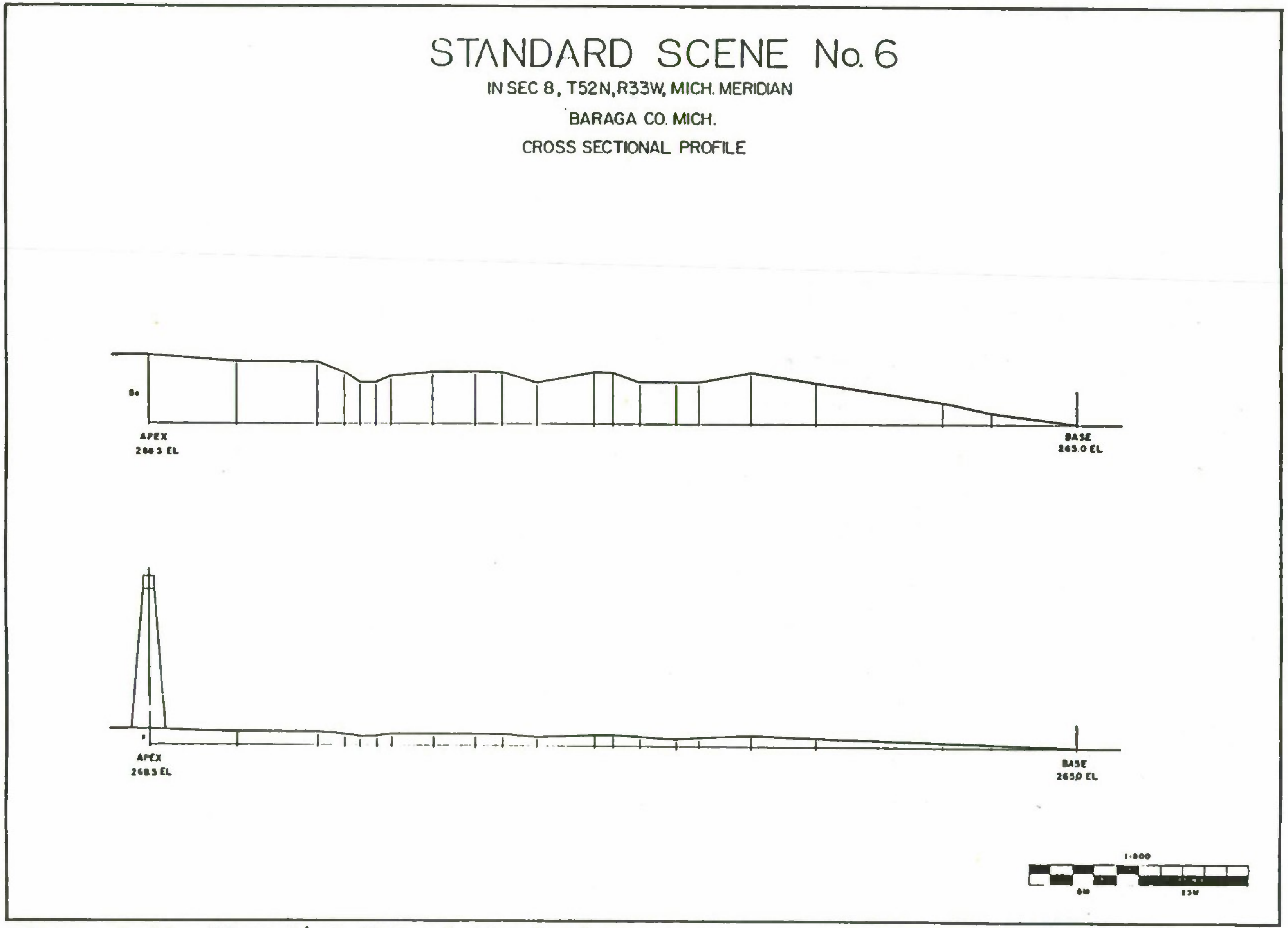

Figure A-18. Elevation Map of Standard Scene VI

A.3.0. <u>Soil Analysis</u>

Knowledge of soil types in an area, and of the properties of these soil types, contributes to tactical decision-making in a variety of ways. In the context of IR sensing, the thermal properties and moisture retaining capabilities of area soils are of particular interest. Soil properties affect the amount of clutter, and the target-background contrast perceived in the IR. Therefore, the Standard Scenes Program included a thorough soil classification survey, the objectives of which were to sample, test and identify the soil types present in each standard scene, and to establish the boundaries of each soil type on site maps. The resulting soil classification maps are presented in Figures A-19 through A-24.

A.3.1. Soil Classification Survey of Standard Scenes. Field work consisted of collecting a bore sample 50 centimeters deep at several designated locations within the standard scene. Figure A-25 shows examples of photographic documentation of bore holes and sampling procedures used. Samples were placed in closed containers to hold moisture content. Samples were labeled and given a general description as to their color and consistency.

Laboratory tests were conducted to identify soil samples according to the Unified Soil Classification System (USGS). This system begins with an examination to determine whether the soil is highly organic (peaty), coarse-grained, or fine grained. A sieve analysis was used to distinguish between types of gravel and sand for the coarse grained soils. More fine grained soils are distinguished in terms of their moisture content and plasticity. Information derived from the sieve analysis included the percentage of clay, silt, and sand present in a sample, and this determined the soil textural classification according to the USDA classification schematic shown in Figure A-26.

Hydrometer analysis was used to determine the particle-size distribution in the fine grained (finer than No. 200 sieve size) fraction of the soil sample. A soil specimen is dispersed in water, and the hydrometer is used to measure the specific gravity of the soil-water suspension. Specific gravity is defined as the ratio of the soil unit weight to the unit weight of the water, and is a necessary quantity in calculations involving the unit weight of a soil.

A.3.2. Soil Thermal Characteristics. Additional information about thermal properties of different soil types were obtained from various sources. Thermal characteristics useful in modeling include soil conductivity and diffusivity[1,2], emissivity, and absorptivity[3].

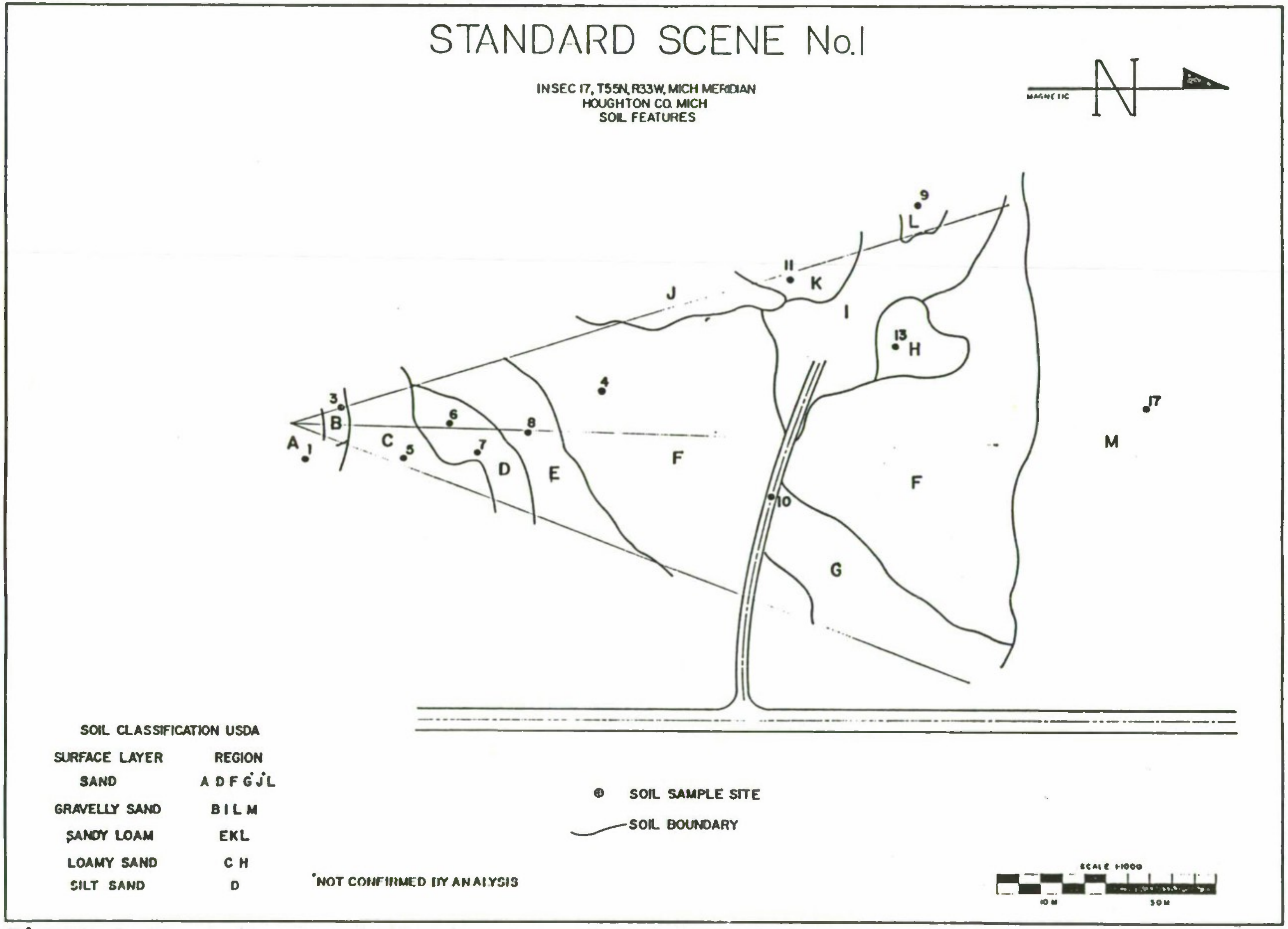

Figure A-19. Soil Classification Map of Standard Scene I

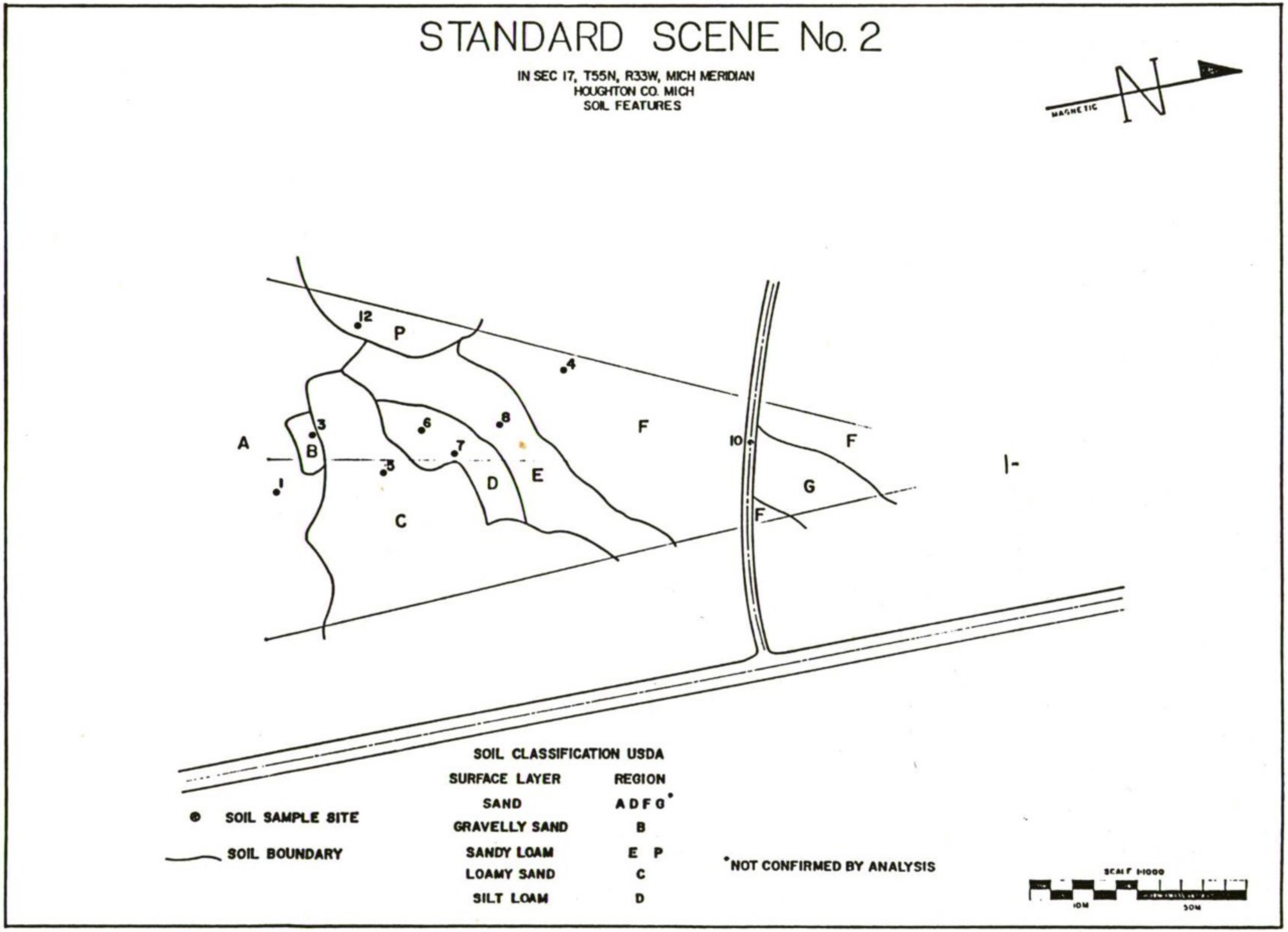

Figure A-20. Soil Classification Map of Standard Scene II

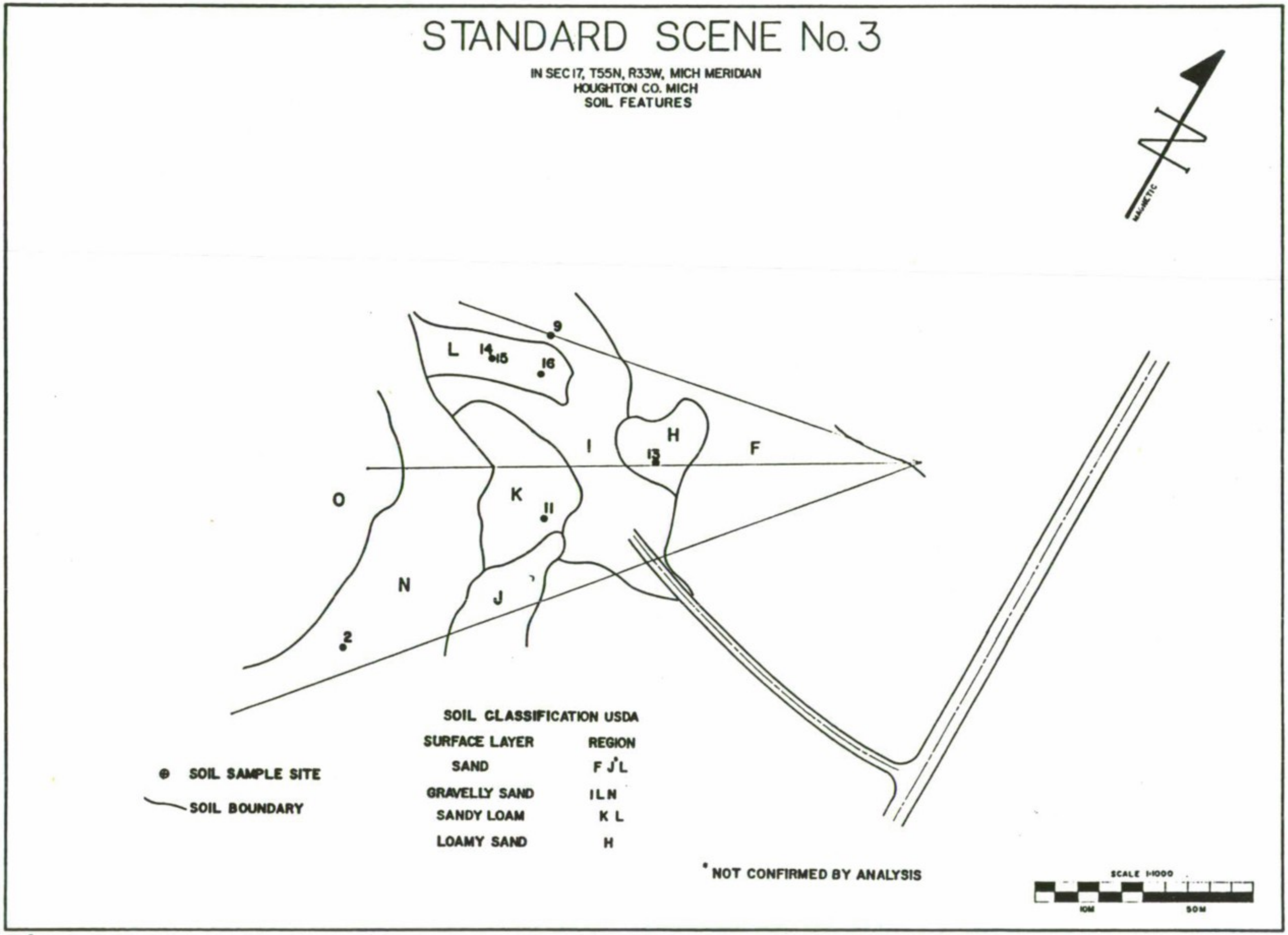

Figure A-21. Soil Classification Map of Standard Scene III

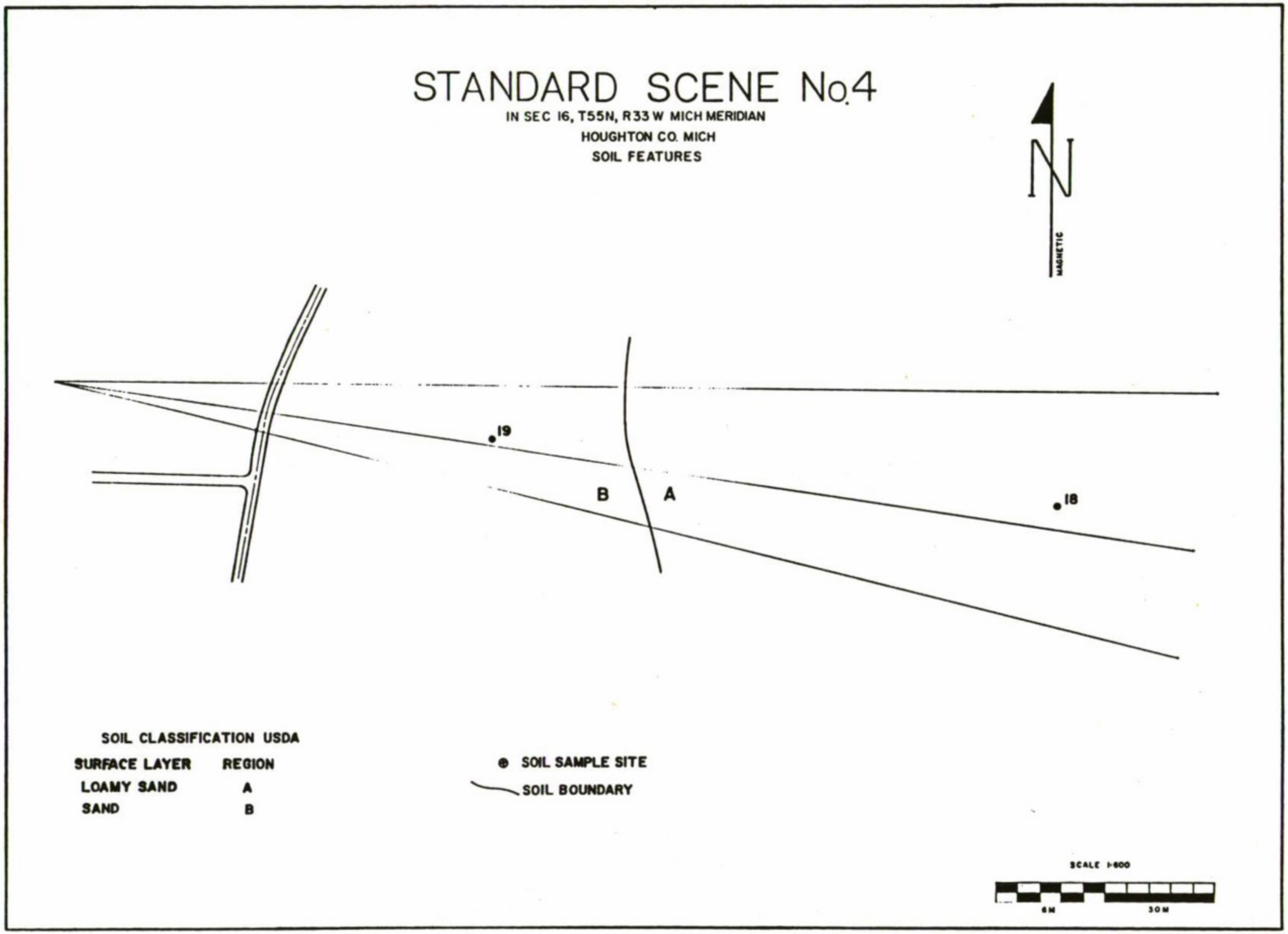

Figure A-22. Soil Classification Map of Standard Scene IV

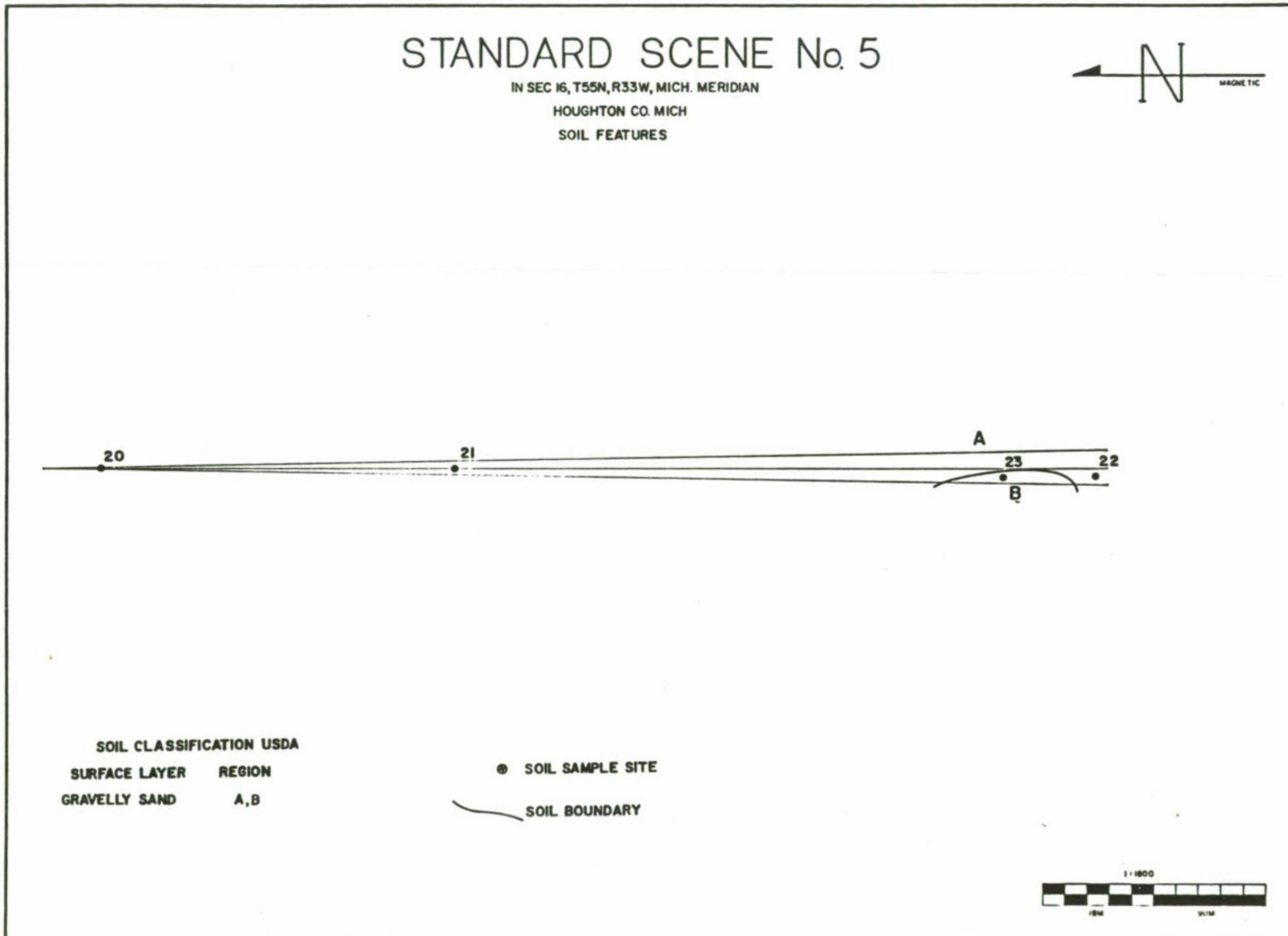

Figure A-23. Soil Classification Map of Standard Scene V

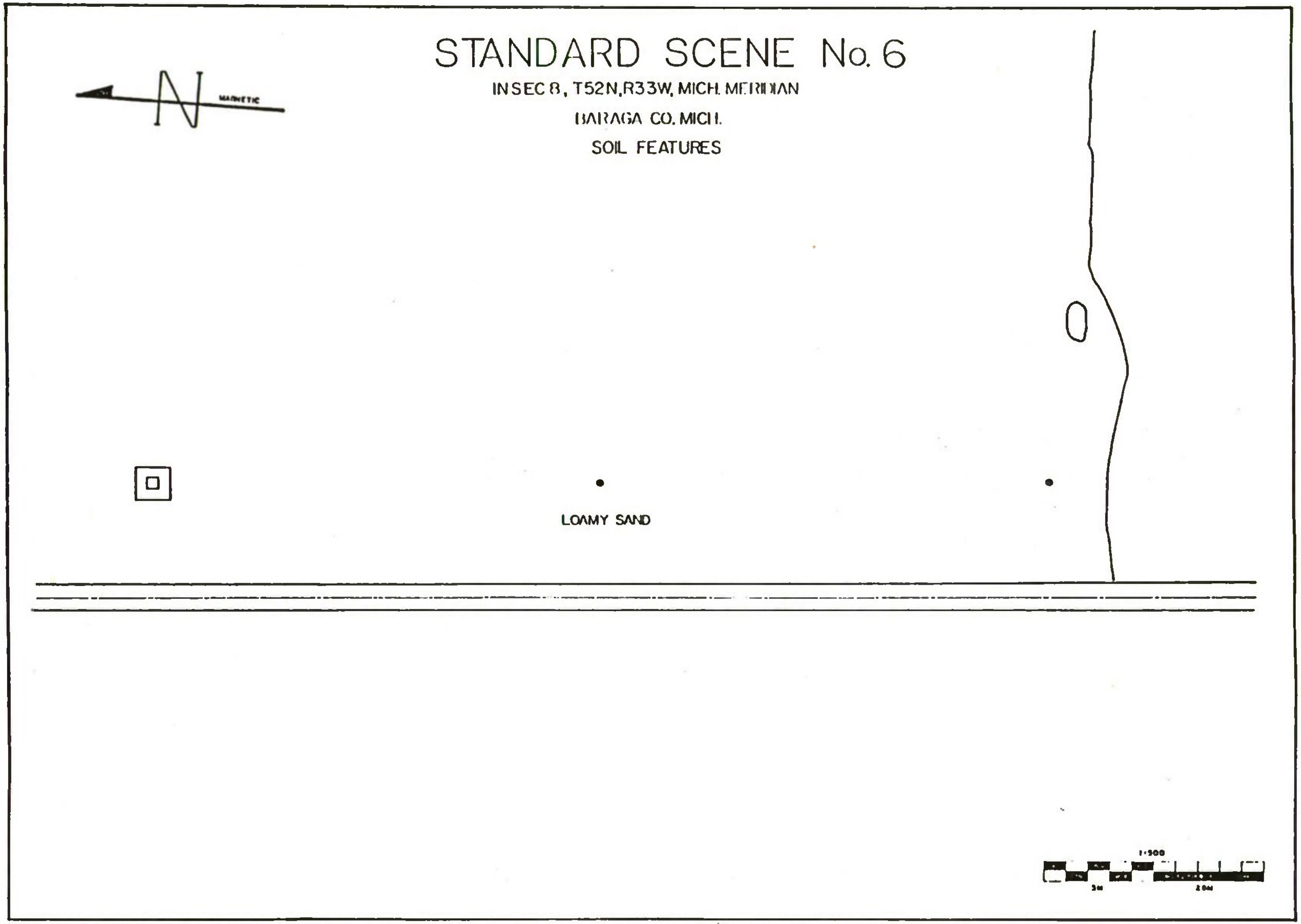

Figure A-24. Soil Classification Map of Standard Scene VI

A. Soil sample 4 from area common to Standard Scenes I and II is a bore sample made with the manual auger shown.

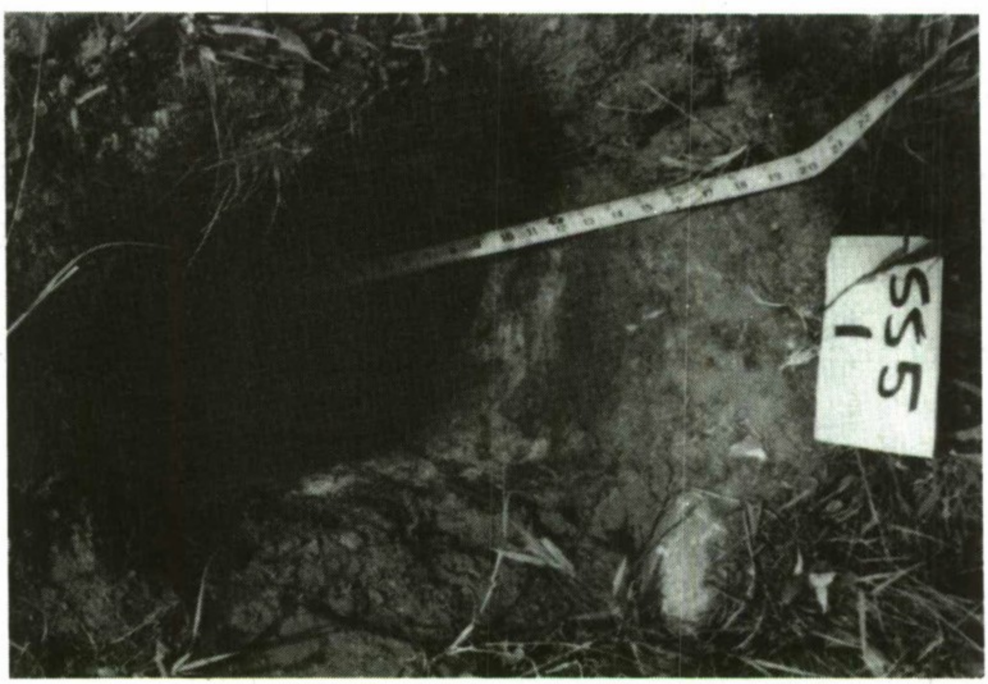

B. Soil sample 1 from Standard Scene V was made with a shovel.

Figure A-25. Soil sample examples

(Using Materials Less Than in 2.0 mm. in Size. If Approx. 20% or more of the soil material is larger than 2.0 mm. the texture term includes a modifier. Example: gravelly sandy loam.

Example of Use: A soil material with 35% clay, 30% silt and 35% sand is a clay loam.

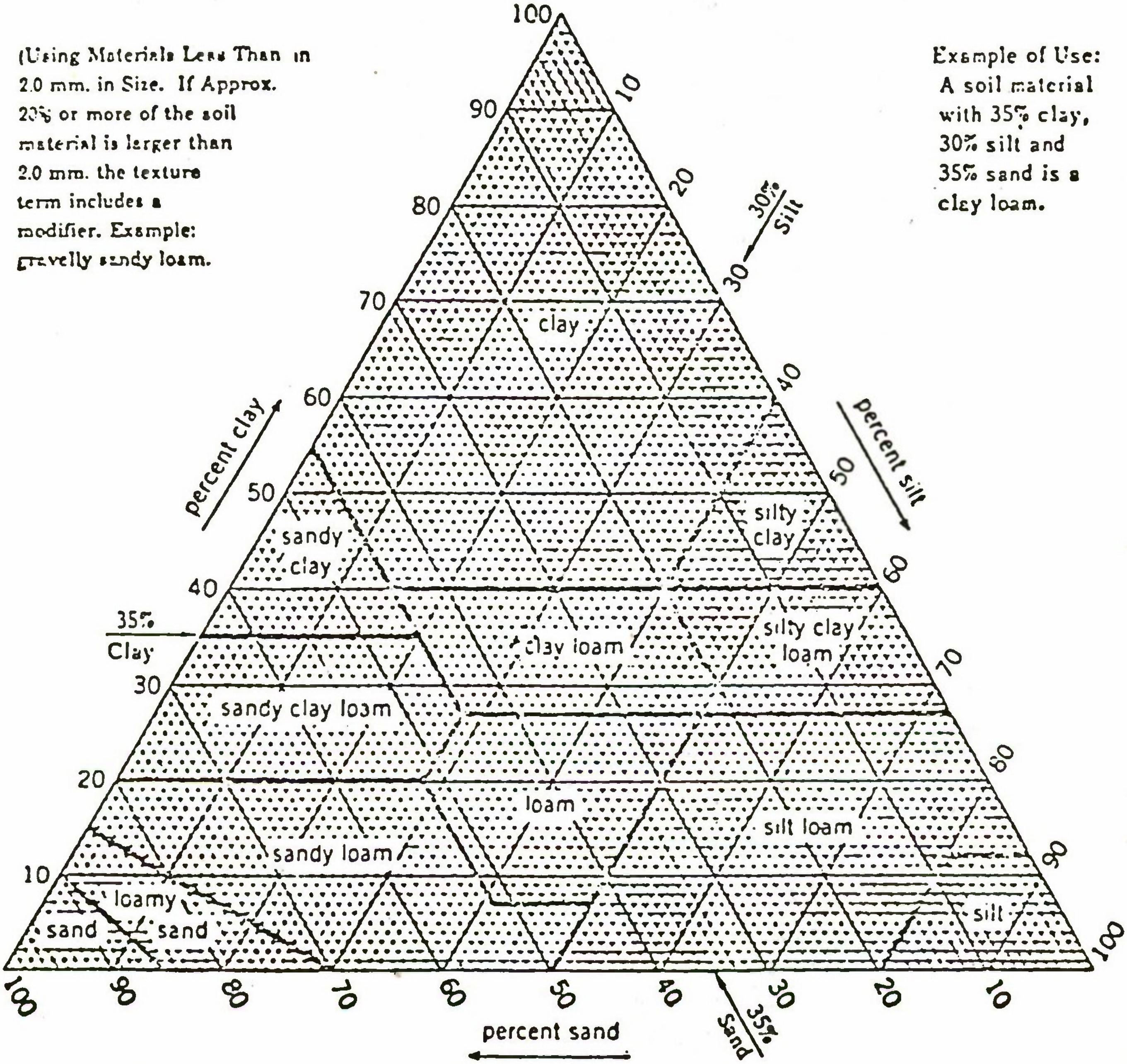

Figure A-26. Guide for USDA soil textural classification

A.4.0. Vegetation Survey

A.4.1. Vegetation Inventory. The principal communities of vegetation types in the standard scenes were identified and delineated. They are shown in the vegetation maps presented in Figures A-27 through A-32. Areas occupied predominantly by a certain community type were measured and staked, and plant collections made from them. Plants were identified at least to genus and, in many cases, species. Two samples of each plant collected were pressed and dried. The plant list given in Table A-2 displays the variety of species present.

Field methods used in the inventory include the step-point transect method which is used to characterize the variou vegetative communities. The method is adapted from the soil-vegetation inventory method used by the U.S. Department of the Interior Bureau of Land Management. The step-point transect method involves identifying and categorizing ground cover, vegetative canopy layers, and phenological stage of development of observed plants. The average hieght in meters, percent ground cover, and number of plants per unit area are recorded for each plant species.

The point-centered quarter method is used in wooded areas to determine density, dominance, and relative frequency of tree species. One notable limitation of this method is that it does not yield the percent cover of the crown, which is an important consideration in terms of thermal effects.

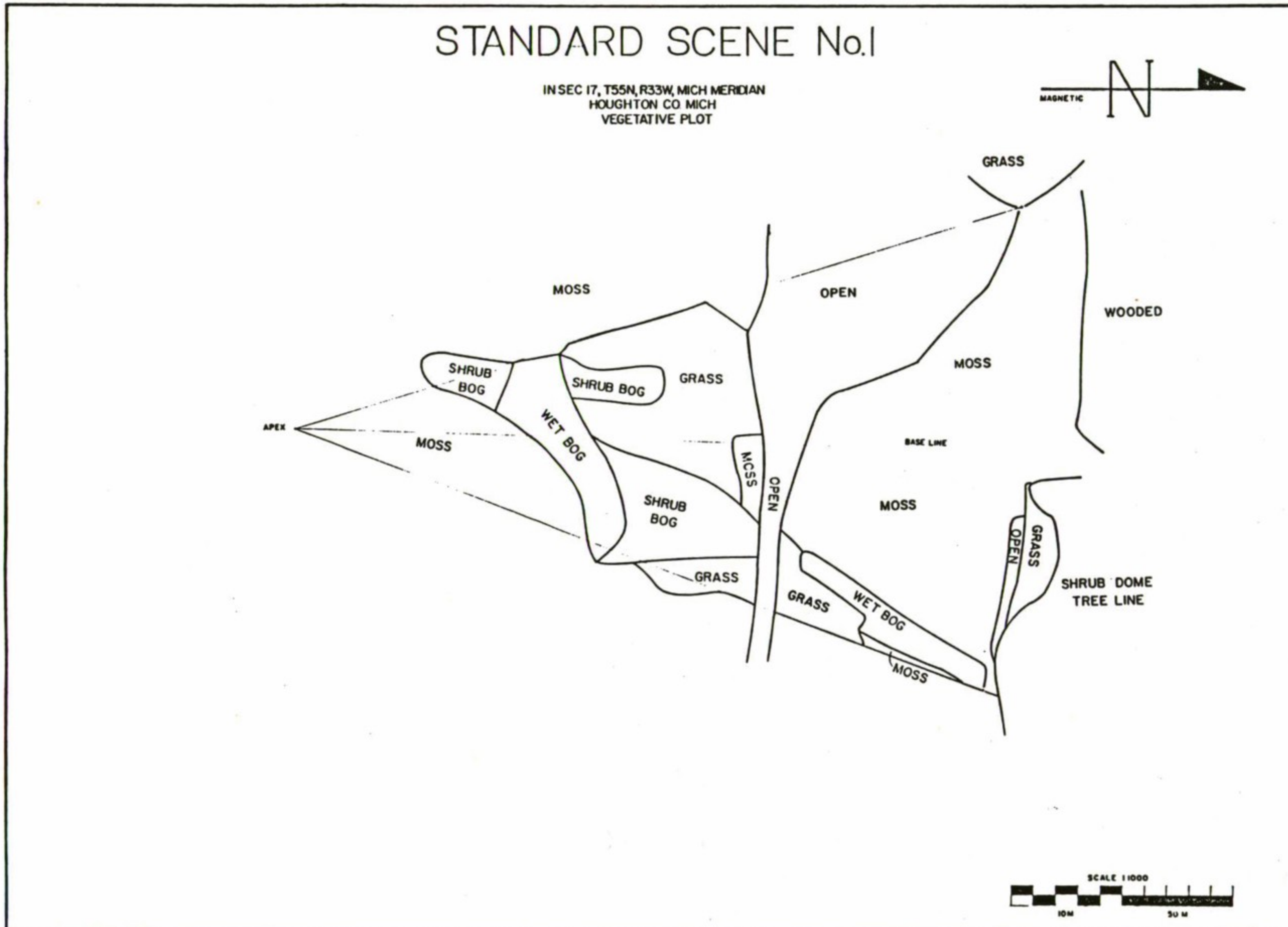

Figure A-27. Vegetation Map of Standard Scene I

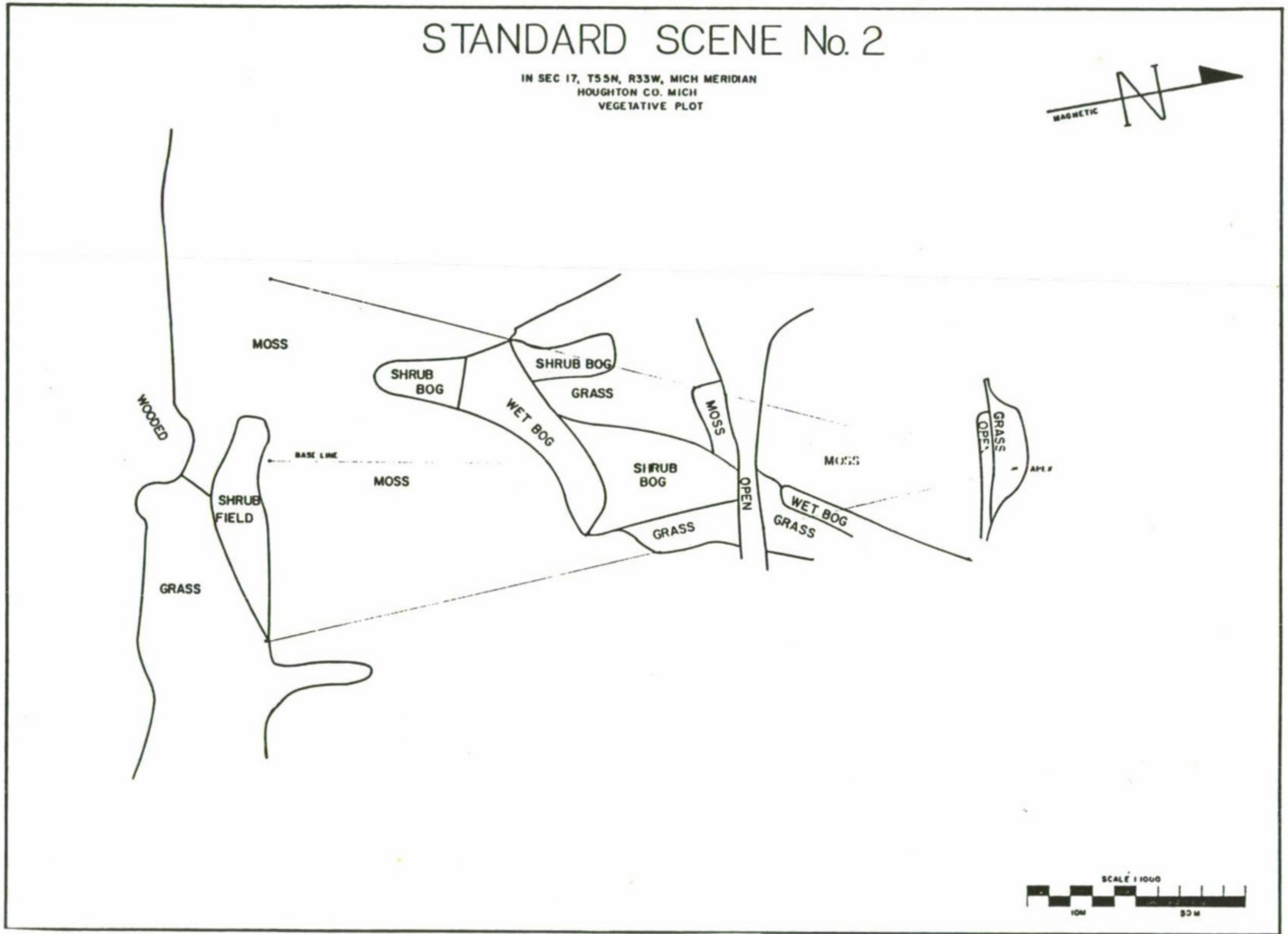

Figure A-28. Vegetation Map of Standard Scene II

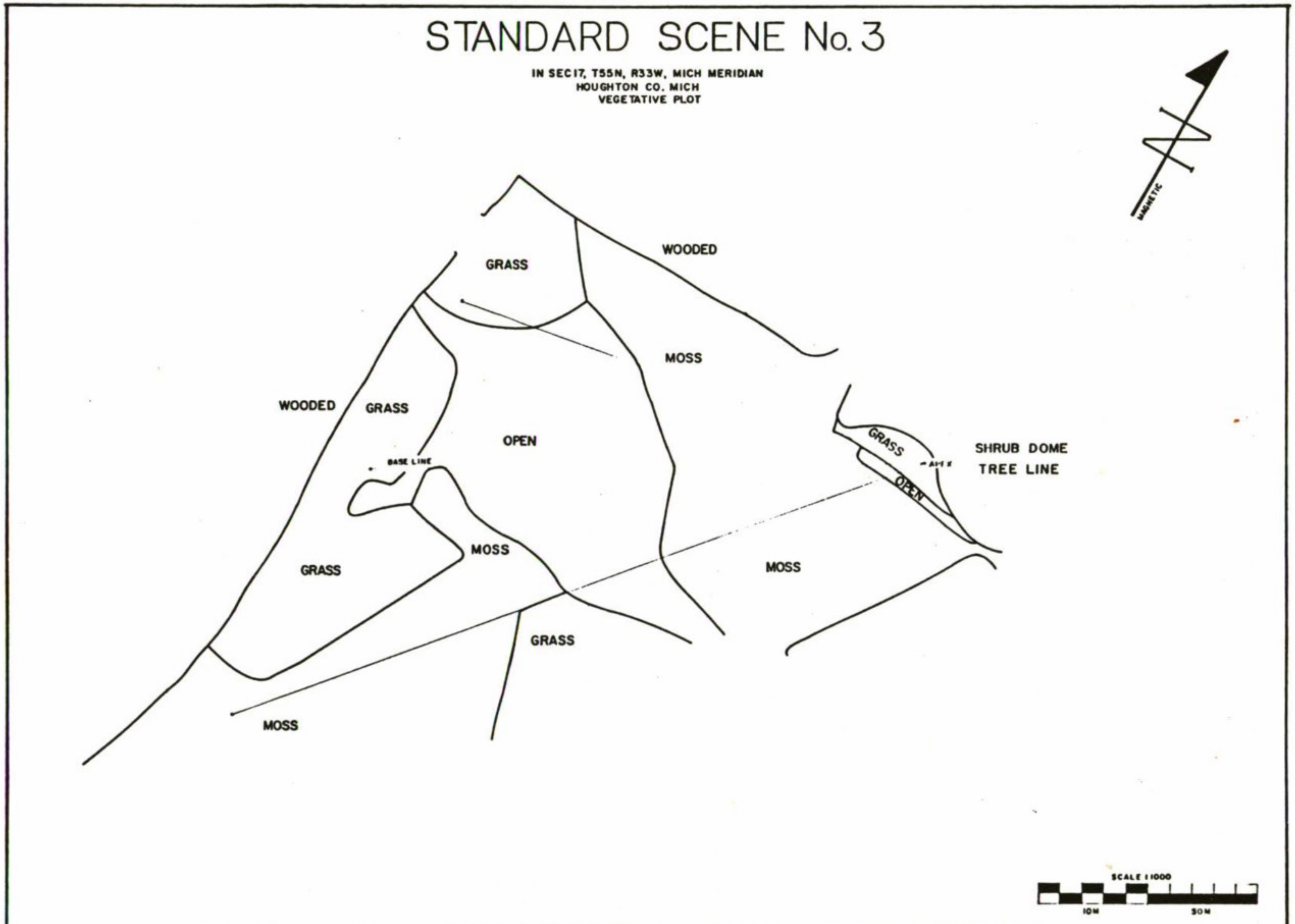

Figure A-29. Vegetation Map of Standard Scene III

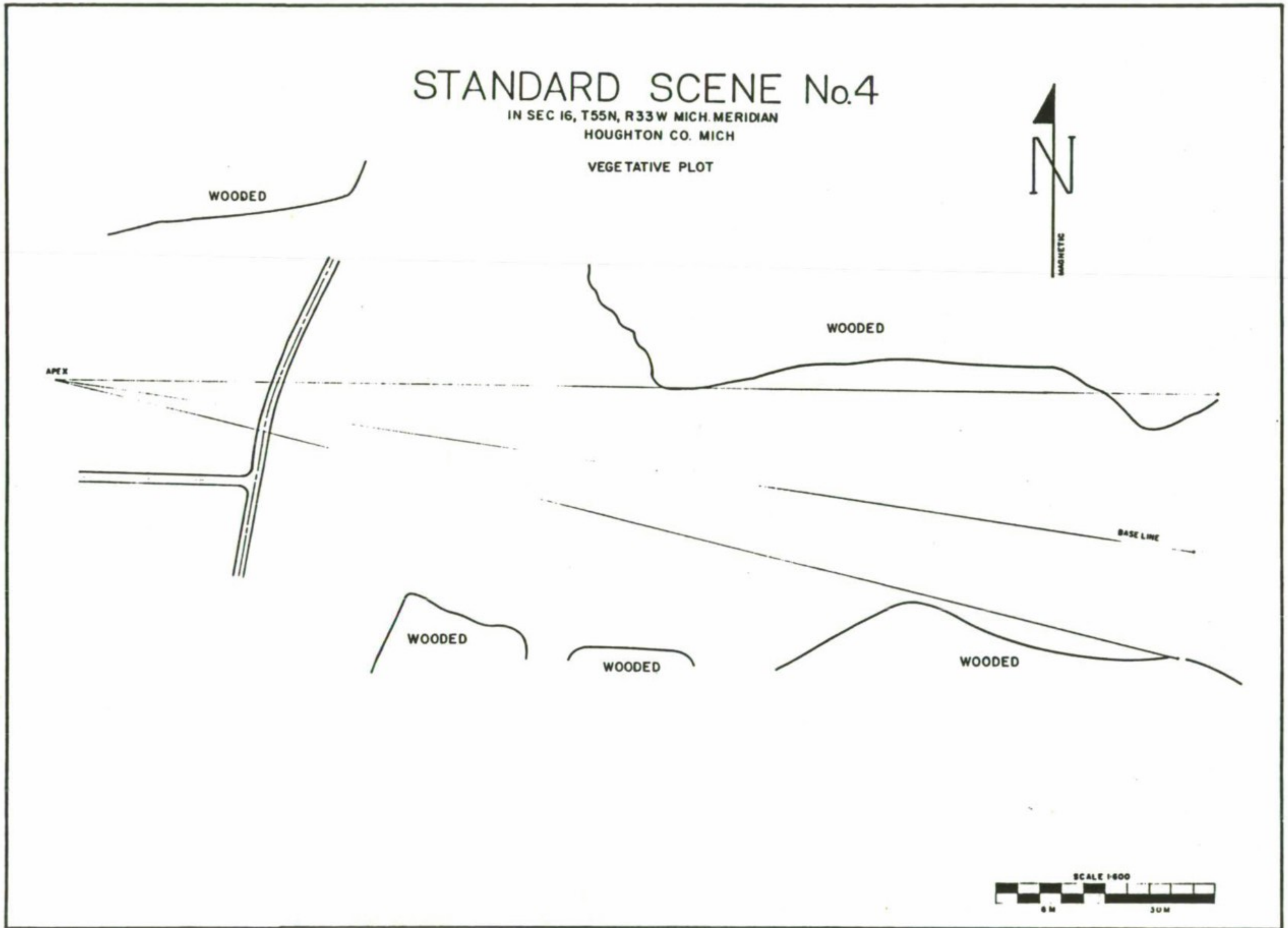

Figure A-30. Vegetation Map of Standard Scene IV

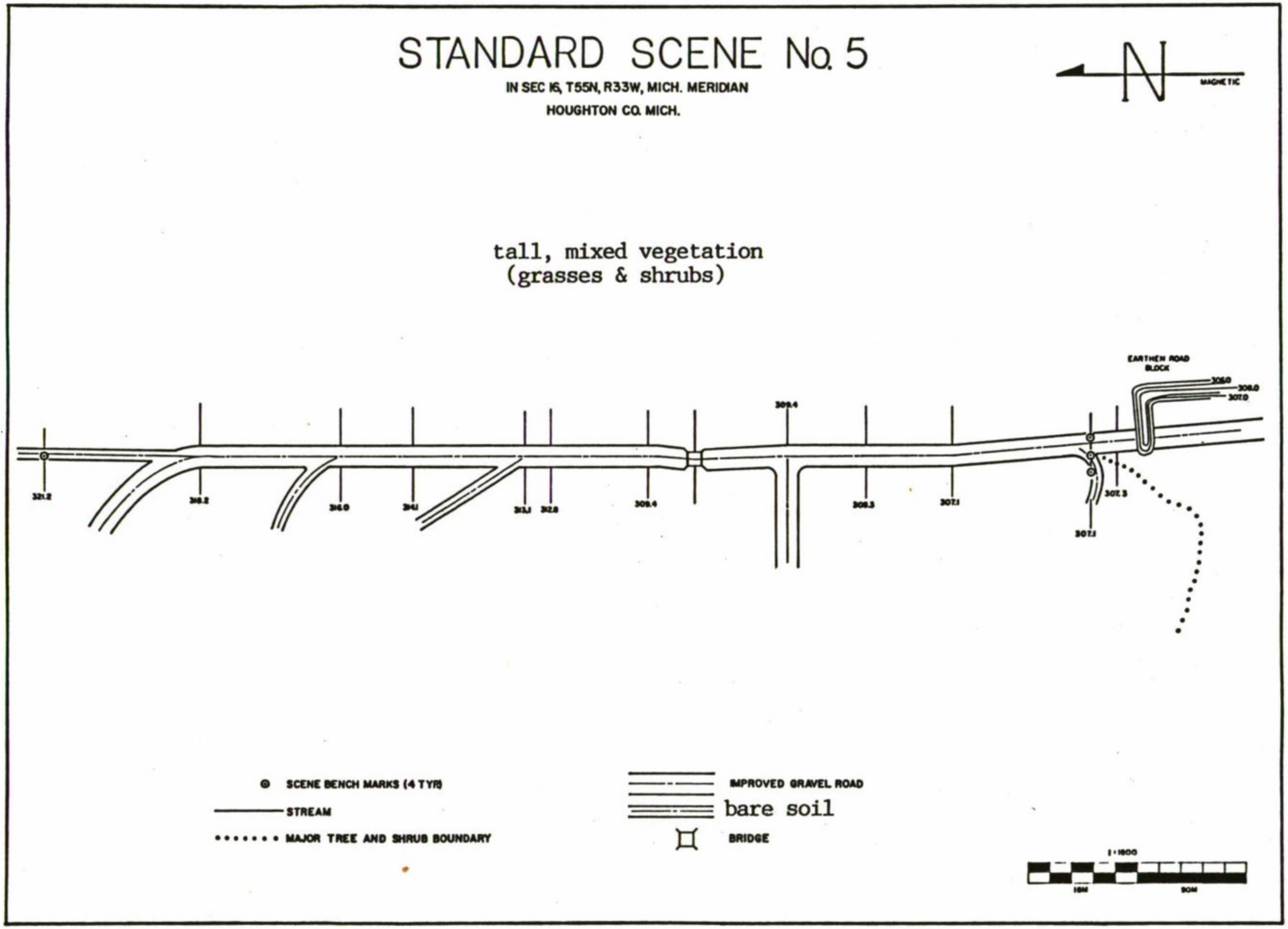

Figure A-31. Vegetation Map of Standard Scene V

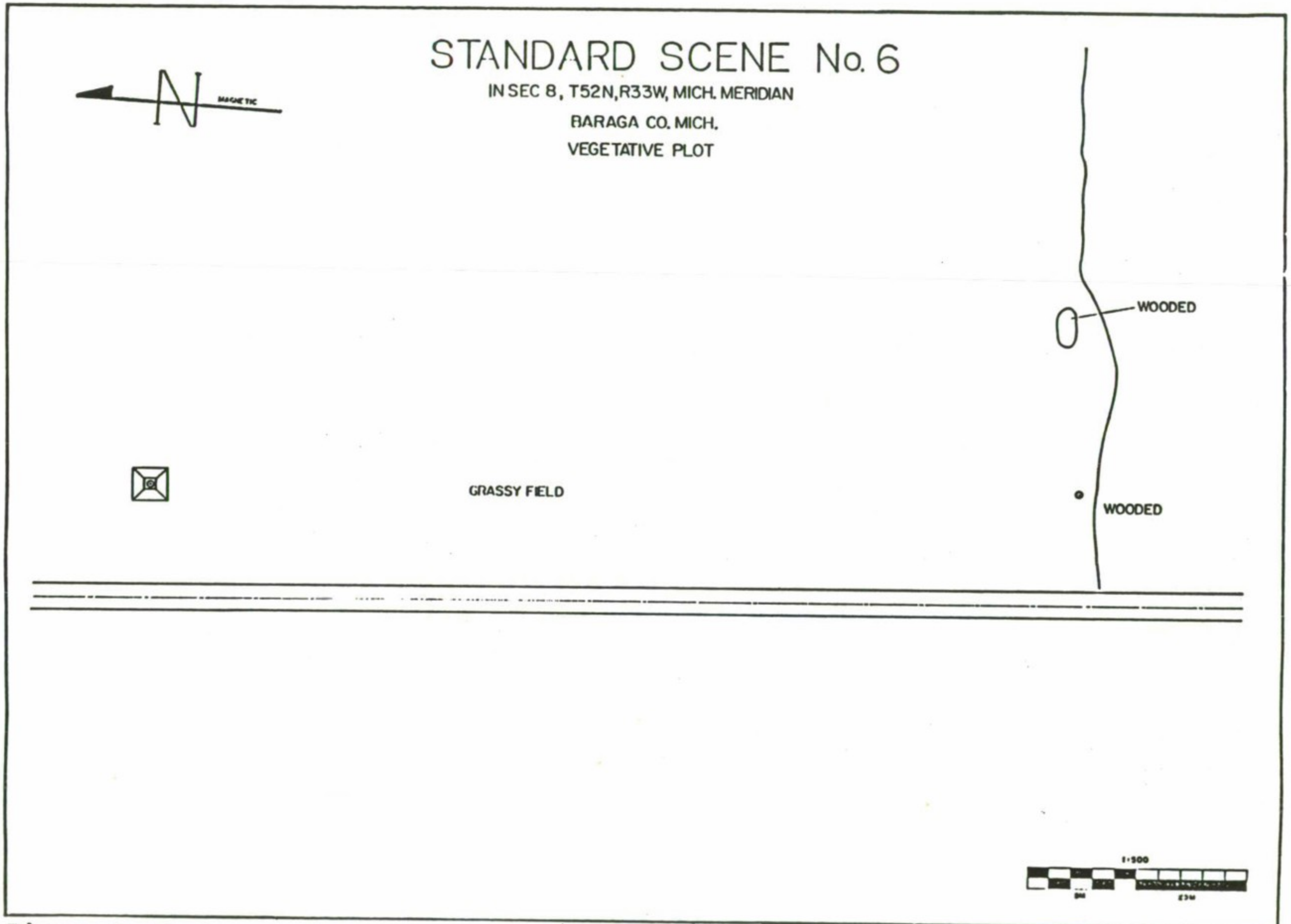

Figure A-32. Vegetation Map of Standard Scene VI

Table A-2. Vegetation species in Standard Scenes

Herbaceous Species (H)

Symbol	Scientific Name	Common Name
ACMI	Achillea millefolium	Yarrow
ANMA	Anaphalis margaritacea	Pearly Everlasting
ASTER	Aster spp.	Species of Aster
ANTE	Antennaria spp.	Pussytoes
CHLE	Chrysantemum leucanthemum	Ox-eye Daisy
CHRYS	Chrysanthemum spp.	Species of chrysanthemum
CIRS	Cirsium spp.	Species of thistle
DIAM	Dianthus armeria	Deptford Pink
EPAN	Epilobium angustifolium	Fireweed
FRVI	Fragaria virginiana	Common strawberry
HABEN	Habenaria spp.	Twayblade
HIAU	Hieracium aurantiacum	Orange Hawkweed or Devil's Paintbrush
HICA	Hieracium canadense	Canada Hawkweed
HIER	Hieracium spp.	Species of Hawkweed
HYPU	Hypericum punctatum	Spotted St. Johnswort
LACT	Lactuca spp.	Species of Lettuce
MACA	Maianthemum canadense	Canada Mayflower
MELIL	Melilotus - alba	White Sweet Clover
	- officinalis	Yellow Sweet Clover
PLLA	Plantago lanceolata	English, or lanceleaf Plantain
PLMA	Plantago major	Common plantain
PTAQ	Pteridium aquilinum	Bracken fern
RAAC	Ranunculus acris	Common, or tall, Buttercup
ROSA	Rosa spp.	Species of Rose
RUAC	Rumex acetosella	Red, sheep, or common sorrel
SICU	Silene cucubalus	Bladder Campion
SMRA	Smilacina racemosa	False Solomon's-seal
SOLID	Solidago spp.	Species of Goldenrod
STELL	Stellaria spp.	Species of chickweed
STRO	Streptopus roseus	Rose Twisted-stalk
TARA	Taraxacum spp.	Species of Dandelion
TRBD	Trientalis borealis	Starflower
TRIF	Trifolium spp.	Species of Clover
TRPR	Trifolium pratense	Red clover
TRRE	Trifolium repens	White clover
VIOLA	Viola spp.	Species of violet

Table A-2, Continued. Vegetation species in Standard Scenes

Shrub and Tree Species (S & T)

Symbol	Scientific Name	Common Name
ACSA	Acer saccharum	Sugar Maple
ALRU	Alnus rugosa	Speckled, or Tag, or Hoary Alder
FRAX	Fraxinus spp.	Species of Ash
OSVI	Ostrya virginiana	Ironwood or Hop-hornbeam
PRPE	Prunus pennsylvanica	Pin Cherry
QURU	Quercus rubra	N. Red Oak
RUBUS	Rubus spp.	Species of Raspberry and Blackberrry
SALIX	Salix spp.	Species of Willow

Grass and Grasslike Species (G)

AGROS	Agrostis spp.	Species of Tickle Grass or Redtop
AGROP	Agropyron repens	Quack Grass
BROM	Bromus spp.	Species of Brome
CAREX	Carex spp.	Species of sedge
EQUIS	Equisetum spp.	Species of Horsetail
JUNCUS	Juncus spp.	Species of Rush
OSCL	Osmunda chlaythoniana	Interrupted Fern
PHLEUM	Phleum pratense	Timothy Grass
POA	Poa compressa	Canada Bluegrass
SISY	Sisyrinchium spp.	Species of Blue-eyed Grass

Moss/Mosslike (M)

Lycop	Lycopodium spp.	Clubmoss

A.5.0. Meteorological and Physical Observations

Meteorological variables and soil temperature are sampled at five minute intervals (solar irradiance is sampled once each minute) throughout each 24-hour field test period. Measurements are made and recorded automatically by a portable weather station maintained by KRC. This data set is supplemented by written observations regarding sky and atmospheric conditions logged by field test personnel, and by observations from the Flight Service Station at the Houghton County Memorial Airport. Observations by the Flight Service Station are recorded hourly, using the form shown in Figure A-33.

A.5.1. Sample Plotted Data. Examples of principal weather variables plotted across a 24-hour period are shown in Figures A-34 through A-38. Data for these figures came from a field test conducted at Standard Scene V, on 9-10 August, 1984.

A.5.2. Weather File Format and Description. Weather data from Standard Scene Program field tests is available in several formats, and KRC has developed software that can be used to select and reformat data on selected meteorological parameters. Data is also available in the format of the weather files used in the PRISM (Physically Reasonable Infrared Signature Model) computer model. An excerpt from KRC's PRISM User's Manual describing the weather file is shown in Table A-3.

A.5.3. Soil Temperature and Moisture Observations. As already mentioned, soil temperature is automatically measured and recorded every five minutes. This is accomplished by means of a soil probe attached to the on-site weather data station. The probe registers soil temperatures at the surface and at 1, 5, 10, 20, and 50 cm depths, for the point in the scene at which the probe is located.

During the 1985 Standard Scene field tests, two or more soil samples were taken from the area of each Standard Scene for the purpose of measuring soil moisture. These samples were taken concurrently with infrared imagery of the scene. At selected spots, soil was sampled from the surface (top 1 cm), and then at successive depths of 5, 10, 25, and 50 cm beneath the surface. The moisture content (percent) and descriptive notes were recorded as shown in Figure A-39.

Figure A-33. Surface Weather Observations Form MFI-10C (65% actual size)

MFI-10C (8-77)

U.S. DEPARTMENT OF COMMERCE
NATIONAL OCEANIC AND ATMOSPHERIC ADMINISTRATION
NATIONAL WEATHER SERVICE

SURFACE WEATHER OBSERVATIONS
(Abridged for use at designated Cred Stations)

To convert LST to GMT ADD 5 hrs. | Time in Column 2 is: GMT ___ LST ✓

STATION: FAA HOUGHTON, MI
DATE: SEPT 1 - 1978

TYPE (1)	TIME (2)	SKY AND CEILING (Hundreds of feet) (3)	VISIBILITY (miles) SURFACE (4)	TOWER (4a)	WEATHER AND OBSTRUCTIONS TO VISION (5)	SEA LEVEL PRESS. (mb.) (6)	TEMP (°F) (7)	DEW PT. (°F) (8)	WIND DIREC-TION (9)	WIND SPEED (kts.) (10)	WIND CHAR-ACTER (11)	ALTIM. SETTING (ins.) (12)	REMARKS AND SUPPLEMENTAL CODED DATA (13)	STATION PRESSURE (ins.) (17)	DRY BULB (°F) (18)	WET BULB (°F) (19)	TOTAL SKY COVER (21)	TOTAL OPAQUE SKY COVER (22)	OBSERVER'S INITIALS (15)
R	0057	250-BKN	40			190	57	54	00	00		008	605 68	28930	57.0	55.2	7	3	TL
R	0158	250-BKN	40			185	57	54	13	06		007		28915	57.0	55.0	6	2	TL
R	0257	100 SCT 250-BKN	40			181	58	53	18	10		006	OCNL LTNG N	28905	58.2	55.3	7	3	TL
R	0358	E100 BKN 250 OVC	40			179	59	55	00	00		005	610	28900	58.5	56.4	10	8	TL
R	0456	E100 BKN 250 OVC	40			179	59	56	00	00		005		28900	59.2	57.0	10	10	TL
R	0557	80 SCT E250 OVC	40			181	58	54	00	00		006		28905	57.6	55.4	10	7	TL
R	0656	100 SCT E250 BKN	20			180	58	55	00	00		005	000 56	28900	57.5	56.6	9	7	TL
R	0755	E80 BKN 250 BKN	20			180	60	57	11	03		005		28.900	60.0	57.9	9	8	JH
R	0856	80 SCT 250 SCT	20			176	62	58	14	08		004		28.890	62.2	59.5	5	2	JH
R	0957	40 SCT 80 SCT 250-BKN	20			166	67	59	15	09		001	814	28.860	67.1	62.2	8	3	JH
R	1056	40 SCT 80 SCT 250-OVC	20			158	72	56	14	08		999		28.840	71.5	61.6	10	3	JH
R	1157	80 SCT 250-OVC	20			145	76	60	17	12		996		28.810	75.5	65.4	10	3	JH
R	1256	80 SCT 250-OVC	20			137	78	60	20	15	G22	994	724 56	28.790	77.6	66.1	10	5	JH
R	1357	60 SCT E250 OVC	20			126	77	61	20	17		990		28.755	77.1	66.5	10	7	JH
R	1456	E60 BKN 250 OVC	20			115	76	59	17	12		987		28.725	75.6	65.1	10	9	JH
R	1556	60 SCT 250-OVC	20			105	76	60	17	17		984	732	28.695	77.5	66.0	10	5	EE
R	1653	60 SCT 250-SCT	15			099	79	60	20	15	G23	982		28.680	78.7	66.7	5	2	EE
R	1750	250-SCT	15			099	77	59	20	15	G23	982		28.680	77.0	65.3	3	1	EE
R	1853	250-SCT	10			099	75	60	20	15	G22	982	605 79	28.680	75.3	65.3	3	1	EE
R	1953	250-SCT	7			099	72	59	21	13		982		28.680	71.5	63.6	1	0	EE
R	2055	CLR	7			105	72	56	21	13		984		28.700	71.6	62.8	0	0	EE
R	2156	CLR	7			109	71	59	21	15		985	310	28.710	70.7	63.5	0	0	EE
R	2250	CLR	7			109	70	58	21	13		985		28.710	70.1	62.6	0	0	EE
R	2356	CLR	7			112	70	59	20	06		986		28.720	70.0	62.8	0	0	TL

TIME (L.S.T.) (40)	NO. (41)	PRECIP. (ins.) (44)	SNOWFALL (ins.) (45)	SNOW DEPTH (ins.) (46)	MAX. TEMP. (°F) (47)	MIN. TEMP. (°F) (48)
0036	X	0	0	0	57	56
0050	•	0	0	0	62	56
0650	•	0	0	0	59	57
1251	•	0	0	0	79	57
1850	•	0	0	0	79	75
MID.	X	0	0	0	75	70

STATION PRESSURE COMPUTATIONS

TIME (L.S.T.) (50)	0055	0654	1253	1855
ATT. THERM. (60)				
OBSERVD. BAR. (61)				
TOTAL CORR. (62)				
STA. PRESS. (63)	28.930	28.900	28.790	28.680
BAROGRAPH (64)	28.940	28.900	28.800	28.675
BAR. CORR. (65)	-.010	0	-.010	+.005

SUMMARY OF DAY (Midnight to Midnight)

24-HR. MAX. TEMP. (°F) (66)	24-HR. MIN. TEMP. (°F) (67)	24-HR. PRECIP. WATER EQUIV. (ins.) (68)	24-HR. SNOWFALL UNMLTD. (ins.) (69)	1200 GMT SNOW (ins.) (70)
79	56	0	0	0

REMARKS, NOTES AND MISCELLANEOUS PHENOMENA (80)

MFI-10C (8-77) SUPERSEDES MFI-10C

☆ U.S. GPO: 1977-0-765-005

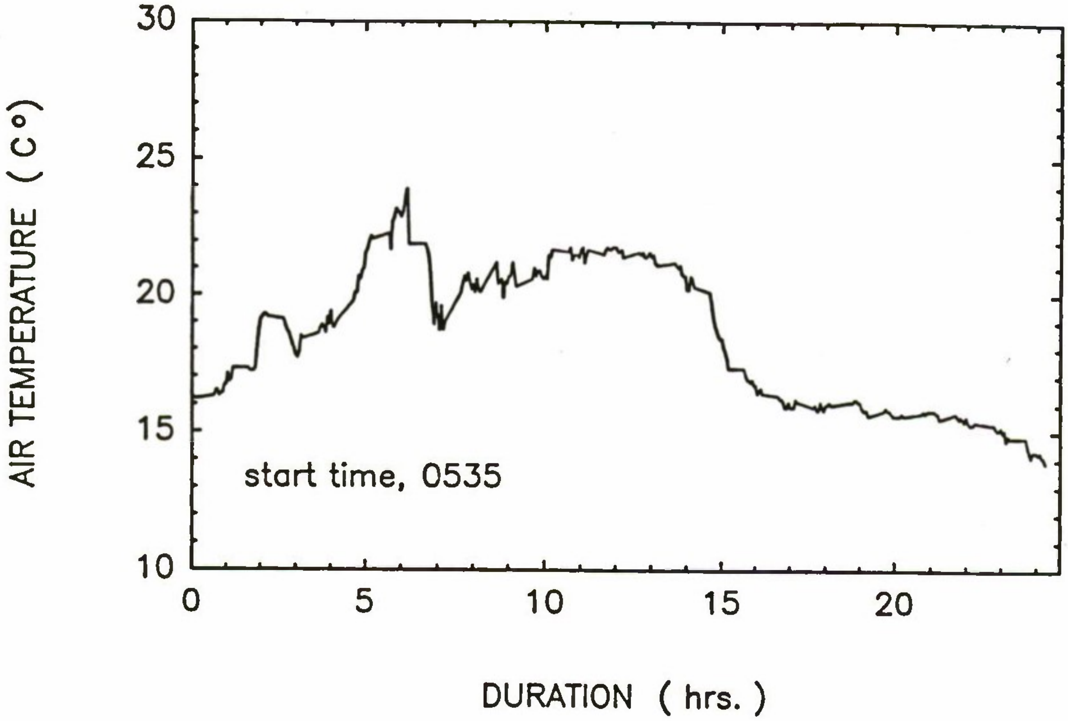

Figure A-34. Air Temperature Across Time, Scene V, 8/9/84.

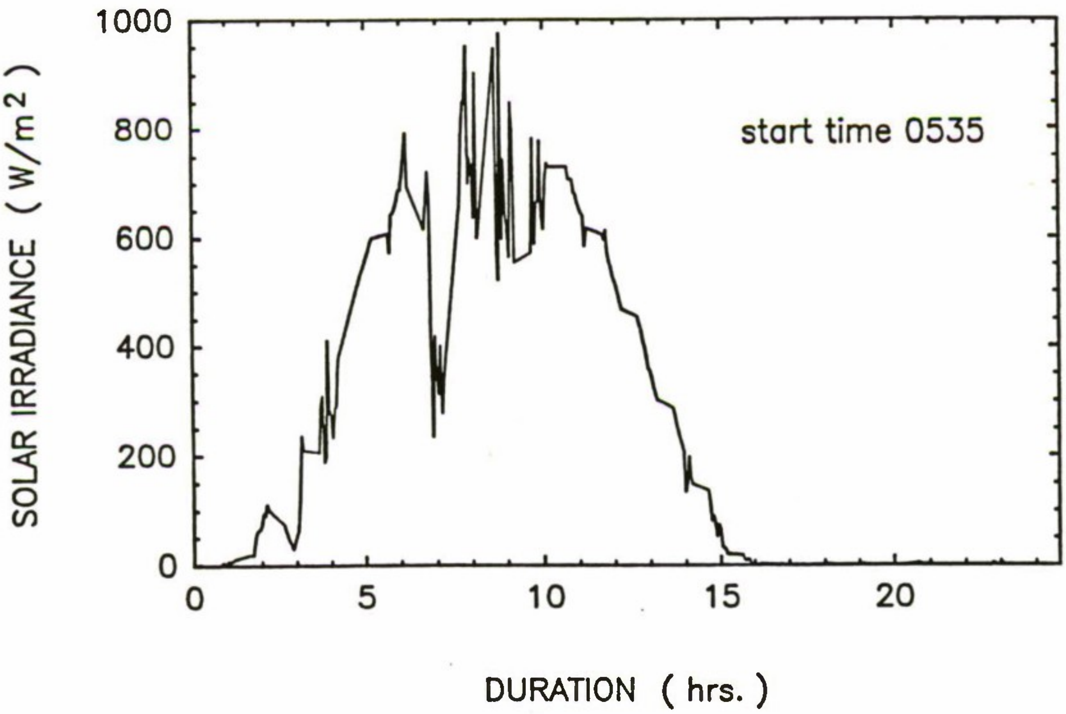

Figure A-35. Solar Irradiance Across Time, Scene V, 8/9/84.

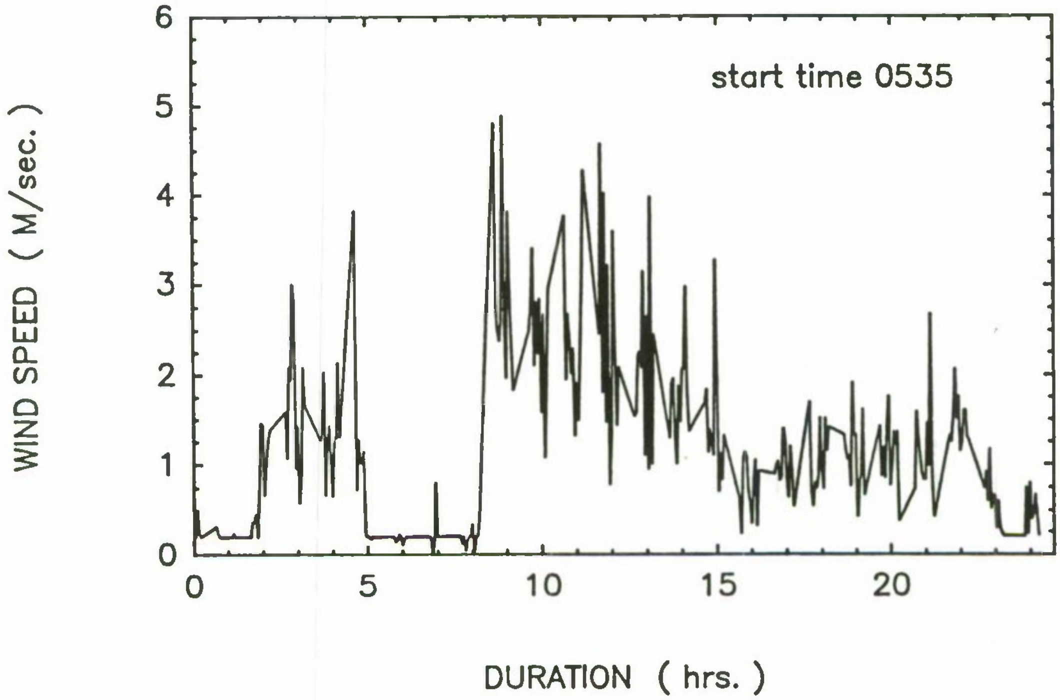

Figure A-36. Wind Speed Across Time, Scene V, 8/9/84

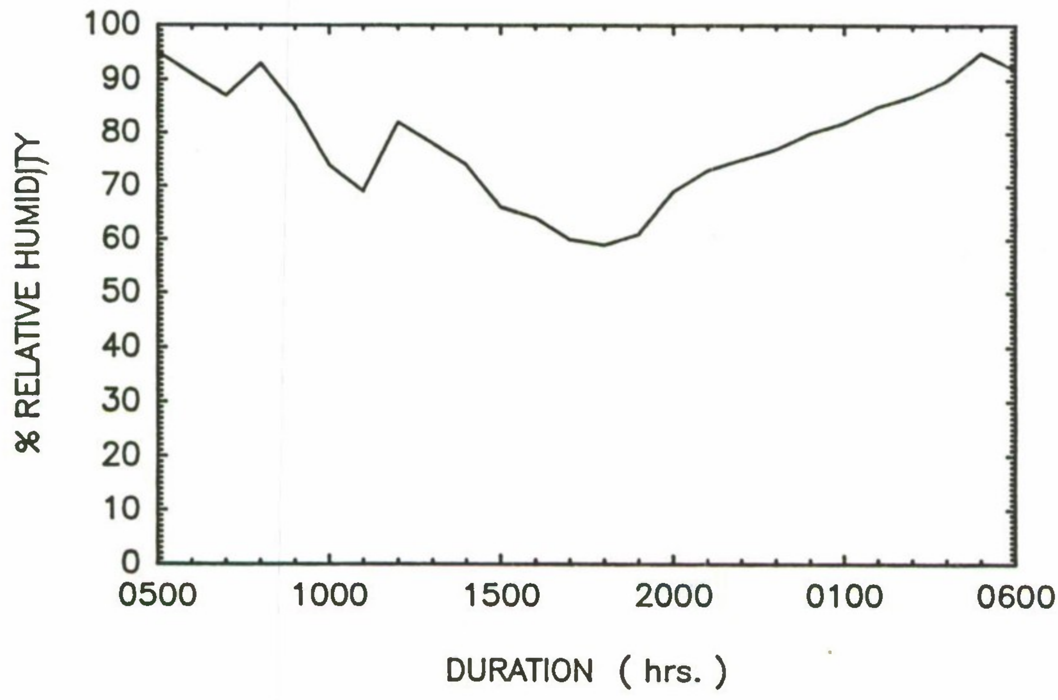

Figure A-37. Relative Humidity Across Time, Scene V, 8/9/84

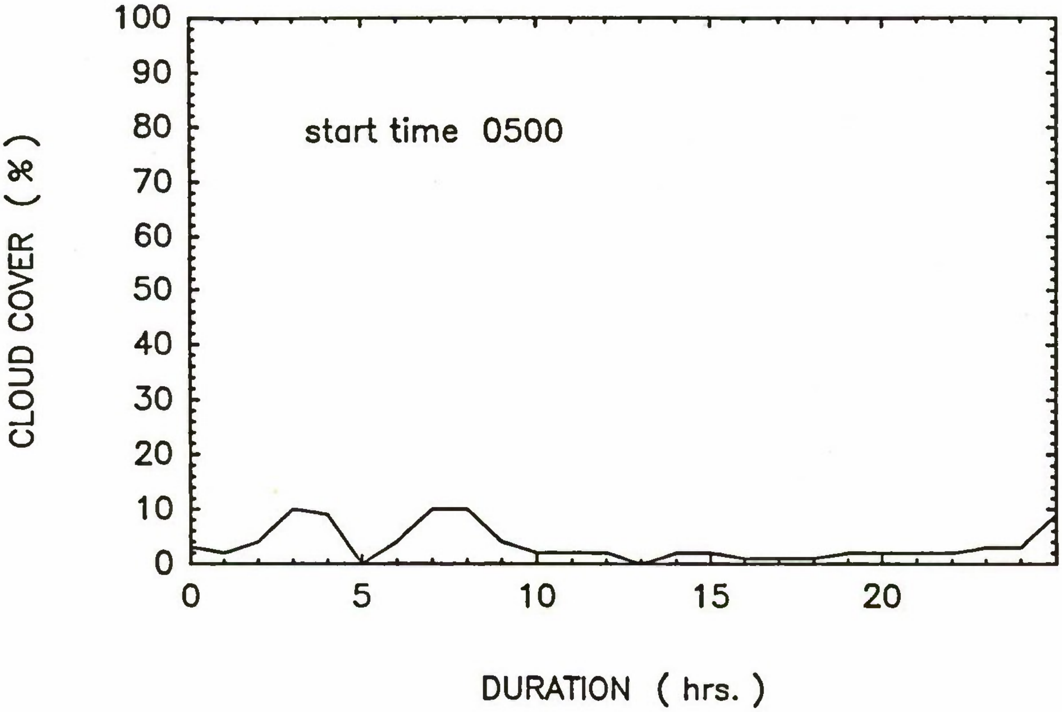

Figure A-38. Cloud Cover Across Time, Scene V, 8/9/89

Table A-3. PRISM weather file description

4.5.1. File Description, Parameters, and Format. The Weather file provides the environmental data that drive the model routines which compute the weather related heating and cooling of the vehicle being modeled.

The Weather file contains records of:

TIME, AIRT, SOLAR, WIND, HUMID, CLOUDS

in the format (2F2.0,5F9.0).

Var	Description
TIME	TIME that the following weather conditions were observed. This is zone time in military style, where 2:30 P.M. is expressed as 1430 hours.
AIRT	AIR Temperature in ^{o}C.
SOLAR	SOLAR irradiance in Watts/M^2.
WIND	WIND speed in M/sec.
HUMID	HUMIDity in percent (0 - 100)
CLOUD	CLOUD cover in tenths. 0 = Clear, 10 = Total Overcast.

4.5.2. Operation. Note that the Weather file is based on the time of day, rather than elapsed time. The model will read the simulation start time from the Scenario file, then read into the Weather file until the corresponding time of day is located. It is only necessary to begin the weather data on the correct day for the start of the simulation, and to ensure that the weather data at least spans the time from the start of the simulation through the end.

4.5.3. Data Generation. Further note that the time interval between weather records is of arbitrary size, and in fact it may vary. The weather routine will linearly interpolate between two records to arrive at the values used by the model.

---

04 Weather for 5/25/82, Grayling, MI

TIME	AIRT	SOLAR	WIND	HUMID	CLOUD
0610	18.800	.000	1.299	78.833	5.000
0615	18.900	2.000	.828	78.250	6.000
0620	18.700	4.000	.903	77.667	6.000
0625	18.600	6.000	1.532	77.083	6.000
0630	18.700	10.000	1.055	76.500	7.000
0635	18.400	20.000	1.630	75.917	7.000
0640	18.400	24.000	1.016	75.333	7.000
.	.	.	.	.	.
.	.	.	.	.	.

Figure 4-4. Sample weather file.

LOT NO. 3

DATE 14 MAY 85 TIME (EDT) 16:45 LOCATION SCENE 4, 7 m S. of TOWER

SOIL SAMPLED BY MMM SOIL ANALYZED BY MMM

BAKEOUT 15 HOURS AT 200 °F

DEPTH	SAMPLE NO.	WET WEIGHT (g)	DRY WEIGHT (g)	DIFF. (g)	PERCENT MOISTURE
0.5 cm	1A	100.3	71.9	28.4	39.5
5 cm	2A	140.4	112.7	27.7	24.6
10 cm	3A	146.7	119.1	27.6	23.2
① 25 cm	4A/4B	136.8/135.2	113.4/117.4	23.4/17.8	20.6/15.2
② 50 cm	5A	169.4	151.6	17.8	11.7

NOTES Surface 100% covered w/ old matted grass + new grass 2-4" high, at least top 5 cm is root zone (like sod).

① soil/sand interface at 25 cm, 4A soil, 4B sand.

② taken in second test hole 1 m S. of 1st hole, because 1st hole had several cm water in it after taking first 4 samples.

version no. 2

Figure A-39. Soil Moisture Data Sheet from Scene IV, 5/14/85

Table A-4. Standard Scenes Soil Moisture Survey October/November 1986

STANDARD SCENE/TIME	LOCATION	DEPTH IN.	WEIGHT SOIL DRY gm	WEIGHT MOISTURE gm	MOISTURE/ DRY SOIL
5/0945	ROAD	.25	505.02	74.19	0.147
5/0945	ROAD	6.0	533.77	24.36	0.046
5/0946	TOWER	.25	347.23	99.19	0.286
5/0946	TOWER	10.0	328.26	96.39	0.294
5/0949	TOWER	17.0	396.38	68.50	0.173
5/1425	ROAD	.25	345.59	34.40	0.100
5/1427	ROAD	6.0	431.32	56.64	0.131
5/1405	TOWER	.28	240.47	80.83	0.336
5/1406	TOWER	10.0	360.20	133.90	0.372
5/1415	TOWER	17.0	339.80	92.30	0.272
4/0850	TOWER	.25	399.61	34.09	0.085
4/0850	TOWER	10.0	434.50	58.30	0.134
4/0850	TOWER	20.0	473.48	49.00	0.103
4/1330	TOWER	.25	202.30	15.10	0.075
4/1330	TOWER	10.0	267.47	63.48	0.237
4/1330	TOWER	20.0	465.10	76.80	0.165
2&3/1510	TOWER	.25	131.78	10.30	0.078
2&3/1510	TOWER	10.0	361.70	25.00	0.069
2&3/1510	TOWER	20.0	276.28	42.90	0.155
1/1320	TOWER	.25	173.30	25.05	0.145
1/1320	TOWER	10.0	319.22	25.78	0.081
1/1320	TOWER	20.0	354.14	48.08	0.136

*"Road" designates the dirt road present in Scene 5. "Tower indicates that soil samples were obtained in the Immediate vicinity of the weatherinstrumentation tower in each scene.

APPENDIX B

Optimetrics Test Reports, 1983 and 1985

OMI-154

INFRARED IMAGERY OF STANDARD BACKGROUND SCENES
SPRING 1985

Charles S. Hall
Lucian W. Chaney
Terence R. Mahone
James E. Rice
Timothy J. Rogne
Kenneth J. Weible

10 January 1986

Prepared for

U.S. Army Tank-Automotive Command
Warren, Michigan

Contract No. DAAE07-81-C-4053

OptiMetrics, Inc.
2008 Hogback Road, Suite 6
Ann Arbor, Michigan 48105-9748

SECURITY CLASSIFICATION OF THIS PAGE

REPORT DOCUMENTATION PAGE

1a REPORT SECURITY CLASSIFICATION: Unclassified	1b RESTRICTIVE MARKINGS: None
2a SECURITY CLASSIFICATION AUTHORITY	3 DISTRIBUTION/AVAILABILITY OF REPORT: Unlimited
2b DECLASSIFICATION/DOWNGRADING SCHEDULE	
4 PERFORMING ORGANIZATION REPORT NUMBER(S): OMI-154	5 MONITORING ORGANIZATION REPORT NUMBER(S)
6a NAME OF PERFORMING ORGANIZATION: OptiMetrics, Inc. / 6b OFFICE SYMBOL (If applicable)	7a NAME OF MONITORING ORGANIZATION: US Army Tank Automotive Command
6c ADDRESS (City, State, and ZIP Code): 2008 Hogback Road, Suite 6, Ann Arbor, Michigan 48105-9748	7b ADDRESS (City, State, and ZIP Code)
8a NAME OF FUNDING/SPONSORING ORGANIZATION: US Army Tank Automotive Command / 8b OFFICE SYMBOL (If applicable)	9 PROCUREMENT INSTRUMENT IDENTIFICATION NUMBER: DAAE07-81-C-4053
8c ADDRESS (City, State, and ZIP Code): Warren, Michigan	10 SOURCE OF FUNDING NUMBERS: PROGRAM ELEMENT NO / PROJECT NO / TASK NO. / WORK UNIT ACCESSION NO.

11 TITLE (Include Security Classification)

INFRARED IMAGERY OF STANDARD BACKGROUND SCENES SPRING 1985

12 PERSONAL AUTHOR(S) Charles S. Hall, Lucian W. Chaney, Terence R. Mahone, James E. Rice, Timothy J. Rogne, Kenneth J. Weible

13a. TYPE OF REPORT	13b. TIME COVERED	14 DATE OF REPORT (Year, Month, Day)	15. PAGE COUNT
Final	FROM 2/4/85 TO 8/30/85	1986 January 10	11

16 SUPPLEMENTARY NOTATION

17 COSATI CODES			18 SUBJECT TERMS (Continue on reverse if necessary and identify by block number)
FIELD	GROUP	SUB-GROUP	Infrared Imagery; Background; Standard Scenes

19 ABSTRACT (Continue on reverse if necessary and identify by block number)

A Texas Medical Instruments Model 910 thermal imaging system was operated at the Keweenaw Research Center (KRC) during the period 11-22 May 1985. The purpose of the measurements was to obtain digital infrared (8-12 μm) imagery of standard background scenes on an hourly basis for 24-hour periods. In all, six scenes were observed. In addition to viewing the natural terrain, a static vehicle (M-113 APC) was positioned near the edge of each scene so that the diurnal dependence of its signature could be compared with that of the background scenes.

20 DISTRIBUTION/AVAILABILITY OF ABSTRACT: ☒ UNCLASSIFIED/UNLIMITED ☐ SAME AS RPT ☐ DTIC USERS	21. ABSTRACT SECURITY CLASSIFICATION: Unclassified
22a NAME OF RESPONSIBLE INDIVIDUAL: Timothy J. Rogne	22b TELEPHONE (Include Area Code): (313) 973-1177 / 22c. OFFICE SYMBOL

DD FORM 1473, 84 MAR — 83 APR edition may be used until exhausted. All other editions are obsolete.

SECURITY CLASSIFICATION OF THIS PAGE: Unclassified

TABLE OF CONTENTS

LIST OF TABLES

INTRODUCTION

A Texas Medical Instruments Model 910 thermal imaging system was operated at the Keweenaw Research Center (KRC) during the period 11-22 May 1985. The purpose of the measurements was to obtain digital infrared (8-12 μm) imagery of standard background scenes on an hourly basis for 24-hour periods. In all, six scenes were observed. In addition to viewing the natural terrain, a static vehicle (M-113 APC) was positioned near the edge of each scene so that the diurnal dependence of its signature could be compared with that of the background scenes.

This report provides descriptions of the reduced digital imagery data obtained during the test. Other data including scene descriptions and weather information are available through KRC.

DATA DESCRIPTION AND COLLECTION PROCEDURES

Six background scenes were observed during the time periods listed in Table 1, with data generally obtained on an hourly basis. The scenes were observed with a standard video camera and a Texas Medical Instruments Model 910 Thermiscope. Table 2 lists a summary of specifications for the TMI system. In scenes 1 through 5 the cameras were located on a stationary platform inside a bus. Scene 6 is a view from a refurbished fire observation tower.

Scenes 1, 2, 3, 4 and 6 are similar, consisting of an open field ending in a well-defined tree line. Scene 5 is a view along a brush-lined tank trail. All scenes contain a static APC.

Scenes 2, 3, 5 and 6 contain a controlled black body with an ambient black body mounted directly above. Scenes 1 and 4 contain the controlled black body only.

The original data collection plan was to make use of a CompuPro microcomputer at the test site as part of a digital data acquisition system. Equipment failure necessitated a backup procedure being used which utilized VHS format video recordings to capture the analog imagery for subsequent off-site digitization. In all, six video tapes were produced during the test.

Analog-to-digital conversion of the image data was performed by a Digital Graphic Systems video image digitizer interfaced to a CompuPro microcomputer. During the digitization process time base problems were encountered resulting in significant frame drift and distortion. An attempt was made to correct this problem by using a time base corrector with very little success. The problem was

TABLE 1. TIME PERIODS DURING WHICH DATA WERE OBTAINED

Scene	Julian Day	Date	Time
1	131 - 133	5/11 - 5/13	7:43 - 6:56
2	138 - 139	5/18 - 5/19	6:30 - 6:58
3	139 - 140	5/19 - 5/20	8:00 - 7:01
4	133 - 135	5/13 - 5/15	7:15 - 7:59
5	136 - 137	5/16 - 5/17	7:10 - 7:04
6	140 - 142	5/20 - 5/22	18:14 - 7:00

TABLE 2. FEATURES OF THE TEXAS MEDICAL INSTRUMENTS MODEL 910 THERMISCOPE

- Thermal sensitivity < 0.05C
- 8-14 μm spectral range
- 525 elements horizontal by 767 lines vertical resolution
- 120 lines per second scan rate
- 33° x 33° field of view
- Thermal reference to internal source stable to better than 0.1C per frame

severe enough as to render approximately 16% of the pertinent digitized frames unusable. Two 9-track computer tapes have been prepared which contain the remaining 165 usable digitized infrared images. Tables 3 and 4 list the contents of the two tapes: Frames 1-83 are on the first tape; frames 84-165 on the second.

There are several items in the tables which deserve some comment. The columns COLD TEMP. and HOT TEMP. list the image temperature span (in units of 0.1 degrees C) reported by the TMI camera. The columns COLD COUNT AND HOT COUNT list the corresponding values in the digitized image data. If black bodies were present in a scene, their temperatures and corresponding digitized value are recorded in the last four columns. The value -99 indicates that the data are missing.

The digitized images are approximately 400 x 400 pixels in size. With a field of view of 33° x 33° in the original image this translates into digitized pixel angular dimensions of approximately 1.4 x 1.4 milliradians.

TABLE 3. BACKGROUND IMAGERY INFORMATION (TAPE 1)

FRAME NUMBER	DATE/TIME CODE JULIAN	HR:MIN	SITE CODE	COLD TEMP. (IN 0.1 C)	COLD COUNT	HOT TEMP. (IN 0.1 C)	HOT COUNT	BB#1 TEMP. (IN 0.1 C)	BB#1 COUNT	BB#2 TEMP. (IN 0.1 C)	BB#2 COUNT
1	131	8: 4	1	180	81	230	227	-99	-99	-99	-99
2	131	9: 0	1	170	78	270	229	-99	-99	-99	-99
3	131	10: 0	1	170	80	270	233	-99	-99	-99	-99
4	131	11: 1	1	170	74	270	230	-99	-99	-99	-99
5	131	12: 1	1	185	72	305	245	-99	-99	-99	-99
6	131	16:59	1	191	78	350	241	-99	-99	-99	-99
7	131	17:57	1	180	83	380	243	-99	-99	-99	-99
8	132	0:15	1	181	83	281	245	199	245	-99	-99
9	132	1: 6	1	170	91	270	248	199	159	-99	-99
10	132	2:17	1	175	72	275	242	199	177	-99	-99
11	132	3: 6	1	153	86	253	242	199	180	-99	-99
12	132	4: 4	1	183	90	254	245	199	168	-99	-99
13	132	5: 5	1	178	87	232	243	199	144	-99	-99
14	132	6: 5	1	211	90	311	242	199	176	-99	-99
15	132	6:59	1	154	61	215	242	199	224	-99	-99
16	132	8: 1	1	148	79	248	238	200	180	-99	-99
17	132	9: 2	1	175	85	325	236	202	117	-99	-99
18	132	10: 0	1	175	79	285	236	224	163	-99	-99
19	132	11: 0	1	160	78	280	235	-99	-99	-99	-99
20	132	12: 0	1	125	67	275	243	245	208	-99	-99
21	132	13: 4	1	155	76	325	246	268	186	-99	-99
22	132	14: 0	1	130	77	310	245	255	205	-99	-99
23	132	15: 0	1	135	80	265	247	265	232	-99	-99
24	132	15:55	1	140	120	280	244	260	228	-99	-99
25	132	17: 6	1	135	70	235	232	240	221	-99	-99
26	132	17:58	1	136	66	235	229	260	220	-99	-99
27	132	19: 0	1	193	88	235	247	225	219	-99	-99
28	132	20: 0	1	168	77	223	250	225	241	-99	-99
29	132	21: 0	1	168	86	227	251	199	195	-99	-99
30	132	22: 3	1	215	85	255	248	-99	-99	-99	-99
31	132	22:55	1	198	71	223	233	-99	-99	-99	-99
32	133	0: 9	1	188	72	218	236	-99	-99	-99	-99
33	133	0:54	1	211	94	230	251	-99	-99	-99	-99
34	133	1:55	1	213	96	233	248	-99	-99	-99	-99
35	133	2:59	1	215	99	239	249	-99	-99	-99	-99
36	133	3:56	1	220	96	244	250	-99	-99	-99	-99
37	133	5:15	1	201	123	281	232	-99	-99	-99	-99
38	133	6:10	1	194	120	255	232	-99	-99	-99	-99
39	133	6:55	1	188	110	258	232	-99	-99	-99	-99
40	134	8: 3	4	205	85	235	234	101	-99	-99	-99
41	134	9:58	4	209	84	239	238	102	180	-99	-99
42	134	11: 6	4	209	81	239	248	116	217	-99	-99
43	134	12: 1	4	115	80	175	254	116	205	-99	-99
44	134	23:58	4	120	71	160	233	120	192	-99	-99
45	135	0:59	4	115	56	155	230	120	197	-99	-99
46	135	1:58	4	117	57	157	240	120	201	-99	-99
47	135	3:59	4	103	55	148	241	120	237	-99	-99
48	135	4:57	4	103	58	143	240	120	222	-99	-99
49	135	6: 0	4	90	55	150	239	105	191	-99	-99
50	135	7: 0	4	196	57	236	234	106	164	-99	-99

TABLE 3. (cont.)

FRAME NUMBER	DATE/TIME CODE JULIAN	HR:MIN	SITE CODE	COLD TEMP. (IN 0.1 C)	COLD COUNT	HOT TEMP. (IN 0.1 C)	HOT COUNT	BB#1 TEMP. (IN 0.1 C)	BB#1 COUNT	BB#2 TEMP. (IN 0.1 C)	BB#2 COUNT
51	135	7:57	4	102	58	162	249	106	174	-99	-99
52	136	7:10	5	165	99	266	242	150	208	89	150
53	136	7:30	5	160	96	260	236	151	223	83	150
54	136	8: 0	5	182	96	242	234	131	219	83	153
55	136	8:30	5	85	88	165	235	131	226	89	157
56	136	9: 0	5	164	86	264	232	131	175	97	143
57	136	9:30	5	167	115	267	235	153	195	100	142
58	136	10: 1	5	140	116	260	233	153	208	100	139
59	136	11: 2	5	140	117	190	232	131	220	100	160
60	136	11:30	5	142	115	202	232	131	222	100	164
61	136	12: 0	5	155	88	235	230	131	205	100	148
62	136	12:57	5	165	84	245	233	131	223	106	183
63	136	13:57	5	110	90	150	236	229	117	173	100
64	136	14:59	5	109	94	149	237	233	116	162	94
65	136	15:56	5	89	94	165	242	234	116	195	86
66	136	17: 5	5	50	98	170	243	210	115	160	78
67	136	17:56	5	85	98	165	249	225	101	179	72
68	136	18:56	5	148	100	199	248	215	86	189	69
69	136	19:56	5	96	102	138	246	101	225	83	72
70	136	20:58	5	195	99	215	247	95	234	72	183
71	136	21:58	5	118	100	173	242	95	200	72	143
72	136	22:59	5	83	101	148	244	95	210	67	155
73	137	24: 0	5	121	99	191	242	90	198	61	151
74	137	1: 5	5	128	118	188	246	90	208	56	136
75	137	1:58	5	88	126	113	238	90	231	56	181
76	137	3: 0	5	82	126	128	239	80	221	56	172
77	137	4: 5	5	135	124	235	238	118	221	33	180
78	137	4:30	5	155	124	215	238	86	215	28	171
79	137	5: 0	5	140	120	220	238	86	216	28	173
80	137	5:30	5	140	124	220	237	87	218	6	164
81	137	6: 0	5	135	121	215	239	85	221	0	170
82	137	6:30	5	135	121	215	241	86	225	0	174
83	137	7: 0	5	140	118	220	240	86	219	22	183

Note: -99 Value indicates missing data

TABLE 4. BACKGROUND IMAGERY INFORMATION (TAPE 2)

FRAME NUMBER	DATE/TIME CODE JULIAN	HR:MIN	SITE CODE	COLD TEMP. (IN 0.1 C)	COLD COUNT	HOT TEMP. (IN 0.1 C)	HOT COUNT	BB#1 TEMP. (IN 0.1 C)	BB#1 COUNT	BB#2 TEMP. (IN 0.1 C)	BB#2 COUNT
84	138	6:30	2	140	110	220	236	85	226	17	171
85	138	7: 0	2	170	114	220	235	85	207	39	158
86	138	7:30	2	99	115	-99	232	93	195	78	184
87	138	8: 0	2	185	114	265	230	168	223	103	176
88	138	8:31	2	195	112	275	228	169	202	122	167
89	138	9: 0	2	195	113	275	227	176	212	128	179
90	138	9:30	2	195	112	275	227	176	208	128	176
91	138	10: 0	2	182	111	282	230	191	218	128	188
92	138	10:32	2	166	110	306	228	192	185	144	155
93	138	11: 0	2	120	113	260	236	191	198	144	170
94	138	11:30	2	101	113	261	233	191	194	156	176
95	138	12: 1	2	101	114	280	233	192	186	167	178
96	138	13: 0	2	110	119	310	234	250	215	178	174
97	138	14: 0	2	110	123	310	234	249	225	183	188
98	138	14:58	2	125	116	325	234	250	196	200	173
99	138	15:59	2	130	112	312	234	250	200	211	178
100	138	17: 0	2	118	113	313	236	250	204	222	185
101	138	18: 0	2	105	125	285	229	250	220	172	171
102	138	19: 0	2	145	122	235	232	250	199	172	187
103	138	20: 0	2	135	89	199	236	184	233	136	181
104	138	21: 0	2	115	85	180	234	169	227	97	129
105	138	22: 5	2	199	87	259	235	152	221	67	107
106	138	22:32	2	142	88	193	236	130	223	56	127
107	138	23: 0	2	115	86	188	235	122	223	44	107
108	139	0: 0	2	153	89	201	238	122	227	42	95
109	139	1: 6	2	233	92	273	236	123	196	78	113
110	139	1:59	2	177	90	231	230	124	171	78	102
111	139	3: 4	2	210	92	292	231	178	141	144	102
112	139	4: 4	2	160	92	240	228	177	229	133	180
113	139	5: 0	2	175	91	225	235	163	234	117	132
114	139	6: 0	2	177	93	207	235	131	219	89	106
115	139	6:58	2	203	94	218	239	132	197	111	113
116	139	8: 0	3	220	89	240	236	132	194	122	162
117	139	8:32	3	189	93	219	239	132	205	122	182
118	139	9: 1	3	207	121	247	231	177	210	156	173
119	139	10: 0	3	205	119	245	231	177	219	156	182
120	139	10:30	3	181	122	322	232	251	215	183	188
121	139	11: 0	3	205	119	305	230	250	217	203	177
122	139	11:30	3	205	119	325	230	250	196	206	169
123	139	12: 0	3	205	120	275	229	245	229	200	197
124	139	12:30	3	213	116	298	236	245	217	211	192
125	139	12:59	3	223	115	306	231	255	210	222	179
126	139	13:29	3	228	115	312	230	255	200	228	177
127	139	14: 0	3	233	115	318	230	255	199	228	175
128	139	14:30	3	236	116	336	230	255	184	222	162
129	139	15: 0	3	218	114	343	229	255	181	217	159
130	139	15:59	3	209	115	332	230	255	193	233	181
131	139	16:58	3	198	113	313	228	255	203	233	194
132	139	18: 0	3	198	115	313	230	255	210	211	181
133	139	18:59	3	189	117	271	230	230	225	211	212

TABLE 4. (cont.)

FRAME NUMBER	DATE/TIME CODE JULIAN	HR:MIN	SITE CODE	COLD TEMP. (IN 0.1 C)	COLD COUNT	HOT TEMP. (IN 0.1 C)	HOT COUNT	BB#1 TEMP. (IN 0.1 C)	BB#1 COUNT	BB#2 TEMP. (IN 0.1 C)	BB#2 COUNT
134	139	19:43	3	150	120	270	236	274	235	167	200
135	139	19:58	3	166	120	231	237	259	237	161	229
136	139	20:58	3	155	120	231	233	237	230	53	161
137	139	21:58	3	137	122	250	231	191	225	78	143
138	139	23: 2	3	131	122	212	232	146	220	56	144
139	140	0: 0	3	124	122	208	232	109	199	33	138
140	140	0:59	3	124	120	204	231	100	192	25	134
141	140	1:59	3	128	97	208	239	100	230	19	145
142	140	3: 0	3	201	99	254	238	100	224	17	132
143	140	3:59	3	207	101	255	245	100	230	14	138
144	140	5: 0	3	205	100	255	244	100	229	39	144
145	140	6: 0	3	205	99	255	244	100	234	28	155
146	140	6:30	3	205	101	255	244	100	234	28	157
147	140	7: 0	3	215	99	255	245	101	228	39	147
148	141	6:58	6	146	99	221	235	123	-99	44	-99
149	141	7: 0	6	155	98	215	232	123	181	44	-99
150	141	8: 2	6	180	97	260	236	152	155	89	-99
151	141	8: 8	6	165	92	315	234	152	-99	89	-99
152	141	9: 0	6	90	91	350	235	213	-99	117	-99
~~153~~	141	9: 4	6	-99	91	-99	237	213	-99	117	-99
154	141	10: 0	6	131	92	371	238	301	-99	150	-99
155	141	19:57	6	110	115	290	249	310	190	217	-99
156	141	20:59	6	59	118	239	252	290	189	183	-99
157	141	22:59	6	134	108	254	231	220	194	67	-99
158	141	23:58	6	137	111	241	235	189	193	56	-99
159	142	0:58	6	49	109	191	233	166	164	58	-99
160	142	1:58	6	47	108	180	233	165	198	50	-99
161	142	2:58	6	127	112	235	236	142	-99	50	-99
162	142	3:58	6	119	113	233	236	142	-99	44	-99
163	142	5: 0	6	155	111	255	234	142	-99	50	-99
164	142	6: 0	6	160	113	260	233	142	-99	50	-99
165	142	7: 0	6	165	110	265	231	142	-99	69	-99

Note: -99 Value indicates missing data

DATA CALIBRATION

The data may be calibrated using the image apparent temperature span reported by the TMI camera, and simply performing a linear interpolation to find the apparent temperature of interesting scene elements. As an example, suppose that we wished to know the apparent temperature of an object in frame 1 (see Table 3) which has a digital image value of 200. In this case:

$$\text{Object Apparent Temp.} = (200-81)*(23.0-18.0)/(227-81) + 18.0$$
$$= 22.1 \text{ C}$$

The reader should be aware that the TMI camera uses a simple method for determining temperature span of a given image. The camera simply compares the magnitude of the scene radiance with that of an internal 300K black body. It then uses a fixed constant (valid at 300K) to convert observed scene radiances (actually radiance differences from the internal black body) to scene apparent temperatures. When the scene temperatures differ significantly from 300K, this procedure causes scene apparent temperatures to be reported which differ from the usual definition (usually the apparent temperature of a scene element is the temperature of a black body which would induce an identical sensor response). Of course one may use the Plank function to convert the TMI reported temperatures if that is desired.

Unfortunately, there is reason to believe that the temperature spans reported by the TMI are not reliable. During field operation sudden shifts in the measured scene temperature range (as reported by the TMI) were observed; these shifts were clearly due to a problem in the TMI

camera. The extent of this problem is unclear. Certainly the presence of these shifts precludes the accurate determination of absolute scene apparent temperatures based on the TMI calibration. It is unclear whether or not scene differential temperatures are accurately represented by the TMI calibration. If this aspect of the TMI calibration is to be used, it should be checked using some of the scene data which includes two black bodies.

In many scene images, one or more black bodies of known temperature are present within the TMI camera field-of-view. Of course when two black bodies are present, they can be used to calibrate the image independently from any information reported by the TMI camera. This is by far the preferred way to calibrate these data. When one black body is present, it can be used to establish the absolute scene temperature; however, the TMI calibration must be used to determine the scene temperature span.

In summary, data obtained at sites 2, 3, and 5 have two black bodies in the image; these data have the greatest potential of being useful. Data obtained at sites 1 and 4 have at most one black body in the image so that TMI calibration information is required to establish the scene temperature range. Finally, although black body data is recorded for scene 6 images, the black bodies are too distant to be of any utility. These images must rely entirely on the TMI calibration.

DIGITAL DATA TAPE DESCRIPTION

Each 1600 bpi, ASCII tape contains one file for each image, each file containing 17 records. The first record is a header record written using a 15I5 format which contains the following information:

Frame number
Julian day
Hour
Minute
Seconds (not used-contains a zero)
Milliseconds (not used-contains a zero)
Site code (corresponds to scene number)
Cold temperature
Cold count
Hot temperature
Hot count
Black body #1 temperature
Black body #1 count
Black body #2 temperature
Black body #2 count

All temperatures are recorded in units of 0.1C. Black body #1 is the controlled temperature black body, and black body #2 is the ambient temperature black body.

Following the header record are 16 records containing the image data. Each record contains 13312 bytes, representing 26 scan lines of 512 bytes each. The unsigned binary value of each byte represents a single image pixel.

APPENDIX C

Report

Climatological Comparison of Houghton, Michigan with the Giessen/Fulda Region of West Germany

Michael J. Hayes

Institute of Snow Research
Keweenaw Research Center
Michigan Technological University
Houghton, Michigan 49931

August, 1985

CLIMATOLOGICAL COMPARISON OF HOUGHTON, MICHIGAN WITH THE GIESSEN/FULDA REGION OF WEST GERMANY

Michael J. Hayes*
Institute of Snow Research
Keweenaw Research Center
Michigan Technological University

INTRODUCTION

A climatological comparison of Houghton, Michigan with the Giessen/Fulda region of West Germany was conducted to determine similarities and dissimilarities occurring between the two climates. The purpose is to ascertain to what extent the field tests conducted in Houghton would be comparable to similar tests conducted in West Germany.

Fulda was chosen for this study due to its strategic military location. Giessen was involved because more data was available, as well as its close distance from Fulda--approximately 60km to the west. The elevations of Giessen and Fulda are approximately 152m and 305m, respectively, which are comparable to Houghton's elevation of 330m [1,2,3]. Thus, in this study, it is assumed that the climates of Giessen and Fulda are nearly identical and will be used interchangeably. These sites are considered within the same climatic region as defined by USAFETAC in <u>Worldwide Airfield Data Vol. X, Part 1</u>, and Figure 1 showing the annual average temperatures for Giessen and Fulda supports this [2]. It should also be mentioned that all three locations--Houghton, Giessen, and Fulda--are defined as being in a vegetation region consisting of mainly deciduous broad-leaved and mixed woods, already suggesting some similarity in their climates [4].

FIGURE 1.

GIESSEN/FULDA DAILY AVERAGE TEMPERATURE COMPARISON

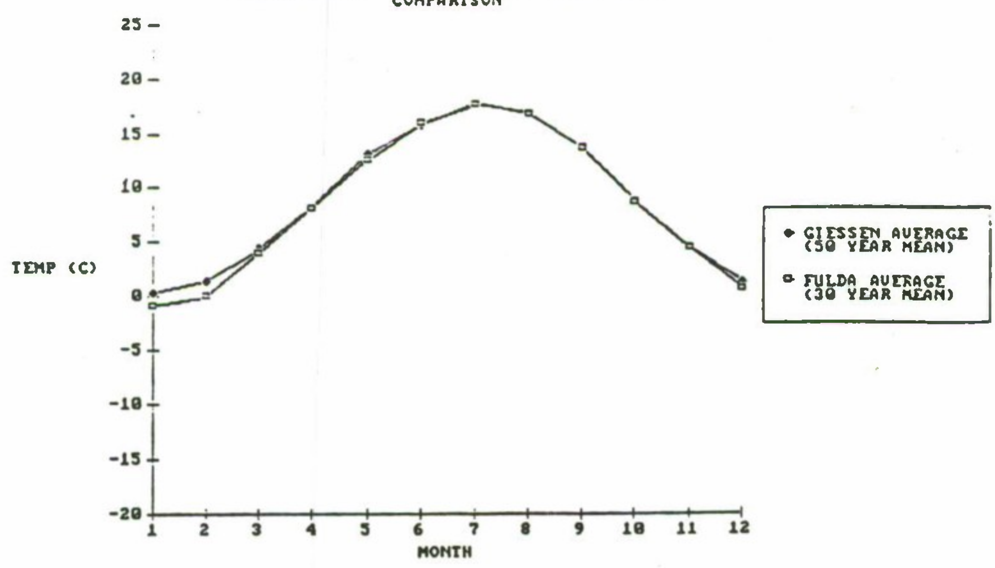

*Visiting student assistant from the Meteorology Department at the University of Wisconsin-Madison.

PROCEDURE

The climatic data available for this study was analyzed by months. Comparisons between Houghton and West Germany were then made using graphs plotted with this monthly information. It should be noted that the monthly comparisons were made not only for corresponding months, say, April-to-April, but also for non-corresponding months, say, April-to-May, April-to-June, April-to-July, etc. Thus, for each climatic parameter studied, every month for Houghton was compared with every month at the German location. This was accomplished by shifting the Giessen or Fulda plots on the various graphs by one month at a time, eventually comparing all the months together. While this was done, the similarities were noted and recorded on a twelve month-by-twelve month chart: Houghton on one axis, Giessen or Fulda on the other. After all the climatic parameters were compared in this manner, all the similarities were plotted on one final twelve month-by-twelve month chart. From the frequency of similarities that then appeared, the overall comparison of the two climates could be made.

CLIMATIC PARAMETERS

TEMPERATURE

The similarities revealed by the comparison of the mean maximum, minimum, and average temperatures for Houghton and Giessen (see Figures 2 and 3) show that the summers and early autumns (June-October) are very similar between the two sites. Temperatures during Houghton's spring (April-June) lag one month behind those in Giessen, and so are similar to March through May in Giessen. This same period in Houghton is also similar to Giessen's autumn and early winter (September-December). Autumn temperatures in Houghton (September and October) are similar to the Giessen spring months (May, April, and March). Meanwhile, the Houghton months of April and November correspond closely to the mid-winter months (December-March) in Giessen. Temperatures during the winter in Houghton are significantly colder than temperatures in Giessen, so that the December-March period in Houghton has no similarities with any months in Giessen. For the entire year, the average maximum temperature of 8.7 $^{\circ}$C in Houghton is lower than the 12.8 $^{\circ}$C in Giessen because of these winter months [1,3]. The average minimum temperatures for the year are -0.3 $^{\circ}$C and 5.0 $^{\circ}$C in Houghton and Giessen respectively [1,3]. Generally, the daily temperature change between the high and the low during the year is quite similar at the two locations, as shown in Figure 4, with Giessen's daily temperatures usually not quite as varied as in Houghton. Finally, Figure 5 shows the comparison of the annual average temperatures for Houghton and Fulda.

PRECIPITATION

Considering precipitation, Houghton receives approximately 26.5 more centimeters of precipitation (liquid water equivalent)

FIGURE 2.

HOUGHTON/GIESSEN DAILY MAXIMUM AND MINIMUM TEMPERATURE COMPARISONS

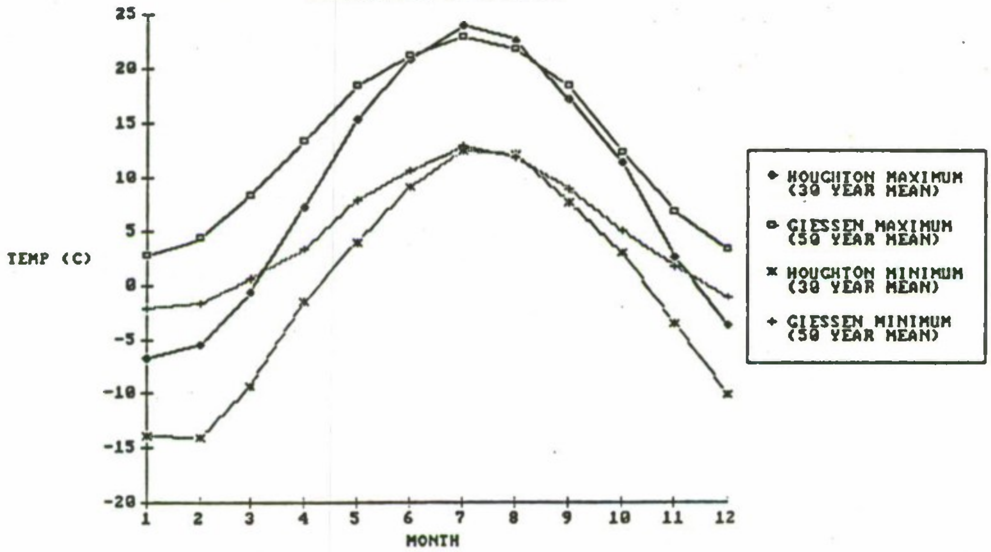

FIGURE 3.

HOUGHTON/GIESSEN DAILY AVERAGE TEMPERATURE COMPARISON

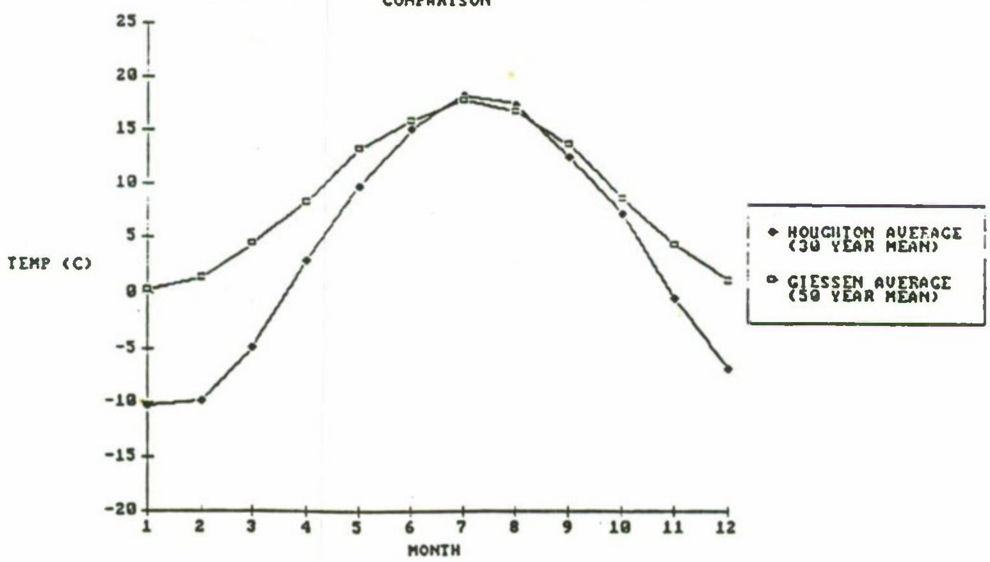

FIGURE 4.

HOUGHTON/GIESSEN DAILY TEMPERATURE CONTRAST (MAX-MIN)

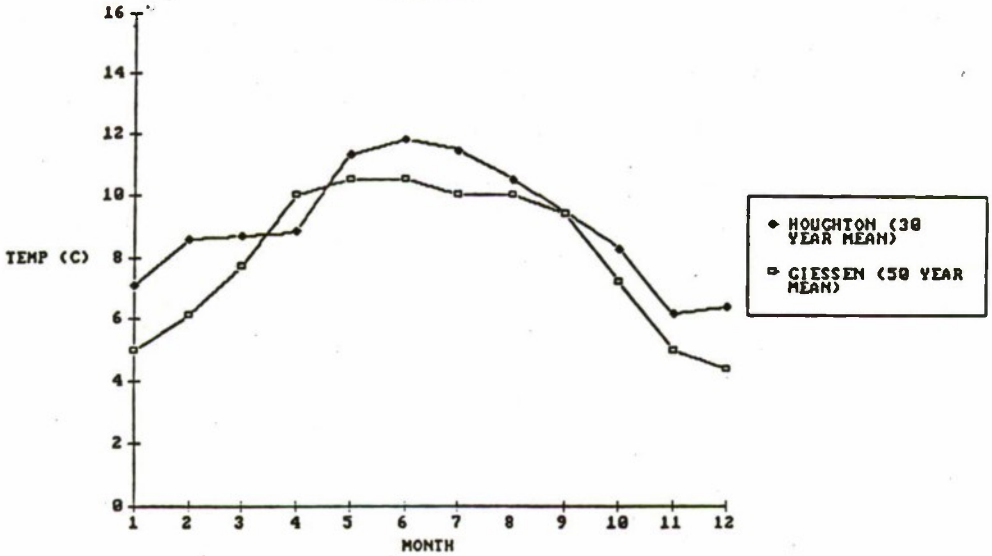

FIGURE 5.

HOUGHTON/FULDA DAILY AVERAGE TEMPERATURE COMPARISON

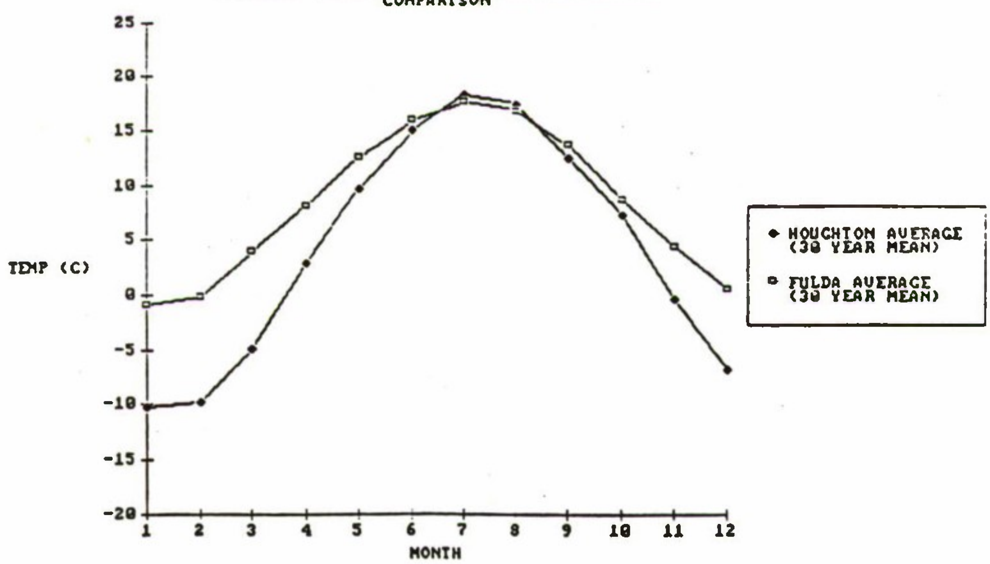

in one year than does Giessen: 86.7cm and 60.2cm respectively [1,3]. The monthly precipitation totals for Houghton and Giessen are shown in Figure 6. The biggest similarity exists between the late winter/early spring months of February, March, and April in Houghton, and the late summer through early winter months in Giessen (August-December). Otherwise, there seems to be no organized pattern of close similarity for the precipitation totals at these two sites.

FIGURE 6.

HOUGHTON/GIESSEN PRECIPITATION COMPARISON

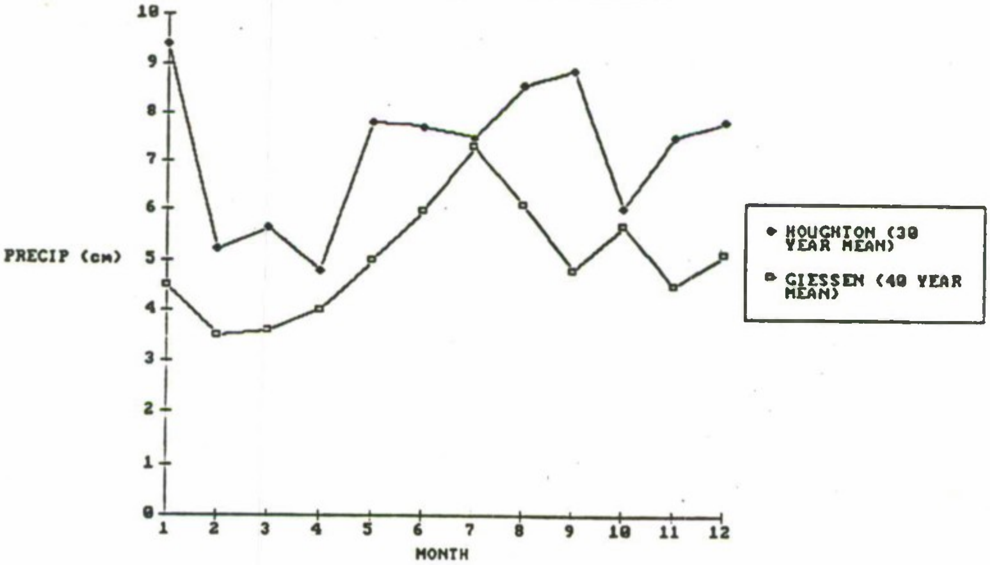

However, when looking at the frequency of observations reporting precipitation at Houghton and Fulda, shown in Figure 7, more similarities become apparent. From May to October, the observations with precipitation at both locations are similar, ranging between 7.1% and 14.7% in Houghton and between 5.9% and 11.5% in Fulda [5,2]. In addition, March, April, and May in Houghton are similar with two periods in Fulda: January-April and December, November, and October. The frequency of precipitation during the winter months in Houghton (November-February) is significantly higher than any month in Fulda, so that there are no months in Fulda similar with this period in Houghton. Only during March in Houghton does the frequency of precipitation become low enough to be considered similar with the winter months in Fulda (December-February).

In all twelve months, Giessen has a monthly average of between 4.5 and 7.5 days with precipitation amounts of 0.254cm (0.1in) or higher [1]. Similarily, for the months of February through November, Houghton has between five and eight days in which at least 0.254cm of precipitation is measured [6]. As Figure 8 shows, only December and January in Houghton have a

FIGURE 7.

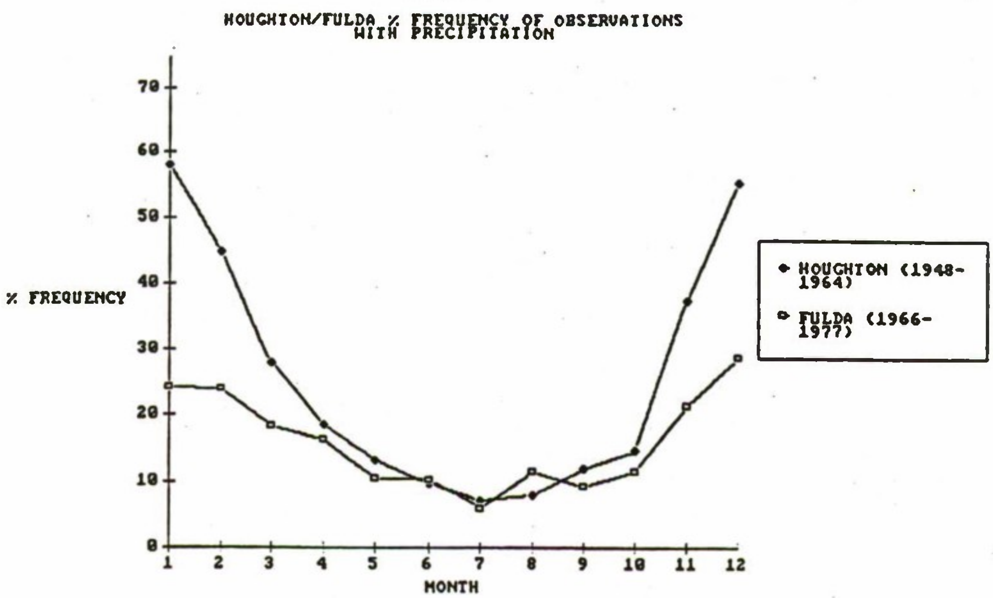

FIGURE 8.

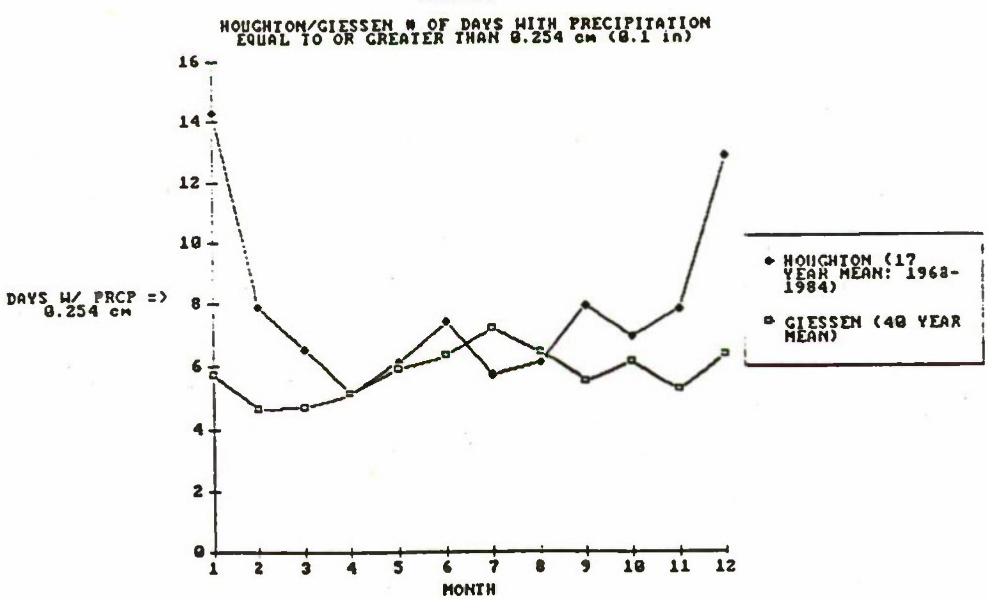

significantly higher number of days with the occurrence of 0.254cm of precipitation and therefore no similarity with any month in Giessen.

Figure 9 compares the percent frequency of hourly observations with snowfall in Houghton and Fulda from September through May. This figure reveals that for the period from November through March Houghton has a much greater frequency of snow than any month during the entire winter in Fulda. The percent frequency in Houghton during those months ranges from 25.5% in March, to 56.7% in January; compared to the season high for Fulda of 8.4% in January [5,2]. Only April and October in Houghton contain snow frequencies similar to the mid-winter months in Fulda (December-February).

FIGURE 9.

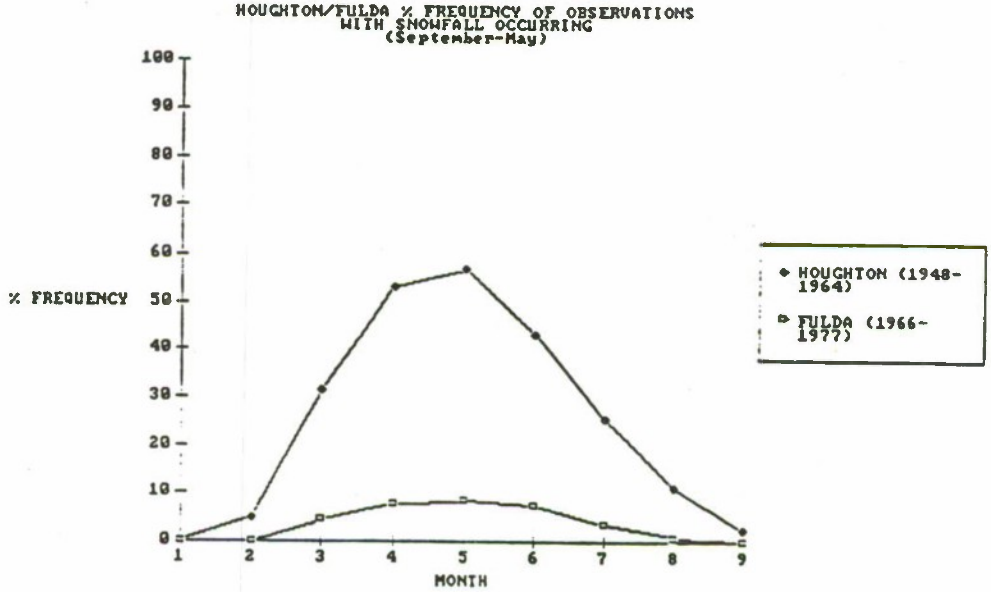

The mean number of days with thunderstorms in Houghton and Giessen, shown in Figure 10, are generally similar year round, with the annual averages being 27.7 and 23.1 days a year respectively [5,1]. Only in September and October Houghton has a higher occurrence of thunderstorms than Giessen does in those same two months. Otherwise, the number of days with thunderstorms in Houghton ranges from around zero for November-February to 6.69 days in June [5]. For Giessen, it ranges from near zero for November-February also, to 5.5 days in June [1].

RELATIVE HUMIDITY

A comparison of the mean relative humidities for Houghton and Giessen (Figure 11) reveals that the annual percent is

FIGURE 10.

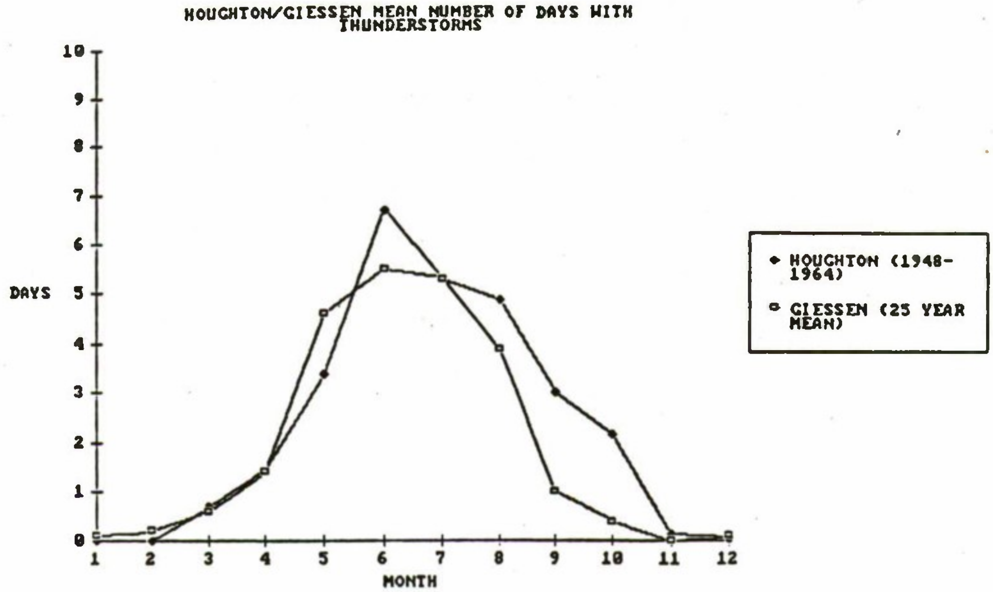

FIGURE 11.

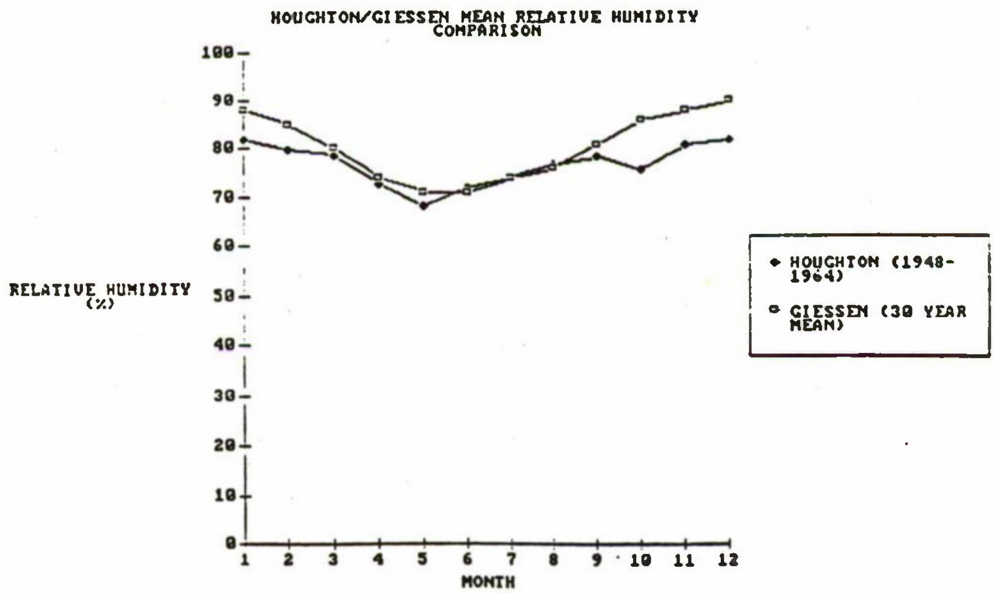

slightly higher at Giessen, 80.3%, than at Houghton, 76.8% [5,1]. During the autumn/early winter months (October-January), Giessen has a higher mean relative humidity than any month during the entire year in Houghton. However, April through September are nearly identical at the two locations, especially during June, July, August. February and March in Giessen are very similar to the winter months in Houghton (November-January).

When comparing early morning mean relative humidities at Houghton and Fulda, Figure 12 shows that every month in Fulda is between 4% and 10% higher than its corresponding month in Houghton [5,2]. The similarities are: June through January in Houghton being similar to the spring months in Fulda (February-April), and the summer months in Houghton (June-September) being similar to the period of November through May in Fulda.

FIGURE 12.

HOUGHTON/FULDA EARLY MORNING MEAN RELATIVE HUMIDITY COMPARISON
(Houghton: 03-05 LST, Fulda: 04 LST)

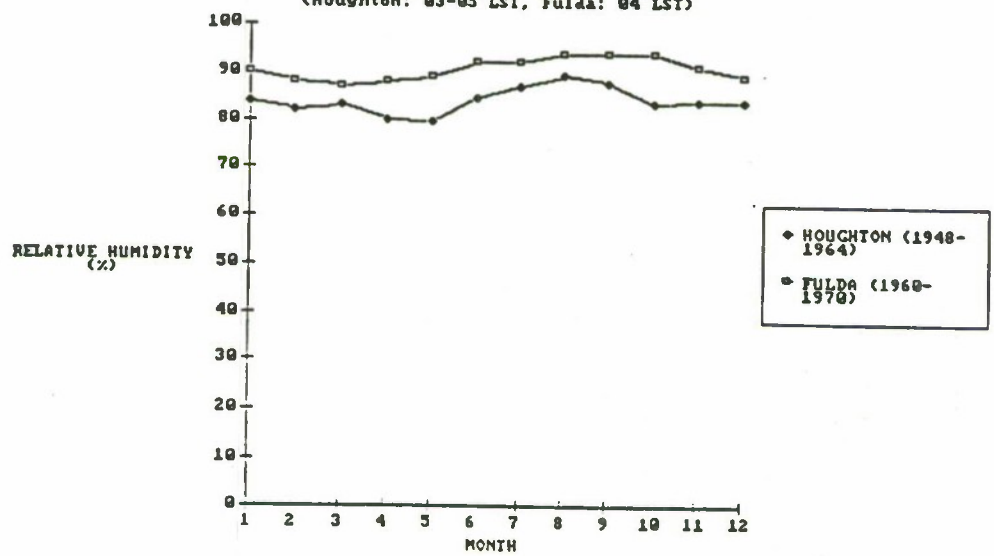

Afternoon mean relative humidities at Houghton and Fulda, shown in Figure 13, are more similar than the morning humidities with the annual means being 68.1% and 70.2% respectively [5,2]. From February through September in Houghton, the humidity is very close to that in Fulda during the corresponding months. In addition, May through August in Houghton is very similar to all the months in the Fulda period of April through August. January through April in Houghton is similar to November, October, and September in Fulda, while September through December in Houghton is similar to Fulda's spring/late winter (April, March, and February).

FIGURE 13.

HOUGHTON/FULDA EARLY AFTERNOON MEAN RELATIVE HUMIDITY COMPARISON
(Houghton: 12-14 LST, Fulda: 13 LST)

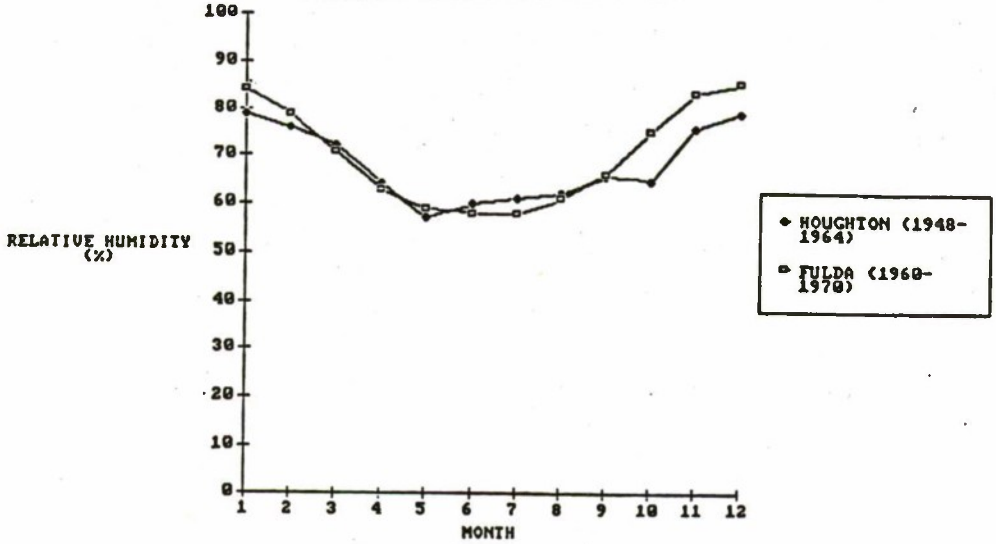

SOLAR RADIATION

The more northerly latitude of Giessen and Fulda is an important factor when comparing the short-wave radiation flux incident on the top of the atmosphere. Figure 14 indicates that during the months of April through September, the amounts of short-wave radiation at Houghton and Giessen or Fulda are very similar--with June in Houghton almost identical with June in the two West Germany cities [7]. However, the amounts from October through March reveal that the German locations have lower solar radiation than in Houghton. In addition, amounts for November through June in Houghton are similar to Giessen or Fulda amounts for the corresponding months of February, January, December, etc., through June.

For the total solar radiation incident at the surface (Figure 15), Houghton is higher than Giessen in every month [7]. During the summer (June-August), or the mid-winter (November-January), no similarities are observed for this parameter. The main similarity between the two sites reveals that Giessen has a one month lag behind Houghton, so that Houghton's January through April and September through December is similar to February through May and August through November, respectively, in Giessen. It should be noted that the effects of latitude, clouds, and obstructions to vision are taken into account in the measurement of this parameter.

FIGURE 14.

HOUGHTON/GIESSEN SHORT-WAVE RADIATION FLUX COMPARISON
(note: measured at the top of the earth's atmosphere)

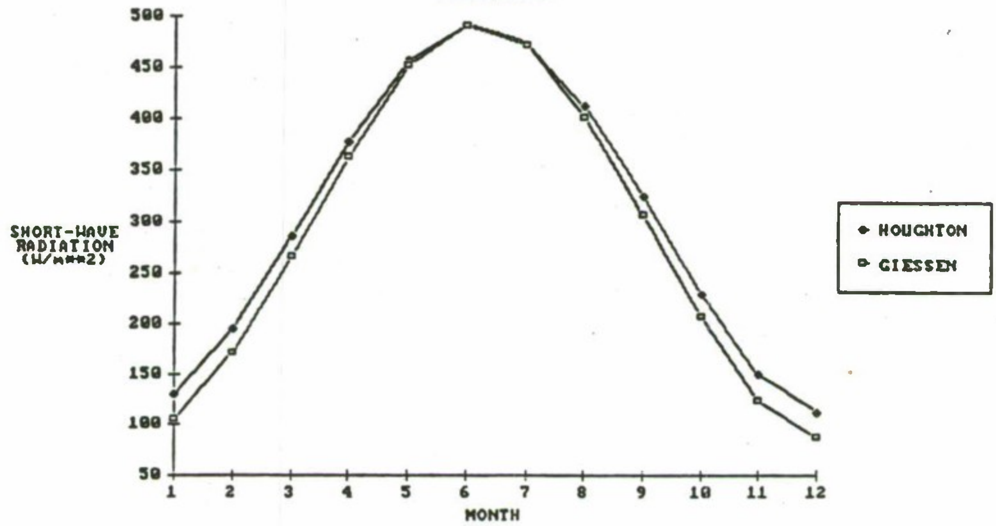

FIGURE 15.

HOUGHTON/GIESSEN TOTAL SOLAR RADIATION COMPARISON
(note: daily means of solar radiation-direct and diffuse-incident on a horizontal surface.)

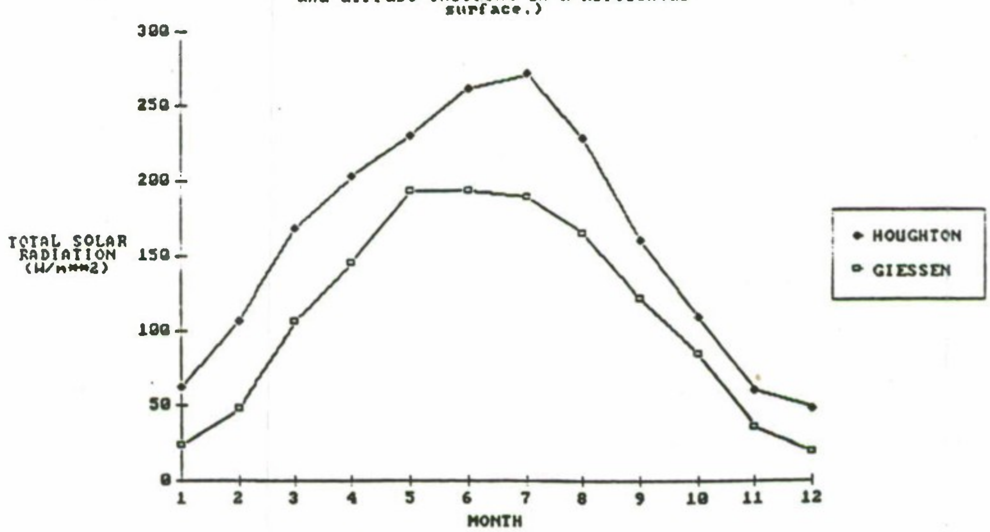

CLOUD COVER

When comparing the amount of cloud cover at Houghton and Giessen, shown in Figure 16, the major similarity noted is that the annual percentages of cloud cover at both locations is 69% [5,1]. The main monthly similarities observed are from March through June, September, and October in Houghton with March through September in Giessen. Because the percent is low enough during July and August in Houghton (54%), these two months do not have the close similarity with any months in Giessen--although the difference is not great as Giessen's August cloud cover is 59% [5,1]. The same is also true for Houghton in December and January when there is somewhat more cloud cover than any month in Giessen. February in Houghton is similar to the winter months in Giessen (November-February).

FIGURE 16.

HOUGHTON/GIESSEN CLOUD COVER COMPARISON

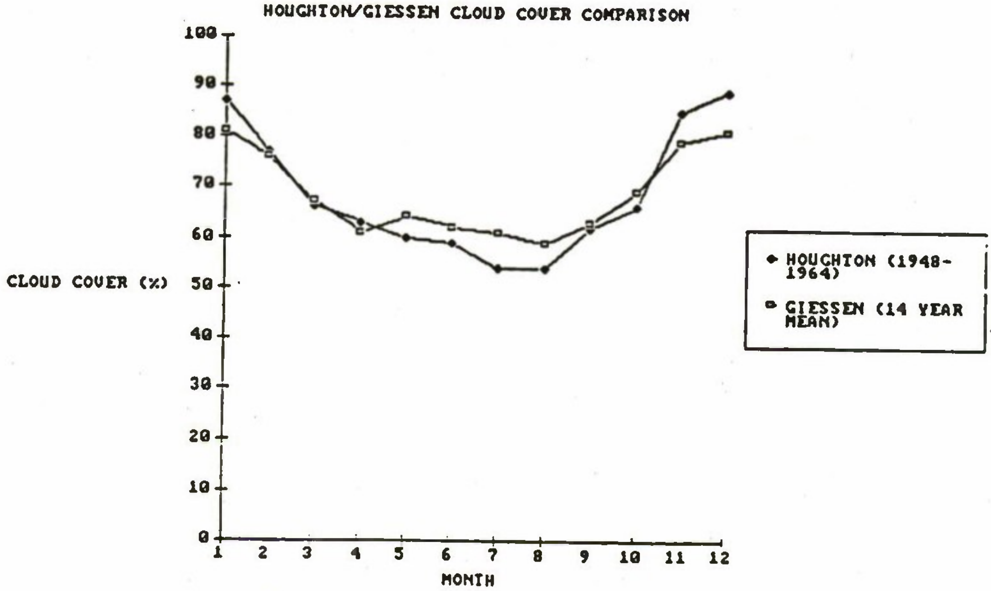

VISIBILITY

Figure 17 shows that the percent frequency with which either a ceiling less than 1524m (5000ft), or the visibility less than 8.045km (5 miles), or both, occurs is greater in Giessen than in Houghton for each of the corresponding months [5,1]. Thus, there are only a few similarities existing for this parameter. One is that Houghton's March and October are similar to the spring and summer months in Giessen (April-August). November and December in Houghton are similar to both January through March, and October and November in Giessen. Finally, Houghton's January and February are similar to October and November in Giessen.

FIGURE 17.

HOUGHTON/GIESSEN % FREQUENCY OF OBSERVATIONS WITH THE CEILING LESS THAN 1524m (5000 FT) AND/OR THE VISIBILITY LESS THAN 8.045 km (5 MILES)

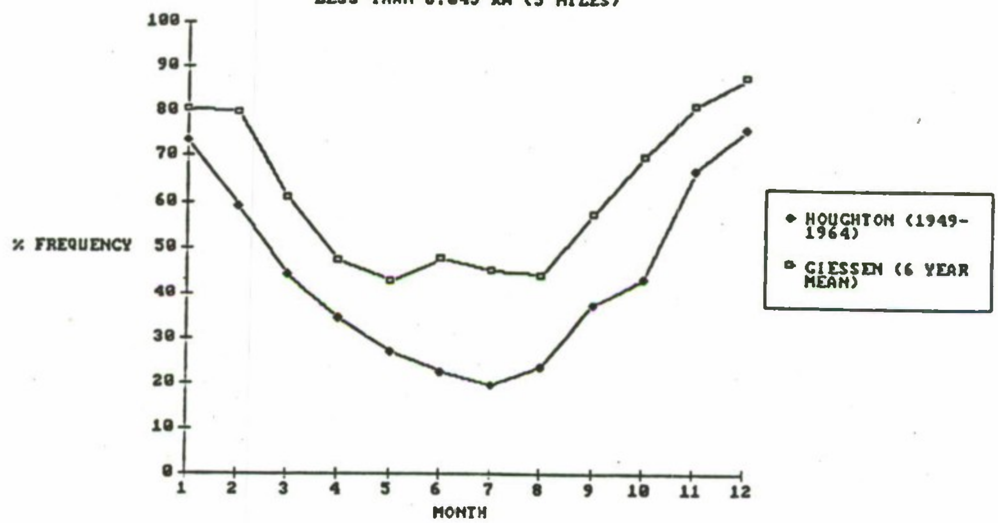

In Figure 18, the percent frequency with which either a ceiling less than 91.4m (300ft), or the visibility less than 1.609km (1 mile), or both, occurs in Houghton and Giessen is shown, and February/February, August/August, September/September, and November/November are all similar [5,1]. In addition, May through October in Houghton is similar to the Giessen months of March and September. Otherwise, there are no additional organized similarities between the two locations. During March through August, Houghton has a higher percent frequency of this occurrence than those same months in Giessen. Meanwhile, for September through December, Giessen has a higher occurrence of the reduced ceiling and/or visibility. For this parameter, it perhaps should be noted that for the station of Wasserkuppe, West Germany--just 15-20km southeast of Fulda (but at a substantially higher elevation of 925m)--there is a significantly greater occurrence of this low ceiling and/or low visibility than at either Houghton or Giessen [2]. This comparison is shown in Figure 19. In December, the frequency is 69% in Wasserkuppe, compared with 10% in Houghton and 15% in Giessen [2,5,1]. While during July, the frequency in Wasserkuppe is 25.5%, compared with 4.2% and 0.8% in Houghton and Giessen [2,5,1]. The annual averages for Houghton, Giessen, and Wasserkuppe are 6.7%, 5.7%, and 41.0% respectively [2,5,1].

Figure 20 shows that compared with Houghton, Fulda has a much higher occurrence of fog throughout the year, with an annual frequency of 24.8% [2]. The annual frequency in Houghton is only 7.9% [5]. The main similarity occurs during the month of May in Fulda when the frequency of fog there is at the minimum for the

FIGURE 18.

HOUGHTON/GIESSEN % FREQUENCY
OF OBSERVATIONS WITH THE CEILING
LESS THAN 91.4m (300 FT)
AND/OR THE VISIBILITY
LESS THAN 1.609 km (1 MILE)

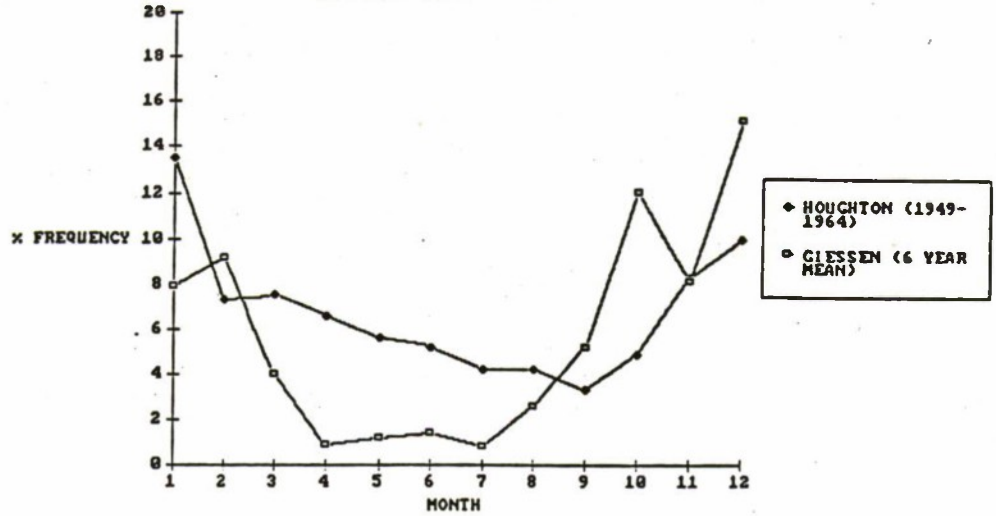

FIGURE 19.

HOUGHTON/GIESSEN/WASSERKUPPE
% FREQUENCY OF
OBSERVATIONS WITH THE CEILING
LESS THAN 91.4m (300 FT)
AND/OR THE VISIBILITY
LESS THAN 1.609 km (1 MILE)

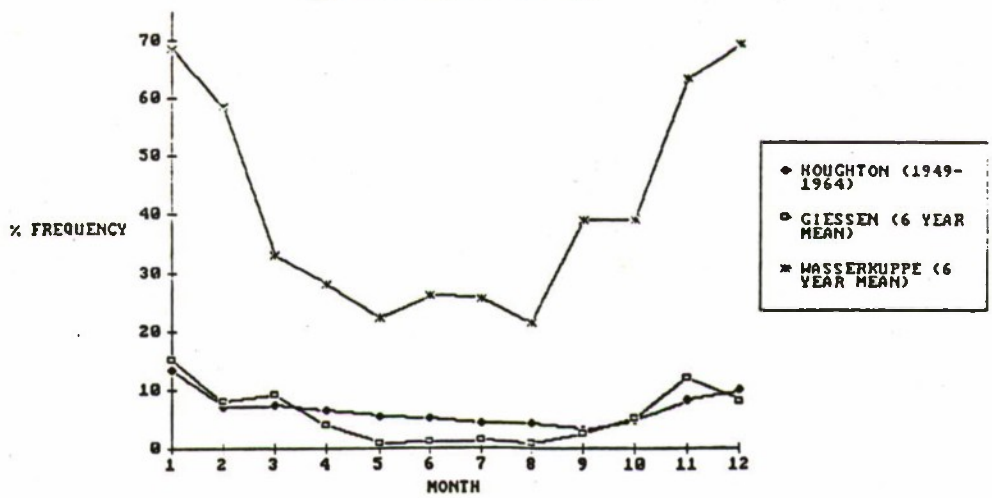

year: 10.6% [2]. This is similar with the Houghton months of April through October when the occurrence of fog is at the maximum for the year. Aside from this similarity, no other significant similarities appear. As for the occurrence of smoke and/or haze, Fulda again has a much greater occurrence than in Houghton so that no similarity exists at all between any two months at the two locations, which is shown in Figure 21. The annual percentage in Fulda is 20.2%, while the frequency of smoke and/or haze being observed in Houghton during the year is only 0.5% [5,2].

FIGURE 20.

HOUGHTON/FULDA % FREQUENCY OF OBSERVATIONS WITH FOG

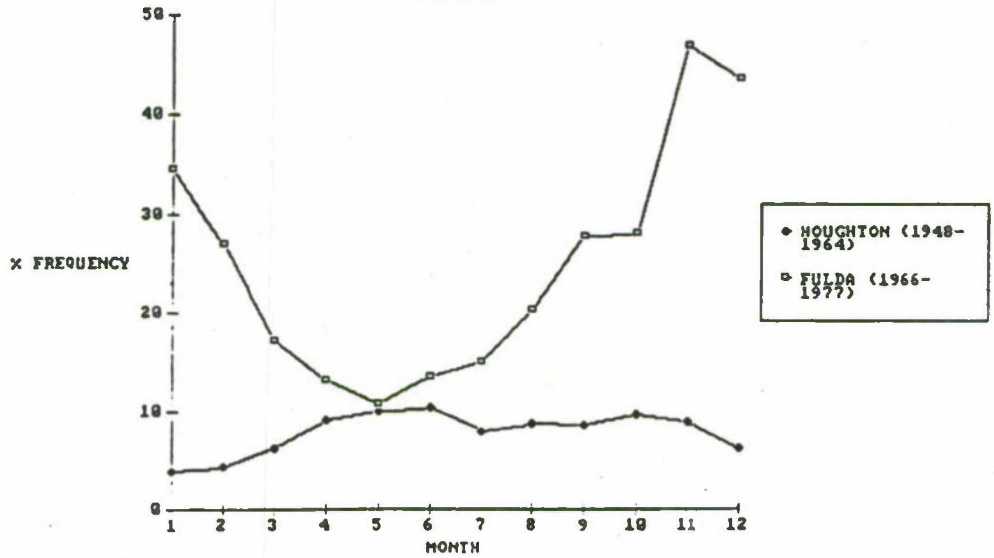

FIGURE 21.

HOUGHTON/FULDA % FREQUENCY OF OBSERVATIONS WITH SMOKE AND/OR HAZE

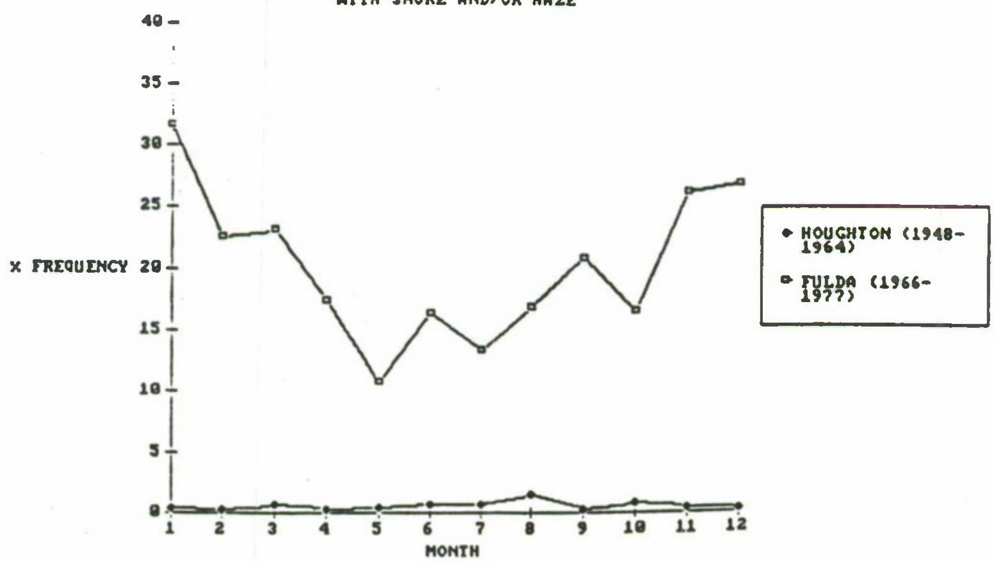

CONCLUSION AND RESULTS

When this climatological comparison was done, the difficulty became obvious in concluding that two climates--in this case Houghton and the Giessen/Fulda region--are similar. A simple comparison can be made for just a temperature or precipitation parameter, or perhaps just for fog, and be reasonably accurate. However, when a multiple of parameters are considered, the chances of finding a dissimilarity greatly increase. For this study, about twenty different climatic parameter comparisons were made, and numerous examples of this occurred. One example of this is that while the mean June maximum temperatures for Houghton and Giessen are 20.8°C and 21.1°C respectively, Houghton receives 261.7 W/m**2 of total solar radiation at the surface and Giessen receives much less than that amount, only 193.8 W/m**2 [3,1,7]. Another example of this can be observed for December in Houghton compared to July in Giessen, with similar precipitation totals for the months of 7.8cm (liquid water equivalent of snow) and 7.3cm (rain), respectively, yet completely dissimilar mean maximum temperatures of -3.7°C and 22.8°C [3,1]. So this must be kept in mind as it is revealed which months in Houghton are similar with which months in West Germany. It is from a greater frequency of climatic parameters being similar--though some may be dissimilar--that these claims of overall similarity are made.

It can be concluded from this climatological comparison that the main similarity between Houghton and the Giessen/Fulda region is from a period of April to September in Houghton and the corresponding months of the same period (April-September) at the West German site. In general, the summer months in Houghton (June-August) appear to be similar with each of the late spring and summer months in Giessen or Fulda region (May-August). In addition, the period of September to December in Houghton is also quite similar with a Giessen/Fulda May, April, March, and February period. Finally, late winter through spring (February-May) in Houghton is similar with a March to June period at the West German locations.

Interestingly enough, December and January in Houghton have a nearly complete dissimilarity with December and January in West Germany. Houghton's January has no apparent similarity with any German month, while its December has some similarity with the Giessen/Fulda months of February, October, and November. There is no month in Houghton during the year which could be said to be similar to all twelve months in West Germany. The same is true for any of the Giessen or Fulda months being similar with all the months in Houghton also.

SIMILARITIES

HOUGHTON	GIESSEN/FULDA
1. Summer(June-August)	Summer(May-August)
2. Autumn/Early Winter (September-December)	Spring/Late Winter (May, April, March, and February)
3. Late Winter/Spring (February-May)	Spring/Early Summer (March-June)
4. December	February, October, and November

MAJOR DISSIMILARITIES

HOUGHTON	GIESSEN/FULDA
1. Late Spring/Autumn (May-October)	Winter(November-February)
2. Winter(November-February)	Spring/Early Autumn (April-Sept.)
3. Mid-winter(December, January)	Mid-winter(December, January)

REFERENCES

1. Hummel, J. R., Climatological Parameters for Germany and Dayton and Comparison Against TSCF Test Episodes, OptiMetrics, Inc., Ann Arbor, Michigan, July 1984.

2. Walker, B. F. and Winn, R. T., Climatological Statistics on Meteorological Factors Affecting Electro-Optics in Germany, Deputy for Development Plans Armament Division, Eglin Air Force Base, Florida, August 1980.

3. Monthly Normals of Temperature, Precipitation, and Heating and Cooling Degree Days 1951-80, National Climatic Center, Asheville, North Carolina, September 1982.

4. Landsberg, H. E., Lippmann, H., Paffen, K. H., and Troll, C., World Maps of Climatology, Springer-Verlag, New York, 1966, pp. 26-27.

5. Revised Uniform Summary of Surface Weather Observations, Data Processing Division USAFETAC, Air Weather Service, Asheville, North Carolina, September 22, 1972.

6. Climatological Data, National Climatic Data Center, Asheville, North Carolina, January 1968-December 1984.

7. deJong, B., Net Radiation Received by a Horizontal Surface at the Earth, Delft University Press, Rotterdam, Netherlands, 1973.

DISTRIBUTION LIST

	Copies
Commander Defense Technical Information Center Bldg. 5, Cameron Station ATTN: DDAC Alexandria, VA 22304-9990	2
Manager Defense Logistics Studies Information Exchange ATTN: AMXMC-D Fort Lee, VA 23801-6044	2
Commander U.S. Army Tank-Automotive Command ATTN: ASQNC-TAC-DIT (Technical Library) Warren, MI 48397-5000	2
Commander U.S. Army Tank-Automotive Command ATTN: AMSTA-CF (Dr. K. Oscar) Warren, MI 48397-5000	1
Director U.S. Army Materiel Systems Analysis Activity ATTN: AMXSY-MP (Mr. Cohen) Aberdeen Proving Ground, MD 21005-5071	1